

# IMPROVING THE FOUNDATION LAYERS FOR CONCRETE PAVEMENTS:

## Lessons Learned and a Framework for Mechanistic Assessment of Pavement Foundations

**Final Report | January 2021**



CENTER FOR  
**CEER**  
EARTHWORKS ENGINEERING  
RESEARCH

National Concrete Pavement  
Technology Center  
Tech Center

IOWA STATE  
UNIVERSITY  
Institute for  
Transportation

### **Sponsored by**

Federal Highway Administration Pooled Fund Study TPF-5(183):  
California, Iowa (lead state), Michigan, Pennsylvania, and Wisconsin

## **About the CP Tech Center**

The mission of the National Concrete Pavement Technology Center (CP Tech Center) at Iowa State University is to unite key transportation stakeholders around the central goal of advancing concrete pavement technology through research, tech transfer, and technology implementation.

## **About the Center for Earthworks Engineering Research**

The mission of the Center for Earthworks Engineering Research (CEER) at Iowa State University is to be the nation's premier institution for developing fundamental knowledge of earth mechanics, and creating innovative technologies, sensors, and systems to enable rapid, high quality, environmentally friendly, and economical construction of roadways, aviation runways, railroad embankments, dams, structural foundations, fortifications constructed from earth materials, and related geotechnical applications.

## **Iowa State University Nondiscrimination Statement**

Iowa State University does not discriminate on the basis of race, color, age, ethnicity, religion, national origin, pregnancy, sexual orientation, gender identity, genetic information, sex, marital status, disability, or status as a US veteran. Inquiries regarding nondiscrimination policies may be directed to the Office of Equal Opportunity, 3410 Beardshear Hall, 515 Morrill Road, Ames, Iowa 50011, telephone: 515-294-7612, hotline: 515-294-1222, email: eooffice@iastate.edu.

## **Disclaimer Notice**

The contents of this report reflect the views of the authors, who are responsible for the facts and the accuracy of the information presented herein. The opinions, findings and conclusions expressed in this publication are those of the authors and not necessarily those of the sponsors.

The sponsors assume no liability for the contents or use of the information contained in this document. This report does not constitute a standard, specification, or regulation.

The sponsors do not endorse products or manufacturers. Trademarks or manufacturers' names appear in this report only because they are considered essential to the objective of the document.

## **Quality Assurance Statement**

The Federal Highway Administration (FHWA) provides high-quality information to serve Government, industry, and the public in a manner that promotes public understanding. Standards and policies are used to ensure and maximize the quality, objectivity, utility, and integrity of its information. The FHWA periodically reviews quality issues and adjusts its programs and processes to ensure continuous quality improvement.

## **Iowa DOT Statements**

Federal and state laws prohibit employment and/or public accommodation discrimination on the basis of age, color, creed, disability, gender identity, national origin, pregnancy, race, religion, sex, sexual orientation or veteran's status. If you believe you have been discriminated against, please contact the Iowa Civil Rights Commission at 800-457-4416 or Iowa Department of Transportation's affirmative action officer. If you need accommodations because of a disability to access the Iowa Department of Transportation's services, contact the agency's affirmative action officer at 800-262-0003.

The preparation of this report was financed in part through funds provided by the Iowa Department of Transportation through its "Second Revised Agreement for the Management of Research Conducted by Iowa State University for the Iowa Department of Transportation" and its amendments.

The opinions, findings, and conclusions expressed in this publication are those of the authors and not necessarily those of the Iowa Department of Transportation or the U.S. Department of Transportation Federal Highway Administration.

### Technical Report Documentation Page

<b>1. Report No.</b> InTrans Project 09-352	<b>2. Government Accession No.</b>	<b>3. Recipient's Catalog No.</b>	
<b>4. Title and Subtitle</b> Improving the Foundation Layers for Concrete Pavements: Lessons Learned and a Framework for Mechanistic Assessment of Pavement Foundations		<b>5. Report Date</b> January 2021	
		<b>6. Performing Organization Code</b>	
<b>7. Author(s)</b> David J. White, Pavana K. R. Vennapusa, and Bora Cetin		<b>8. Performing Organization Report No.</b> InTrans Project 09-352	
<b>9. Performing Organization Name and Address</b> National Concrete Pavement Technology Center and Center for Earthworks Engineering Research (CEER) Iowa State University 2711 South Loop Drive, Suite 4600 Ames, Iowa 50010-8664		<b>10. Work Unit No. (TRAIS)</b>	
		<b>11. Contract or Grant No.</b>	
<b>12. Sponsoring Organization Name and Address</b> Federal Highway Administration Transportation Pooled Fund 1200 New Jersey Avenue SE Washington, DC 20590		<b>13. Type of Report and Period Covered</b> Final Report	
		<b>14. Sponsoring Agency Code</b> TPF-5(183)	
<b>15. Supplementary Notes</b> Visit <a href="https://cptechcenter.org/">https://cptechcenter.org/</a> for color PDF files of this and other research reports.			
<b>16. Abstract</b> <p>This report summarizes the key findings and lessons learned from the series of field, laboratory, and advanced numerical studies performed under Federal Highway Administration (FHWA) Transportation Pooled Fund Study TPF-5(183). This research program was established by the partnering state departments of transportation (DOTs) to identify opportunities to document the as-constructed conditions and advance the quality and economy of the foundation layers for portland cement concrete (PCC) pavements, leading to improved support for long-life pavement systems.</p> <p>The key findings and lessons learned are drawn from detailed pavement foundation test programs in the participating states of California, Iowa, Michigan, Pennsylvania, and Wisconsin. The key findings are presented with an emphasis on the measurement and characterization of the design input values for the foundation layers. The focus of the lessons learned is on the challenges involved in the mechanistic characterization of pavement foundation engineering properties.</p> <p>Through this study, it was determined that current practices for pavement foundation quality inspection, specifically mechanistic characterization, are limited by the methods of measurement and frequency of testing. Ultimately, important pavement foundation parameters are not being measured in practice or controlled in situ, and therefore their impact on pavement performance is not well understood or accounted for in modern pavement design.</p> <p>A new performance-based framework is presented that rethinks the mechanistic assessment of pavement foundation layers and outlines an improved approach going forward. The goal of improving the measurement and performance of pavement foundation layers is to promote long-life concrete pavements. Improved workflows and better in situ measurement technologies are needed to ultimately produce more sustainable and longer lasting pavements.</p>			
<b>17. Key Words</b> concrete pavement—geostatistics—pavement foundation—pavement subbase—pavement subgrade—quality assurance—quality control—spatial analysis		<b>18. Distribution Statement</b> No restrictions.	
<b>19. Security Classification (of this report)</b> Unclassified.	<b>20. Security Classification (of this page)</b> Unclassified.	<b>21. No. of Pages</b> 141	<b>22. Price</b> NA





# **Improving the Foundation Layers for Concrete Pavements: Lessons Learned and a New Framework for Mechanistic Assessment**

**Final Report**  
January 2021

## **Research Team Members**

Tom Cackler, David J. White, Jeffery R. Roesler, Barry Christopher, Andrew Dawson,  
Heath Gieselman, Pavana Vennapusa, Peter Becker, Jia Li, Yang Zhang, Alex Johnson,  
and A. J. Wolfe

## **Authors**

David J. White, Pavana K. R. Vennapusa, and Bora Cetin

## **Sponsored by**

Federal Highway Administration Pooled Fund Study TPF-5(183):  
California, Iowa (lead state), Michigan, Pennsylvania, and Wisconsin

Preparation of this report was financed in part  
through funds provided by the Iowa Department of Transportation  
through its Research Management Agreement with the  
Institute for Transportation  
(InTrans Project 09-352)

## **National Concrete Pavement Technology Center and Center for Earthworks Engineering Research (CEER)**

Iowa State University  
2711 South Loop Drive, Suite 4700  
Ames, Iowa 50010-8664  
Phone: 515-294-5798  
<https://cptechcenter.org/>



## TABLE OF CONTENTS

ACKNOWLEDGMENTS .....	xi
EXECUTIVE SUMMARY .....	xiii
CHAPTER 1: INTRODUCTION .....	1
The Challenge .....	1
Research Objectives.....	2
Summary of Lessons Learned.....	2
Addressing Nonuniformity in Foundation Layer Engineering Support Values .....	8
Establishing a New Framework for Pavement Foundation Assessment .....	13
Organization of the Report.....	13
CHAPTER 2: LESSONS LEARNED FROM FIELD STUDIES .....	15
Field Verification of the Mechanistic Design Parameters of the Foundation Layers.....	15
Design Parameters Used by Different State Agencies.....	15
Field Testing and Interpretation Methods.....	17
Field Testing Results and Comparisons with Design Input Values.....	20
Spatial Nonuniformity of the Mechanistic Properties of the Foundation Layer.....	25
Field Testing Results.....	26
Influence of Foundation Input Properties on Design and Performance Predictions.....	34
Impact of Nonuniform Support Conditions on Mechanistic Pavement Responses.....	37
Impacts of Loss of Support on Mechanistic Pavement Responses.....	37
In Situ Assessment of Distressed Pavement Sections.....	40
Assessment of Frost Heave and Joint Deterioration on US 30 near Ames, Iowa.....	40
Assessment of Joint Deterioration on Urbandale Drive in Urbandale, Iowa.....	43
Evaluation of Premature Pavement Distresses on US 34 near Mount Pleasant, Iowa .....	46
In Situ Assessment of Rehabilitated Pavement Sections.....	50
Pennsylvania SR-422 Pavement Rehabilitation Project .....	50
California I-15 Pavement Rehabilitation Using Precast Concrete Panels .....	57
Impact of Seasonal Variation on Pavement Foundations and Performance .....	59
Seasonal Temperature Variation and Frost Depth.....	59
Seasonal Variations in In Situ Foundation Layer Properties.....	60
Laboratory Characterization of Frost Heave and Thaw Weakening Susceptibility .....	64
CHAPTER 3: MECHANISTIC CHARACTERIZATION OF PAVEMENT FOUNDATION LAYERS .....	70
A Brief History of the Evolution of Rigid Pavement Design .....	70
Geotechnical Input Parameters in Rigid Pavement Design .....	72
Modulus of Subgrade Reaction (k) Value .....	77
Foundation Layer Resilient Modulus.....	87
Nonuniformity and Loss of Support .....	89
Influence of Seasonal Variations .....	91
Foundation Layer Drainage Properties .....	96
Empirical Relationships and Associated Uncertainties/Risks .....	97
CHAPTER 4: MECHANISTIC PAVEMENT FOUNDATION SPECIFICATION FRAMEWORK.....	100

Review of the Current State of the Practice for Design and Construction QC/QA .....	100
Framework for Performance-Based Mechanistic Pavement Foundation Testing .....	105
Step 1: Selection of Pavement Design Method.....	107
Step 2: Selection of Foundation Layer Design Input Parameters .....	107
Step 3: Development of a Program/Method for Selection of These Input Parameters...	108
Step 4: Complete Design Calculations and Establish Field Target Values .....	110
Step 5: Implement Specifications with 100% Geospatial Mapping .....	111
Steps 6, 7, and 8: Evaluate the Results and Perform Independent QA Testing .....	111
CHAPTER 5: CONCLUSIONS AND RECOMMENDATIONS .....	112
REFERENCES .....	115
AASHTO Standards, American Association of State Highway and Transportation Officials, Washington, DC.....	115
ASTM Standards, ASTM International, West Conshohocken, PA .....	115
Author-Date References.....	115



## LIST OF FIGURES

Figure 1. Selected field test projects showing the wide range of material used in pavement foundation construction .....	3
Figure 2. Key factors for evaluating the challenges in designing, constructing, and testing pavement foundation systems .....	7
Figure 3. Spatial plots of IC measurement values for a special backfill subbase layer (left) and the overlaid RPCC base layer (right) showing reflections of the “hard” areas from the subbase layer into the base layer and base layer in situ elastic modulus values .....	11
Figure 4. Nonuniform support conditions leading to underdesign/overdesign and increased pavement stresses (top) and target field support conditions achieved through more uniform support values, including improvement in reworked areas (bottom).....	12
Figure 5. Mechanistic-based in situ test methods used in this study .....	18
Figure 6. In situ PLT results near Sta. 495+00 – Wisconsin US 10 construction project .....	21
Figure 7. In situ $k$ values from FWD testing – Wisconsin US 10 construction project.....	21
Figure 8. Which is the correct $k$ value? Date compares the design target $k$ value with measured and estimated $k$ values from various field and laboratory measurements – Wisconsin US 10 construction project.....	22
Figure 9. Backcalculated $E_{SB}$ values for the CTB/sand subbase layer from FWD tests over a 5.5 m wide x 92 m long area: (a) spatial contour map and (b) measurements longitudinally along the roadway – Michigan I-96 reconstruction project.....	23
Figure 10. Backcalculated subgrade modulus ( $E_{SG}$ ) values beneath the base/subbase layer from FWD tests over a 5.5 m wide x 92 m long area: (a) kriged spatial contour map and (b) measurements longitudinally along the roadway – Michigan I-96 reconstruction project.....	24
Figure 11. $E_{LWD}$ measurements across the pavement width near Sta. 1394+60 – Iowa US 30 construction project.....	26
Figure 12. Surface of the RPCC-modified subbase layer across the width of the pavement foundation layer near Sta. 1394+60 – Iowa US 30 construction project (photographs taken on August 8, 2011) .....	27
Figure 13. Description of a typical experimental and spherical semivariogram and its parameters .....	29
Figure 14. Field testing in a dense grid pattern on an open-graded drainage course granular base layer consisting of recycled steel slag (classified as GP and A-1-a) – Michigan I-94 construction project (photograph taken on May 28, 2009) .....	30
Figure 15. Spatial contour maps of (a) $\gamma_d$ and (b) $E_{SB}$ values and histogram plots of (c) $\gamma_d$ and (d) $E_{SB}$ values based on LWD measurements on a compacted open-graded drainage course granular base layer – Michigan I-94 construction project.....	31
Figure 16. Semivariograms of $E_{SB}$ measurements from LWD testing: (a) from testing in a dense grid over a small area and (b) from sparse testing over a large area – Michigan I-94 construction project .....	32
Figure 17. IC measurement values obtained at different amplitude (a) settings on a special backfill subgrade treatment layer placed over the subgrade and on the overlaid RPCC subbase layer in the same area – Iowa I-29 reconstruction project .....	34

Figure 18. Stress ratio values for different pavement joint LTE cases, foundation support $k$ values, and pavement thicknesses for a standard 80 kN (18 kip) AASHTO single-axle dual-wheel loading near a corner .....	35
Figure 19. EverFE simulation results depicting principal stresses in the pavement layer (left) and surface deflections (right) .....	38
Figure 20. FE model with two jointed slabs and 80 kN standard single-axle loading (with dual-wheel sets) near the joint/corner and an area of void beneath the slab for different LOS conditions.....	39
Figure 21. Influence of LOS and magnitude of gap on SR values for LOS for different pavement thickness cases.....	40
Figure 22. Heave near joints and drilling, coring, and sampling in February and March 2010 on an existing pavement with severe joint distresses – Iowa US 30 existing pavement evaluation project.....	41
Figure 23. Average moisture contents of core specimens at various depths – Iowa US 30 existing pavement evaluation project.....	42
Figure 24. Spatial contour plots of vertical heave near four selected joints – Iowa US 30 existing pavement evaluation project.....	43
Figure 25. Joint deterioration (left) and CHP test in a drilled core hole at a joint obtained on November 7, 2013 (right) – Iowa Urbandale Drive project.....	44
Figure 26. Extracted core from a joint (with the right side representing the top of the pavement) showing freeze-thaw-related damage near the bottom of the sawcut (photograph taken on November 7, 2013) – Iowa Urbandale Drive project .....	46
Figure 27. (a) Corner cracking on concrete panel, (b) longitudinal cracking, and (c) cracks observed on embankment fill slope near mile post 194 on US 34 WB, photograph taken on July 27, 2012 – Iowa US 34 pavement evaluation project.....	47
Figure 28. Box plots comparing FWD test results at locations with and without cracking: (a) peak deformations beneath the plate under an applied load of 40 kN and (b) backcalculated $k$ value – Iowa US 34 pavement evaluation project.....	49
Figure 29. Foam injection process: (a) drilling equipment used to drill injection holes, (b) foam injection, (c) mechanical gauges used to monitor pavement panel rise, and (d) dowel bar retrofitting performed at selected crack locations (photographs taken in October 2009) – Pennsylvania SR-422 rehabilitation project .....	51
Figure 30. (a) Patch area showing OGS and HDP mixture boundary and (b) close-up view of the OGS and HDP mixture sample extracted from the patch area (photograph taken in October 2009) – Pennsylvania SR-422 rehabilitation project .....	52
Figure 31. Results of elevation monitoring near joints and cracks on nine panels: (a) plan view of elevation monitoring locations, foam injection locations, and A-A, B-B, and C-C survey lines and (b) change in elevation ( $\Delta$ Elevation) shortly after HDP foam injection along A-A, B-B, and C-C survey lines .....	53
Figure 32. (a) $D_0$ at the joints, (b) $D_0$ at the cracks, (c) $D_0$ midway between the joint and the crack, (d) intercept at the joints, (e) intercept at the cracks, (f) intercept midway between the joint and the crack, before and after HDP/grout stabilization and dowel bar retrofitting at the cracks – Pennsylvania SR-422 rehabilitation project .....	55
Figure 33. (a) LTE at the joints and (b) LTE at the cracks, before and after HDP/grout stabilization and dowel bar retrofitting at the cracks – Pennsylvania SR-422 rehabilitation project .....	56

Figure 34. Estimated frozen zones (shaded areas) at mile post 143.68 from 2011 to 2015 – Iowa US 30 reconstruction project .....	59
Figure 35. Freeze-thaw cycles at various depths from 2011 to 2015 using $\pm 0.5^{\circ}\text{C}$ and $\pm 1^{\circ}\text{C}$ as cycle boundary values – Iowa US 30 reconstruction project .....	60
Figure 36. Testing results from Plainfield, Iowa, test site: (a) zero-degree isotherm with time, (b) seasonal variations in $D_0$ , and (c) seasonal variations in $k_{\text{FWD-Static-Corr}}$ .....	62
Figure 37. PCI versus pavement age in the present study compared to results presented in White and Vennapusa (2014) and White et al. (2008).....	63
Figure 38. Side-by-side specimen assembly before/after freeze-thaw testing (1 in. = 25.4 mm) .....	64
Figure 39. Idealized view of the temperature control chamber .....	65
Figure 40. Comparison of frost heave rates and post-test CBR values for all stabilized and unstabilized material samples .....	66
Figure 41. Relationships between post-test CBR values and measured heave rates with a comparison to the ASTM D5918 criteria.....	68
Figure 42. Sensitivity of change in $k$ value on the design life of a pavement using the AASHTO (1993) rigid pavement design procedure .....	77
Figure 43. Interpretation of plate load testing results per (a) the AASHTO Road Test and AASHTO design procedures and (b) AASHTO and PCA design procedures .....	79
Figure 44. Comparison of the relationships between $M_r$ and $k$ value obtained from U.S. Department of Defense (2018), AASHTO (1993), and the ACPA web-based prediction tool .....	83
Figure 45. Relationships between $k$ and CBR published in the literature and data points from the present study and others (1 pci = 0.27 kPa/mm).....	84
Figure 46. Static $k_{\text{PLT}}$ values versus $k_{\text{FWD-Dynamic}}$ measurements reported in the literature .....	86
Figure 47. Deformed shape and stress contours for slabs with surface-initiated cracks and edge loading.....	89
Figure 48. Color contours of major principal stresses in a jointed concrete slab (200 mm [8 in.] thick) subjected to 80 kN (18 kip) AASHTO single-axle dual-wheel loading, with different $k$ values and a gap modeled beneath the slab when LOS = 1 .....	90
Figure 49. Variation in $F_U$ with changes in degree of saturation.....	94
Figure 50. Estimating the reliability of a predicted value based on the standard error of the estimates from empirical relationships .....	98
Figure 51. Workflow for field verification of pavement foundation design input parameters.....	106
Figure 52. Step 3a of workflow for field verification of pavement foundation design input parameters – for evaluation of support conditions under existing pavements prior to rehabilitation .....	107

## LIST OF TABLES

Table 1. Ranges of coefficient of variation values for field-measured parameters from multiple project sites .....	9
Table 2. Summary of foundation design input parameters currently in use by the participating state agencies .....	16
Table 3. Summary of design, in situ-measured, and laboratory-measured values – Michigan I-96 reconstruction project.....	25
Table 4. Summary of mean and COV values of foundation layer properties from multiple sites .....	28
Table 5. Sensitivity of AASHTOWare Pavement ME Design input variables on predicted performance indicators – jointed rigid pavement .....	36
Table 6. Summary of in situ test results – Iowa Urbandale Drive project.....	45
Table 7. Summary of Student’s <i>t</i> -test results on FWD deflection basin parameters near mid-panel on cracked and uncracked slabs – Iowa US 34 pavement evaluation project.....	48
Table 8. Summary of t-test analyses on FWD deflection basin parameters near mid-panel on new versus old pavement – California I-15 rehabilitation project.....	58
Table 9. Summary of project sites in Iowa selected for seasonal variation testing .....	61
Table 10. Frost susceptibility classification.....	65
Table 11. Proposed frost heave and thaw weakening susceptibility classification for stabilized soils based on data from this study .....	68
Table 12. Influence of foundation layer properties on rigid pavement layer distresses .....	73
Table 13. Summary of rigid pavement design procedures and foundation layer input parameters .....	74
Table 14. Summary of the state of the practice for PCC pavement design, pavement foundation testing, and stabilization .....	101
Table 15. Summary of testing methods to determine mechanistic properties of geomaterials ...	108



## ACKNOWLEDGMENTS

This research was conducted under Federal Highway Administration (FHWA) Transportation Pooled Fund Study TPF-5(183), involving the following state departments of transportation (DOTs):

- California
- Iowa (lead state)
- Michigan
- Pennsylvania
- Wisconsin

The authors would like to express their gratitude to the FHWA, the Iowa DOT, and the other pooled fund state partners for their financial support and technical assistance.

Numerous people from each of the participating states assisted in identifying and providing access to the project sites, obtaining project design information, and obtaining field quality assurance test results. Several graduate and undergraduate research assistants from Iowa State University assisted with field and laboratory testing. All of their help was greatly appreciated.



## EXECUTIVE SUMMARY

Improving the in situ measurement of important mechanistic parameter values is the next major step forward in advancing the design, construction, and quality inspection practices for pavement foundations. By enabling in situ measurement of the correct parameters (e.g., resilient modulus), the resulting quality of the foundation layers will be known, corrective improvements can be made before the pavement is placed, and long-life pavement systems can be delivered more reliably.

The project described in this report was performed under Federal Highway Administration (FHWA) Transportation Pooled Fund Study TPF-5(183). The research program was initiated by the partnering state departments of transportation (DOTs)—California, Iowa (lead state), Michigan, Pennsylvania, and Wisconsin—to identify opportunities to document the as-constructed conditions and advance the quality and economy of the foundation layers for portland cement concrete (PCC) pavements, leading to improved support for long-life pavement systems.

This report describes how needed improvements to pavement foundation design, construction, and quality inspection practices were identified using results from an extensive field testing program, advanced numerical studies, and a detailed review of the engineering parameters used in pavement foundation design. A major goal of the research was to better connect pavement system design requirements to the parameters that should be measured during construction to ensure quality acceptance.

The lessons learned from the extensive field testing program described in this report focus on the challenges of mechanistic characterization of pavement foundation engineering properties. The wealth of data from these detailed field investigations are available in separately published project reports for a wide range of pavement foundation geomaterials and conditions, including freeze-thaw conditions.

The following key challenges regarding current practices were documented during the field investigations and analyses:

- The geomaterials used in pavement foundations construction are variable and complex.
- No field verification of the engineering parameters used in the mechanistic design of pavement foundations is being used for quality acceptance during construction.
- While parametric studies of pavement design have shown that pavement performance has a low sensitivity to the support provided by the foundation materials, poor support conditions are well documented as affecting the long-term field performance of pavements.

- Substantial spatial variability (nonuniformity) exists in newly constructed pavement foundations for the range of materials tested.
- If the subgrade layer is nonuniform, the overlying aggregate base layer will be nonuniform.
- Uniformity of support is an important characteristic of pavement foundation systems. New finite element analyses quantify the effects of this characteristic on pavement performance.
- Loss of support due to irreversible plastic deformation in the foundation layer can significantly decrease the fatigue life of the pavement.
- Permanent (irreversible) deformation of the pavement foundation layers is not considered in modern pavement design or measured as part of the construction verification process.
- Limited geotechnical testing (covering less than 1% of a given work area) is used to accept the engineering support values of pavement foundations, resulting in low reliability.
- Constructed pavement foundation layers often show isolated areas of poor quality that contribute to localized pavement performance issues.
- Limited technology is available to help earthwork and paving contractors improve the field control of pavement foundation layers during construction.
- Modern laboratory testing to determine the stress-dependent resilient moduli of foundation materials does not accurately represent/replicate field boundary conditions.
- More frost heave and thaw testing is needed to characterize complex pavement foundation geomaterials, especially stabilized materials. In addition, the impact of wetting and drying cycles on these materials should be evaluated and characterized in terms of changes in volume, stiffness, and strength.
- Characterizing the soil water characteristics curves (SWCCs) of foundation layer materials is important, especially if the new mechanistic-empirical design procedure used in AASHTOWare Pavement ME Design is followed, because SWCCs have a direct impact on modeling the post-construction variations in the resilient moduli of these materials over the design life of the pavement.
- The current practice for selecting design input parameters for pavement foundation geomaterials (e.g., modulus, post-construction changes in modulus) is still largely empirical.
- Most methods for quality inspection testing do not qualify as direct mechanistic measurements.



An ideal foundation layer for long-life concrete pavements should achieve the following:

- Uniform support
- Balance between excessive softness and stiffness
- Adequate drainage
- No plastic (permanent) deformation
- Use of sustainable methods and materials

Each of the separately published project reports provides key outcomes specific to the materials and test results for each site. Several additional peer-reviewed publications derived from this research have contributed to the state of the art and practice. With this previously published work and the lessons learned described in this report, and given the need for improved pavement foundation solutions, a new performance-based specification workflow was developed to improve future construction and in situ verification.

According to the assessments and surveys of state practices described in this report, current specifications for pavement foundation layers are a combination of construction method requirements (e.g., lift thickness, number of roller passes) and end-results requirements (e.g., minimum relative compaction). These requirements serve a practical function but limit advancement in terms of pavement foundation improvement.

This report proposes a performance-based specification approach that specifies the support conditions provided by the pavement foundation layer in terms of the pavement designers' requirements (e.g., resilient modulus or modulus of subgrade reaction) and includes a new requirement for uniformity (e.g., coefficient of variation of resilient modulus).

The following are the key features of a performance-based construction specification:

- Measurement technologies that provide near 100% sampling coverage
- Acceptance and verification testing procedures that measure the performance-related parameters that are relevant to the mechanistic design inputs
- Protocols for establishing target values for acceptance based on design
- Quality statements that require achievement of spatial uniformity

- Protocols for data analysis and reporting that ensure that the construction process is field-controlled in an efficient manner

The starting point for moving toward a performance-based specification is to develop an entirely new quality inspection workflow involving communication between the designer, engineer, contractor, and inspector. This report provides a description of the key elements of a performance-based workflow.

## **CHAPTER 1: INTRODUCTION**

This report provides a summary of key findings from a series of field, laboratory, and advanced numerical studies performed under Federal Highway Administration (FHWA) Transportation Pooled Fund Study TPF-5(183) that focused on the characterization of pavement foundation engineering properties. The lessons learned from these studies are presented in this report with an emphasis on the measurement and characterization of design input values for pavement foundation layers.

Through these studies, it was determined that current practices for pavement foundation quality inspection and mechanistic characterization are limited in terms of the methods of measurement and frequency of testing. A framework for a new type of performance-based workflow is presented that outlines an approach for the improved mechanistic assessment of pavement foundation layers. The goal of improving the measurement and performance of pavement foundation layers is to promote long-life (longer than 40 years) portland cement concrete (PCC) pavements.

### **The Challenge**

As an integral component of concrete pavement systems, pavement foundations are relied upon by contractors to serve as a suitable construction platform and by pavement engineers to provide adequate long-term support for the pavement. When pavement foundations are constructed in preparation for paving, there is a critical need to ensure that their as-constructed engineering properties are satisfactory.

Modern pavement design tools, such as the new mechanistic-empirical (ME) design method used in AASHTOWare Pavement ME Design, require more accurate characterization of the pavement foundation's geotechnical parameters than was previously necessary (AASHTO 2015). There are several geotechnical parameters (Christopher et al. 2006) and many different pavement foundation geomaterials to consider, including recycled materials and various chemical and mechanical stabilization options (Saeed 2008, Tutumluer 2013, Tutumluer et al. 2018, White et al. 2018). Meanwhile, recent developments in geotechnical asset management (Vessely et al. 2019) emphasize consideration of the pavement foundation as an asset with long-term value. With improved in situ characterization of pavement foundation systems and an understanding of the geomechanical behavior of the foundation layers, continued design improvements are expected to follow (see Darter et al. 1995).

However, the series of field investigations undertaken during this project shows that current in situ quality inspection practices do not directly measure the key geotechnical parameter values that are assumed during the design phase. Therefore, a disconnect exists between pavement design assumptions and construction inspection practices. This disconnect significantly limits the advancements that can be made in understanding pavement foundations, hindering efforts to improve design practices and methods for verifying that pavement foundation systems are of sufficient quality to support long-life pavements.

For example, uniformity of support, which is widely recognized as critically important to providing adequate pavement support (Richart and Zia 1962, Hudson and Matlock 1966, Levey and Barenberg 1970, Huang 2004, Birkhoff and McCullogh 1979, Westergaard 1927, White et al. 2005) is not typically included in acceptance practices for foundation layers and is not generally tested for acceptance criteria during construction. Additionally, though limiting irreversible plastic behavior (Huang and Wang 1974) is recognized as essential to achieving long-term performance for concrete pavements (Christopher et al. 2006), this parameter is also not measured or controlled during construction.

Ultimately, important pavement foundation parameters are not being measured in practice or controlled in situ, and therefore their impact on pavement performance is not well understood or accounted for in modern pavement design. Improvements through better process workflows and in situ measurement technologies are needed to achieve more sustainable and longer lasting pavements.

## **Research Objectives**

The research program described in this report was established by the five state departments of transportation (DOTs) partnering under TPF-5(183)—California, Iowa (lead state), Michigan, Pennsylvania, and Wisconsin—to identify opportunities to document as-constructed conditions and advance foundation quality and economy, leading to improved support for long-life (longer than 40 years) concrete pavement systems. With improved long-term quality, pavement foundations can be an important geotechnical asset throughout a pavement’s design life and for future repaving (see Vessely et al. 2019).

The aim of this report is to provide a technical framework and workflow of suggested practices that can be used to ensure that both short-term and long-term foundation construction and engineering performance requirements are achieved. Several knowledge gaps in current practices are identified that require future research, training, and specification development. Although measurement technology in this field is progressing, new specifications and training programs for improving pavement foundations are not being developed and implemented. Making important strides toward improving pavement foundations will require hard work and implementation strategies involving the development of new specifications, new and economical geomaterial stabilization solutions/products, better technologies for rapid field measurement, and improved education/training for contractors, engineers, and inspectors.

## **Summary of Lessons Learned**

Data used in the development of this report are based on several field studies of newly constructed and in-service concrete pavements in Iowa, Michigan, Wisconsin, California, and Pennsylvania. Figure 1 highlights some of the geomaterials and conditions at selected project sites to illustrate the range of materials used in pavement foundation construction.





I-15 near Ontario, California CTB layer after removal of pavement (June 28, 2010)



I-29 in Monona and Harrison Counties, Iowa, recycled pavement special backfill material over compacted subgrade



I 94 in St. Clair and Macomb Counties, Michigan, woven geotextile separator installed on top of the subgrade



SR-22 near Clyde in Indiana County, Pennsylvania, Construction of drainage CTB layer.



US Highway 422 in Indiana, Pennsylvania, injected HDP foam into OGB under the pavement surface



US Highway 10 just north of Junction City, Wisconsin, variable clay subgrade material

**Figure 1. Selected field test projects showing the wide range of material used in pavement foundation construction**

As expected, the project sites showed that pavement foundation materials have a wide range of material index properties and resulting engineering support conditions with complex behaviors during loading. Foundation materials are also subjected to a wide range of freeze-thaw environmental conditions, as evident in the varying climate conditions at the field test sites.

Several field studies and detailed analyses, including three-dimensional (3D) modeling of pavement foundation nonuniformity, are described in full in separately published project reports. The following summarizes the key points learned from the extensive field research program:

- A wide range of geomaterials with variable engineering properties is used for pavement foundations, with virtually no field verification of the design engineering parameter values (e.g., modulus of subgrade reaction, resilient modulus, drainability, deformation behavior). Construction acceptance of pavement foundation layers was sometimes approved based on in situ moisture and relative compaction measurements.
- Parametric studies conducted using AASHTOWare Pavement ME Design show that pavement performance has a low sensitivity to changes in the type and stiffness of foundation materials for selected slab thicknesses. However, the sensitivity of pavement performance to poor support conditions (nonuniformity, stiffness, permanent deformation) is well documented in the literature, indicating that the foundation layer properties affect the long-term field performance of rigid pavement systems (Lytton et al. 2019, Christopher et al. 2006).
- Substantial spatial variability (nonuniformity) exists in the engineering values of newly constructed pavement foundations, setting the conditions for the development of increased tensile stresses in the pavement layer (as verified using finite element [FE] modeling) for certain loading conditions. Uniformity of support is an important characteristic of pavement foundation systems.
- Loss of support (LOS) due to irreversible plastic deformation or erosion beneath the pavement significantly decreases the fatigue life of the pavement. A gap as small as 1.3 mm (0.05 in.) between the pavement and the foundation layer can lead to a loss of support.
- Permanent (irreversible) deformation of the pavement foundation layers (including the embankment, subgrade, and base layers) is not considered in pavement design and is not measured as part of the construction verification process.
- Overall, limited geotechnical testing (amounting to less than 1 percent of the area of the foundation layers) is used to characterize pavement foundation engineering values; as a result, testing has a low reliability in detecting conditions that do not meet the assumed design requirements.
- Constructed pavement foundation layers often have isolated areas of poor quality that are believed to contribute to localized pavement performance issues.

- Limited technology is available to help earthwork and paving contractors improve the field control of the subgrade and subbase layers and thereby improve the construction of the foundation layers.
- Even with modern laboratory testing to determine the stress-dependent resilient moduli of foundation materials, various challenges limit understanding of in situ conditions, including nonrepresentative boundary conditions and the lack of consideration of stress transfer or interactions between multiple foundation layers.
- In practice, the frost heave and thaw softening behavior of foundation layer materials is assessed mostly using soil classification, but the findings from this research show that soil classification is not always a reliable indicator. A broader program of laboratory testing and characterization is needed to assess frost heave and thaw softening behavior but is not often performed during pavement foundation design.
- The current state of the practice in selecting design input parameters (e.g., modulus) is largely based on historically convenient values or empirical relationships with surrogate or indirect test measurements. Empirical approaches offer much lower up-front costs than direct measurement approaches but introduce greater risks because of the (largely unquantified) uncertainties associated with the possibility that the predicted values will not match the actual field conditions. Some empirical procedures (e.g., calculating composite modulus of subgrade reaction using a method developed by the American Association of State Highway and Transportation Officials [AASHTO] [1993]) can result in unrealistic values that do not represent field conditions.
- Although a variety of in situ test methods are available that allow for the rapid evaluation of foundation layer mechanistic properties, most tests do not qualify as direct determinations of the values of design input parameters. Without direct measurement, agencies must rely on local calibrations to design input parameters.

The ideal support conditions for concrete pavement foundation layers include (1) uniform support, (2) balance between excessive softness and stiffness, (3) adequate drainage, (4) no irreversible plastic deformation, and (5) use of sustainable methods and materials.

Building long-life pavements with design lives of 40 or more years will require sustainable solutions and pavement foundation systems that not only support pavements uniformly during their service lives but also support rehabilitation design solutions after the pavements' initial service lives. The problem with poor support conditions is that defects cannot be overcome by increasing the thickness of the pavement layer.

To economically construct optimal foundation layers and ensure that they are long lasting, new inspection workflows and specifications are required to promote the field verification of design assumptions. If credible field measurements are taken during construction, appropriate corrective

actions can be taken to fix problematic areas prior to paving. Better measurement technologies are critical to making significant advances in this area.

Furthermore, although pavement design is increasingly becoming more sophisticated, selection of the input parameter values for pavement foundation design still often relies upon limited test data and empirical estimations from indirect measurements. Reliance on limited information to assess critical engineering performance characteristics, neglecting to control materials and quality inspection practices related to foundation uniformity, and failing to account for potential degradation of support due to poor drainage, erosion, and changes in soil volume all introduce substantial risks that the pavement system will not perform in a way that meets the requirements of long-term pavement design.

The findings from this research and prior literature indicate that little emphasis is currently placed on the in situ verification of the values of design input parameters. In addition, a disconnect currently exists between design and construction in terms of how the geotechnical properties of the foundation layers influence the long-term performance of PCC pavements. New technologies for the in situ assessment of parameters such as modulus and strength are expected to improve material selection and field process control through geospatial documentation that can verify design parameters in the field during construction.

Figure 2 outlines in detail the goals and key challenges associated with designing, constructing, and testing pavement foundation systems. The figure also details the key objectives of pavement foundation design; the associated failure mechanisms, distresses, and contributing factors; the measurement methods to quantify the different parameter values; typical target values and the controls and measures that can be established to achieve the target values; and the attributes needed in future specifications to address the control measures.

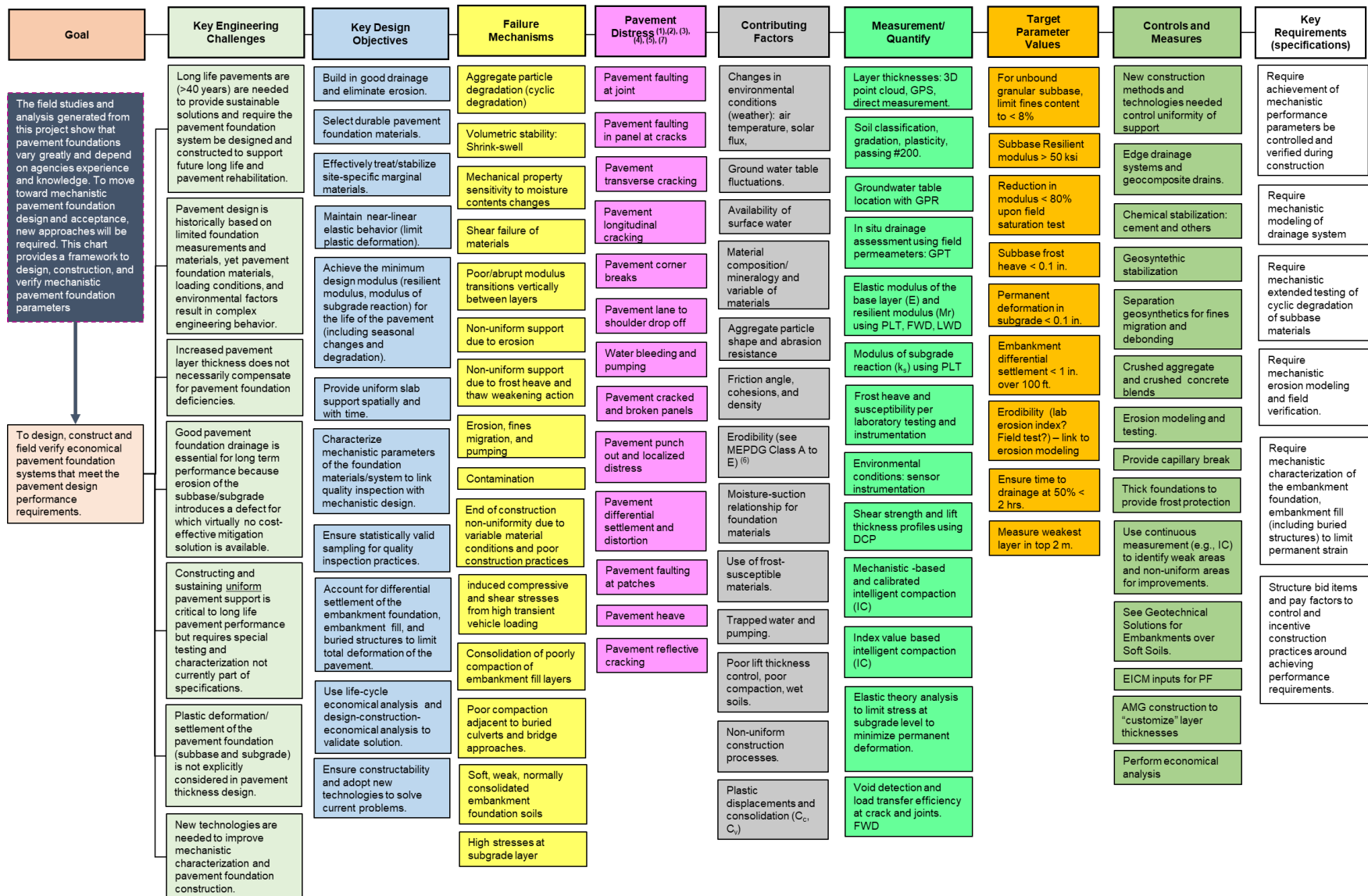


Figure 2. Key factors for evaluating the challenges in designing, constructing, and testing pavement foundation systems

## Addressing Nonuniformity in Foundation Layer Engineering Support Values

Nonuniform foundation support conditions can have detrimental effects on the service life and ride quality of pavements. Partly in response, uniformity of support was one of the primary areas of research emphasis throughout this study. According to the American Concrete Pavement Association (ACPA), uniformity of the subgrade and subbase layers is more important than the strength or stiffness of those layers (ACPA 2008). Based on field performance surveys, ACPA (2008) reported that many miles of old concrete pavements constructed on naturally uniform subgrades were in excellent condition, while pavements constructed over subgrades without proper subgrade compaction control (resulting in nonuniform conditions) were not. ACPA (2007) has also stated that the risk of premature failures increases when a nonuniform condition exists beneath a concrete pavement.

White et al. (2004) demonstrated through site characterization and pavement modeling that the benefits of uniform subgrade support for concrete pavements are evident in the reduction in maximum deflections and principal stresses in the PCC surface layer. Based on field studies conducted as part of the present project and additional pavement modeling, Brand et al. (2014) claimed that “nonuniform subgrade support is a complex interaction between the  $k$  value range, the magnitudes of  $k$  values, the distribution of the support stiffness relative to the critical loading location, and the size of the predefined area.” Nonuniformity of support is a complex problem that has not been well studied, primarily due to the lack of high-quality data available nationally.

Generally, in pavement design the foundation is considered to be a layered medium with uniform material properties and support conditions. However, geomaterial engineering parameter values generally show significant spatial variation in the field. Spatial variations in the support conditions provided by pavement foundation layers are documented by Vennapusa (2004) and White et al. (2004) and in several of the field studies from the present project. Table 1 summarizes the ranges of coefficient of variation (COV) values for field-measured parameters from the field projects conducted under this research.

**Table 1. Ranges of coefficient of variation values for field-measured parameters from multiple project sites**

<b>Measurement Property</b>	<b>Treated and Untreated Base/Subbase</b>	<b>Untreated Subgrade</b>	<b>Field Studies</b>
Elastic Modulus, $E_{LWD-Z3}$	19% to 63%	17% to 65%	WI US 10; IA US 30; PA SR-22; MI I-94; MI I-96
Modulus of Subgrade Reaction, $k_{PLT}$	30% to 34%	27% to 30%	WI US 10; MI I-94
California Bearing Ratio, CBR	22% to 34%	28% to 79%	WI US 10; IA US 30; MI I-94; MI I-96
Coefficient of Permeability, $K_{sat}$	86% to 135%	NA	PA SR-22; MI I-94; MI I-96
Dry Density, $\gamma_d$	2% to 6%	2% to 3%	WI US 10; PA SR-22; MI I-94; MI I-96
Moisture Content, $w$	12% to 21%	13% to 15%	

Although it is well known that uniformity of support is desired for concrete pavement foundation layers, uniformity of support is not yet well defined. The questions that need to be answered are “What level of nonuniformity is considered acceptable?” and “How is nonuniformity measured?”

The effects of spatial variability on the performance of geotechnical structures have been considered for a wide range of geotechnical applications (e.g., Mostyn and Li 1993, Phoon et al. 2000, White et al. 2004, Griffiths et al. 2006). One challenge in this area of study has been to collect enough information to make use of spatial statistics. Traditional quality control/quality assurance (QC/QA) programs for pavement foundation testing include rather sparse and infrequent testing. Special testing efforts are required for geospatial sampling that can adequately capture the real spatial variability.

As part of this project, special field testing operations were conducted at several construction sites using a dense grid pattern (i.e., less than 1 m spacing between points) over a small area and a sparse sampling pattern over a larger area. The goal was to measure the various foundation support characteristics (i.e., moisture content, dry density, strength, and stiffness) and assess their spatial variability and nonuniformity at both short and long ranges. Detailed results of the test measurements and their analyses are presented in the separately published project reports prepared as part of this research (see Chapter 5 for a complete list of reports and papers). The measurement parameters assessed included elastic modulus determined from lightweight deflectometer (LWD) testing ( $E_{LWD-Z3}$ ), dynamic cone penetration index (DCPI) of the subbase and subgrade layers ( $DCPI_{subbase}$ , and  $DCPI_{subgrade}$ ) using dynamic cone penetrometer (DCP)



testing, and dry unit weight ( $\gamma_d$ ) and moisture content ( $w$ ) determined from the nuclear gauge (NG) testing.

In practice, it is often misconceived that placing an aggregate base/subbase layer improves uniformity or provides uniform support. This is contrary to the findings of this study; placing an aggregate base/subbase over a nonuniform subgrade does little to improve uniformity. For example, Figure 3 shows intelligent compaction (IC) mapping for a project in Iowa involving a recycled PCC (RPCC) aggregate base layer overlaid on a special backfill subbase (subgrade treatment). The figure illustrates how the “soft” and “hard” areas identified in the subbase layer (left) reflect into the upper granular layer (right).



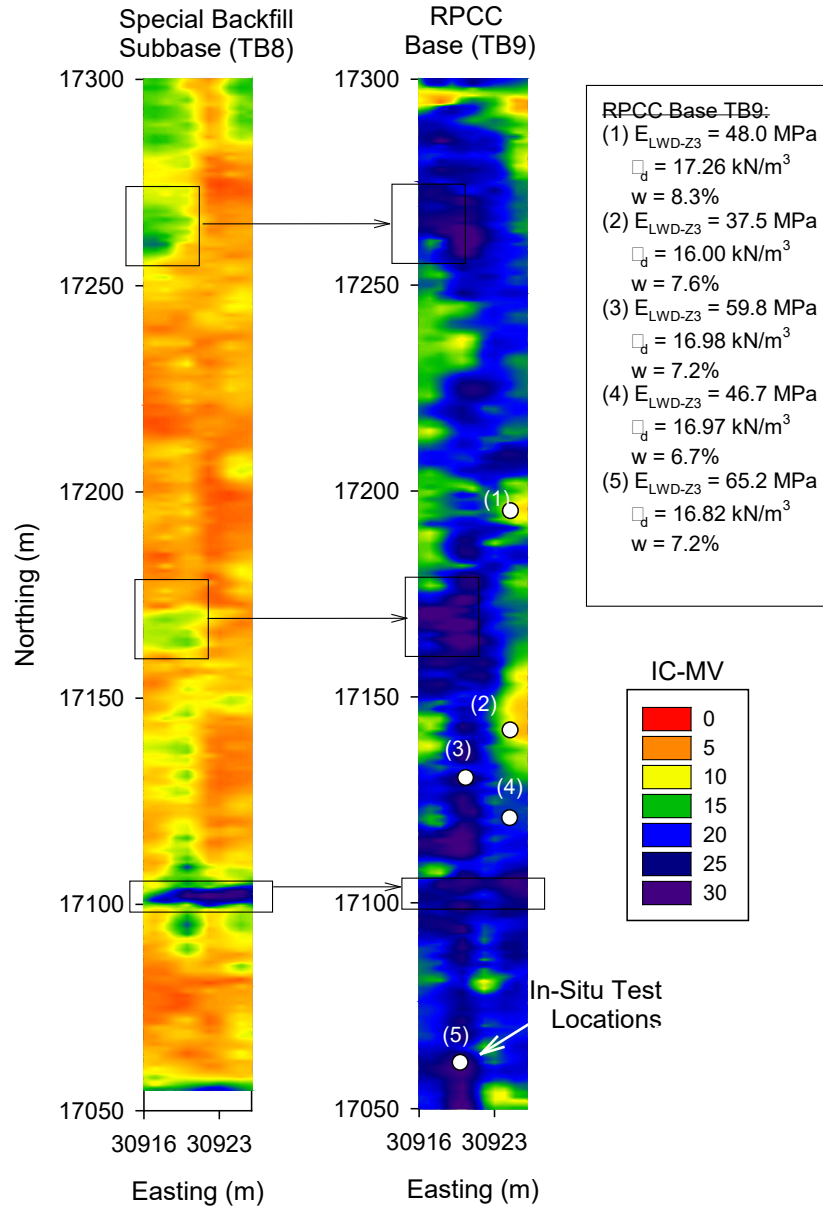


**Figure 3. Spatial plots of IC measurement values for a special backfill subbase layer (left) and the overlaid RPCC base layer (right) showing reflections of the “hard” areas from the subbase layer into the base layer and base layer in situ elastic modulus values**

ACPA (2007) notes that the primary purpose of aggregate base/subbase layers is to reduce erosion and pumping of fines from the subgrade and provide adequate drainage to quickly remove moisture from the pavement system. Therefore, proper subgrade preparation and stabilization are critical in helping the subgrade serve as a stable and uniform sublayer during the service life of a pavement. The present study suggests that the best means of obtaining uniform support for concrete pavements is not simply to place an aggregate base over a nonuniform subgrade but to improve the subgrade support conditions so that they provide uniform and stable support for the overlaid aggregate base layer.

Nonuniformity is best addressed during construction of the foundation layers starting from the bottom up. The effects of nonuniformity are illustrated in Figure 4.

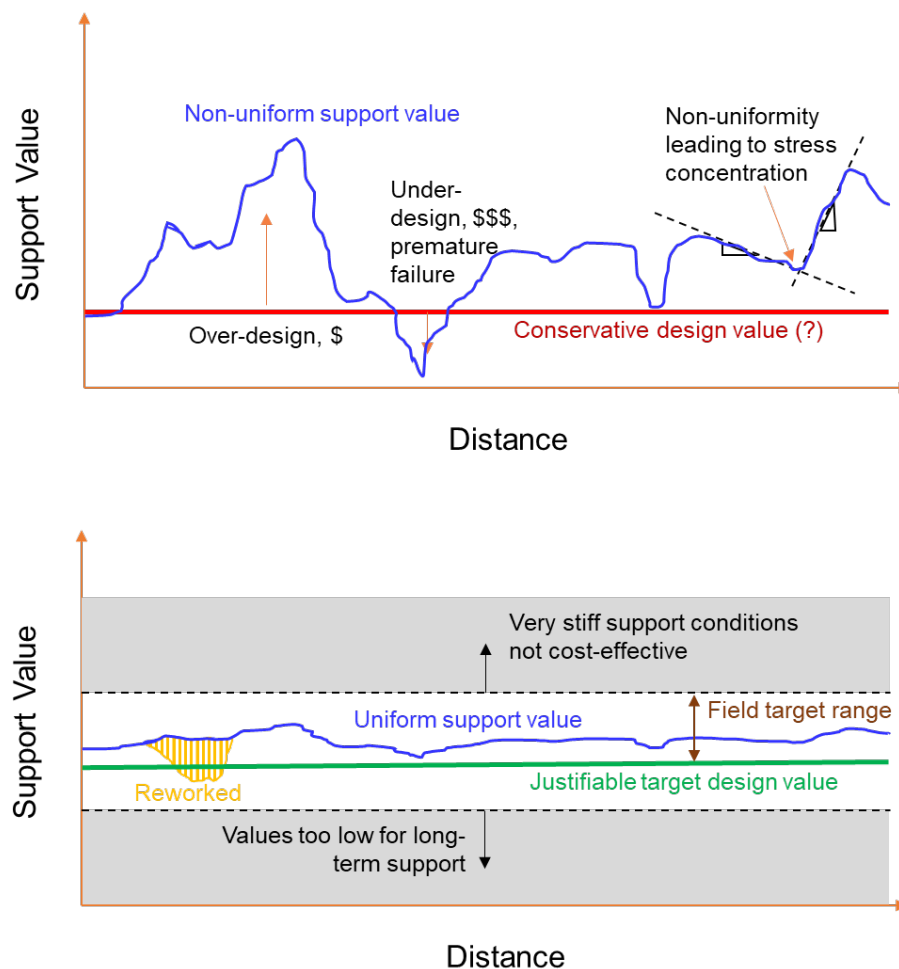


**Figure 4. Nonuniform support conditions leading to underdesign/overdesign and increased pavement stresses (top) and target field support conditions achieved through more uniform support values, including improvement in reworked areas (bottom)**

The upper chart in the figure shows nonuniform support conditions with design assumptions that can result in either underdesigned or overdesigned sections of a roadway and that can create abrupt changes in stiffness. This can be avoided by fixing the isolated low-stiffness areas during construction so that the entire stretch of roadway achieves a minimum justifiable target value, maintaining the support values within a certain range, and avoiding abrupt changes, as shown in the lower chart in the figure. This concept is relatively simple, but current practice does not use the quality inspection workflow processes or the testing technologies needed to implement this approach.

## **Establishing a New Framework for Pavement Foundation Assessment**

The assessment of pavement foundation systems should include the verification of critical design values and require at least some minimum control of the foundation construction process to do the following:

- Ensure that appropriate pavement foundation materials are selected to meet the requirements for the projected traffic loading conditions and environmental factors affecting the engineering behaviors of these materials (e.g., volumetric stability)
- Provide good pavement foundation drainage, which is essential for good long-term performance because erosion of the subbase/subgrade introduces a defect for which virtually no cost-effective mitigation solution is available
- Construct and sustain (during the pavement's service life) uniform pavement support, which is critical for achieving good long-term pavement performance and requires detailed characterization and observation during construction
- Limit differential plastic deformation/settlement of the pavement foundation layers (subbase and subgrade) because plastic deformation is not explicitly considered in pavement thickness design

Based on the findings from this study, the authors' experience, and a review of the current state of the practice for design, a new framework and workflow for field process control and testing is provided in this report (Chapter 4) for different levels of quality standards. Key elements of the proposed framework include measuring the values of the pavement foundation's important mechanistic design parameters, establishing statistically valid sampling/inspection plans, and selecting appropriate improvement options (e.g., stabilization or better compaction) that will help the foundation meet the performance requirements for the project.

## **Organization of the Report**

The remaining chapters of this report are organized as follows:

- Chapter 2 provides an overview of the extensive field and laboratory testing program performed as a part of this project. Key findings are synthesized based on engineering parameters measured from all sites.
- Chapter 3 presents a brief history of the evolution of rigid pavement design; a discussion of the important geotechnical input parameters, including how those parameters were measured by different agencies when the design equations were developed; and an overview of the different in situ evaluation methods (direct and indirect). A quantitative approach to assessing the reliability of an empirical prediction method is also discussed in Chapter 3.

- Chapter 4 presents a review of the current state of the practice for the five participating states in terms of design and QC/QA, a discussion of the links between QC/QA and design, a review of some recently developed performance-based earthwork specifications, and a new framework for the mechanistic characterization of pavement foundations with a workflow to link design target values with QC/QA.
- Chapter 5 provides a summary of findings and recommendations from the extensive test program undertaken under this project.

The findings from this report should be of interest to researchers, practitioners, and agencies that deal with the design, construction, and maintenance of PCC pavements. This report is one of several project reports developed as part of the TPF-5(183) and FHWA DTFH 61-06-H-00011:WO18 studies.

## **CHAPTER 2: LESSONS LEARNED FROM FIELD STUDIES**

Extensive field and laboratory testing was conducted at 11 pavement foundation project sites including new, reconstruction, and rehabilitation projects in California, Iowa, Michigan, Pennsylvania, and Wisconsin. Of these, eight projects focused on the field evaluation of pavement foundation layer properties during reconstruction and three projects focused on linking the performance of the existing pavement and the observed distresses to the mechanistic properties of the foundation layers. Of the latter three projects, two focused on evaluating the pavement foundation following rehabilitation. In addition to these projects, five test sections across Iowa with varying ages and distress conditions were tested multiple times over a two-year period to evaluate seasonal variations in the support conditions of the pavement foundation layer.

The results from the field project sites were compiled in a large database of foundation layer properties and were used to draw comparisons between design input parameters and assessments of the effects of these properties on pavement performance. Detailed results and findings from each project site are documented in separately published project reports. The purpose of this chapter is to review the pavement designs that the different states used at the project sites in terms of the required foundation layer parameters and to summarize the key findings and observations from the test results.

### **Field Verification of the Mechanistic Design Parameters of the Foundation Layers**

#### *Design Parameters Used by Different State Agencies*

The design input parameters used for foundation layers vary among agencies depending on the choice of the pavement design method. A summary of these parameters for the five state agencies involved in this study is provided in Table 2.

**Table 2. Summary of foundation design input parameters currently in use by the participating state agencies**

State Agency	Pavement Design Method	Foundation Design Moduli Parameter(s)	Drainage Design Input Parameter(s)
California	Caltrans Highway Design Manual (Chapter 620)	California R-value and resilient modulus ( $M_r$ ) – Typical values for different material types provided in the manual	Specific drainage input parameters not defined
Iowa	PCA (1984)	Composite modulus of subgrade reaction ( $k_{\text{comp-PCA}}$ ) – Calculated based on modulus of subgrade reaction ( $k$ ) and aggregate layer thickness above subgrade	Specific drainage input parameters not defined
Michigan, Pennsylvania	AASHTO (1993)	Composite modulus of subgrade reaction ( $k_{\text{comp-AASHTO (1993)}}$ ) – Calculated using subgrade $M_r$ , elastic modulus of base/subbase layer ( $E_{\text{SB}}$ ) above subgrade, and thickness of base/subbase layer using a nomograph chart	Coefficient of drainage ( $C_d$ ) – Determined based on the time and degree of drainage desired and the anticipated duration the layer is expected to be in near-saturated condition
Wisconsin	AASHTO (1972)	Modulus of subgrade reaction ( $k$ ) and composite modulus of subgrade reaction ( $k_{\text{comp-AASHTO (1972)}}$ ) – Calculated using subgrade $M_r$ , elastic modulus of base/subbase layer ( $E_{\text{SB}}$ ) above subgrade, and thickness of base/subbase layer using a nomograph chart	Specific drainage input parameters not defined

The foundation support condition for rigid pavement design is characterized by the modulus of subgrade reaction ( $k$ ) value in the AASHTO (1972), AASHTO (1993), and Portland Cement Association (PCA) (1984) design methods. When an aggregate base layer is present over the subgrade, the  $k$  value is increased and is defined as the  $k_{\text{comp}}$  value, although the procedure to determine the  $k_{\text{comp}}$  value varies by design procedure. PCA (1984) provides a set of  $k_{\text{comp}}$  values as a function of the subgrade layer  $k$  value, the thickness of the base layer, and the type of the base layer (untreated versus cement-treated base). The AASHTO design procedures (AASHTO 1972, 1993) present nomographs to determine  $k_{\text{comp}}$  based on the subgrade layer resilient modulus ( $M_r$ ), the thickness of the base layer ( $H$ ), and the elastic modulus of the subbase/base layer ( $E_{\text{SB}}$ ) above the subgrade. The nomographs were developed based on elastic layer simulations of a flexible loading plate on different base and subgrade combinations.

The Caltrans *Highway Design Manual* (HDM) (2018) presents a design catalog that includes a set of thickness design tables developed based on past empirical design methods used by the agency and an early version of AASHTOWare Pavement ME Design (version 1). The design

catalog considers the traffic level, climate region, subgrade soil type, and lateral support as influencing factors, and pavement cross-section recommendations (for pavement and base layer thicknesses) are provided for different combinations of these factors. The Caltrans design guide refers to the use of the  $R$ -value and  $M_r$  for the subgrade and aggregate base layers to characterize the foundation layers.

The modern design method used in AASHTOWare Pavement ME Design uses the stress-dependent  $M_r$  value for foundation layer support, which is then converted into a dynamic  $k$  value internally in the design software. The procedure for this calculation is described in the second edition of the *Mechanistic-Empirical Pavement Design Guide* (MEPDG) (AASHTO 2015).

Another important foundation layer property that affects pavement performance is subsurface drainage, which, if not sufficient, can contribute to cracking and faulting distresses due to pumping, erosion, and concrete durability problems. Drainage is addressed in the AASHTO (1993) design procedure via an index parameter called the coefficient of drainage ( $C_d$ ). The  $C_d$  is selected based on the quality of drainage (i.e., the time required for the water to drain) and the percent of time the pavement structure is exposed to moisture levels approaching saturation. The time required for the water to drain is calculated based on the pavement geometry, type of drainage features (daylighted or subdrain), thickness of the base, and the saturated hydraulic conductivity of the material ( $K_{sat}$ ). The other design guides referenced in Table 2 do not reference a specific design input parameter for drainage but rather address drainage with the inclusion of appropriate drainage features within the system.

### *Field Testing and Interpretation Methods*

The  $k$ ,  $k_{comp}$ ,  $M_r$ , and  $E_{SB}$  values were measured in this study using a variety of commercially available equipment for in situ research and testing (Figure 5) and empirical estimations.





Falling weight deflectometer testing on open graded drainage course layer on I 94 project in Michigan (May 30, 2009)



Light weight deflectometer testing on granular subbase layer on I 35 project in Iowa (August 30, 2010)



304.8 mm diameter static plate load test setup on compacted subgrade on US 10 project in Wisconsin (May 25, 2010)



Air permeability testing on cement treated base layer on SR-22 project in Pennsylvania (September 17, 2009)



Dynamic cone penetrometer testing on open graded drainage course layer on I 94 project in Michigan (May 30, 2009)



Intelligent compaction roller mapping on subgrade layer on SR-22 project in Pennsylvania (September 20, 2009)

**Figure 5. Mechanistic-based in situ test methods used in this study**



The in situ test methods used in this study included (a) static plate load tests (PLTs) using a 304.8 mm (12 in.) diameter loading plate, (b) dynamic falling weight deflectometer (FWD) tests using a machine manufactured by Kuab with a 300 mm (11.8 in.) diameter loading plate, (c) dynamic LWD tests using a machine manufactured by Zorn with a 300 mm (11.8 in.) diameter loading plate, and (d) DCP tests. Details on the testing procedures, data interpretation methods, and calculations for each of the test methods are described in the separately published project reports. A summary of these procedures is provided below.

PLTs were conducted directly on the subgrade or aggregate base/subbase layers. The  $k$  values determined from the static PLT are referred to as  $k_{\text{PLT}}$  values. The  $k$  values referenced in the design procedures were determined using a static PLT with a 762 mm (30 in.) diameter loading plate. Therefore, the  $k_{\text{PLT}}$  values determined using a 304.8 mm (12 in.) diameter loading plate in this study were corrected for plate size using theoretical relationships suggested by Terzaghi and Peck (1967). The corrected  $k_{\text{PLT}}$  values are referred to herein as  $k_{\text{PLT}}^*$ .

FWD tests were conducted over the pavement surface layer to determine backcalculated  $k$  values. The backcalculated  $k$  values were determined using the AREA factor method described in AASHTO (1993) and were then corrected for finite slab size per Croveti (1994) and static loading conditions per AASHTO (1993). These corrected  $k$  values are reported herein as  $k_{\text{FWD-Static-Corr}}$ .

LWD tests were conducted to determine elastic modulus values based on peak deformation response and are referred to herein as  $E_{\text{LWD}}$  values. DCP tests were conducted to determine the penetration resistance profile and empirically calculate the California bearing ratio (CBR),  $M_r$ , and the  $k$  values of the foundation layers. Additionally, measurements based on IC index values, including compaction meter value (CMV), were obtained at select project sites to assess on-site correlations with in situ point test measurements, such as those obtained using LWD and DCP tests, and to characterize the spatial nonuniformity of the support conditions.

The  $k$  values determined from these different testing and interpretation procedures are compared in the following sections, and the notations for the different procedures are as follows:

- $k_{\text{PLT}}^*$  – determined from the static PLT (and corrected for plate size). No moisture correction for post-construction moisture changes was applied to the PLT results.
- $k_{\text{FWD-Static-Corr}}$  – determined from the FWD test and corrected for slab size and static conditions.
- $k_{\text{AASHTO(1993)}}$  – determined using subgrade  $M_r$  values from DCP-CBR testing and thawed CBR values from laboratory testing using the charts provided in AASHTO (1993) and dividing the  $M_r$  value by 19.4 per AASHTO (1993) to calculate  $k$  in units of psi for  $M_r$  in units of psi.  $M_r$  values determined from laboratory testing on an undisturbed sample extracted from the field were also used for calculations.

- $k_{PCA(1984)}$  – determined from CBR values using charts provided in PCA (1984).
- $k_{comp-AASHTO(1972)}$  – determined per AASHTO (1972) using subgrade  $M_r$  and subbase layer modulus ( $E_{SB}$ ) values from DCP-CBR testing and the thickness of the base/subbase layers ( $H_{SB}$ ) as interpreted from DCP profiles.
- $k_{comp-AASHTO(1993)}$  – determined per AASHTO (1993) using subgrade  $M_r$  and  $E_{SB}$  values from DCP-CBR testing and the thickness of the base/subbase layers ( $H_{SB}$ ) as interpreted from DCP profiles.  $M_r$  values determined from laboratory testing on an undisturbed sample extracted from the field were also used for calculations.
- $k_{comp-ACPA(2012)}$  – determined using subgrade  $M_r$  and  $E_{SB}$  values from DCP-CBR testing per AASHTO (1993) and  $H_{SB}$  values from DCP profiles. These values were used as inputs in the ACPA (2012) online estimator.

The geotechnical parameter for assessing the drainage capacity of a base/subbase layer is the  $K_{sat}$  value. During field testing, the rapid air permeability test (APT) device was used to directly measure the in situ  $K_{sat}$  values. Due to the ability of the APT device to perform the test in a few seconds, the tests were performed at multiple test locations over a relatively small area to assess the influence of the segregation of aggregate particles and fines near the surface. A photograph of the APT is provided in Figure 5. The  $K_{sat}$  calculation procedures are provided in detail in White et al. (2013) as well as in the separately published project reports. AASHTO (1993) details a procedure that uses  $K_{sat}$  values and pavement geometry to calculate the time for a desired degree of drainage, which is then related to the  $C_d$  value. The time for drainage was calculated using the Excel-based software tool Pavement Drainage Estimator (PDE) developed at Iowa State University (Vennapusa 2004).

### *Field Testing Results and Comparisons with Design Input Values*

In this section, the foundation layer modulus values determined from field testing conducted at two field projects are presented and compared with the modulus values assumed during design for the respective projects.

The first project was completed in Wisconsin and involved the new construction of US Highway 10 in Portage County. The design included a 254 mm (10 in.) thick jointed PCC pavement to be supported over a 152 mm (6 in.) thick dense aggregate base over 610 mm (24 in.) of Grade 1 select borrow granular fill and compacted subgrade. The rigid pavement design was performed using the AASHTO (1972) procedure. A modulus of subgrade reaction of  $k = 41$  kPa/mm (150 pci) was used in the design. Selection of this  $k$  value was based on a database of the relationships between subgrade soil type and  $k$  value. A  $k_{comp}$  value accounting for the base/subbase layers was not used for this project.

Static PLTs were conducted on the compacted subgrade at 27 locations along a 65 m (213 ft) stretch of the roadway. The  $k_{PLT^*}$  values are presented in Figure 6.

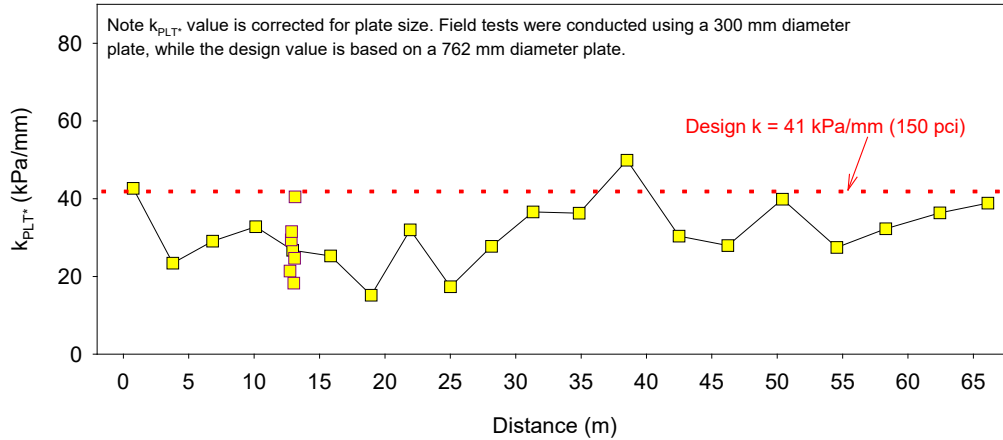


**Figure 6. In situ PLT results near Sta. 495+00 – Wisconsin US 10 construction project**

The results showed that only 2 out of the 27 test locations met the minimum design  $k$  value of 41 kPa/mm (150 pci). The average  $k_{PLT*}$  was about 30.5 kPa/mm (112 pci), which is about 26% lower than the design  $k$  value.

FWD tests were also conducted for this project on a section of the finished pavement layer near the subgrade test section. The  $k_{FWD-Static-Corr}$  values are presented in Figure 7.

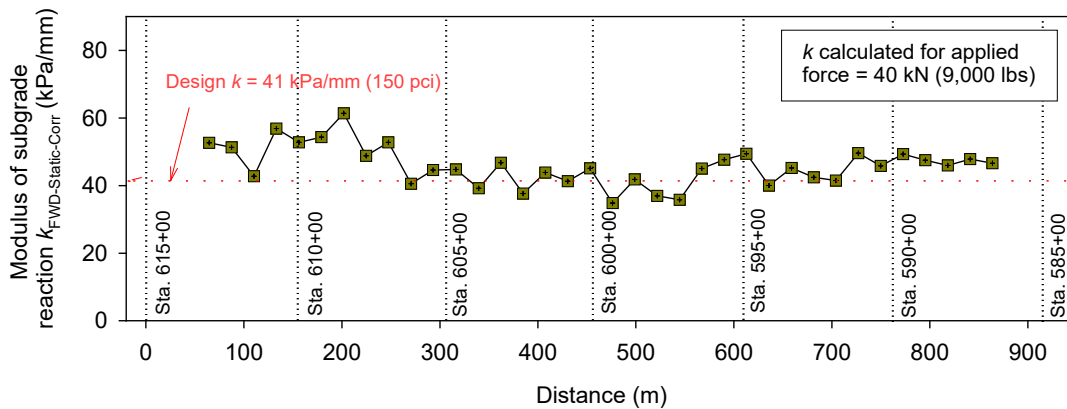


**Figure 7. In situ  $k$  values from FWD testing – Wisconsin US 10 construction project**

The results showed that the  $k_{FWD-Static-Corr}$  values were higher than the  $k_{PLT*}$  values, which is expected because the foundation beneath the pavement consists of about 762 mm (30 in.) of base/subbase above the compacted subgrade layer. The  $k_{FWD-Static-Corr}$  values for 6 out of 36 measurements did not meet the minimum design  $k$  value of 41 kPa/mm (150 pci).

The average  $k$  and  $k_{comp}$  values estimated using the different procedures (FWD, PLT, and DCP-CBR) are plotted in Figure 8.

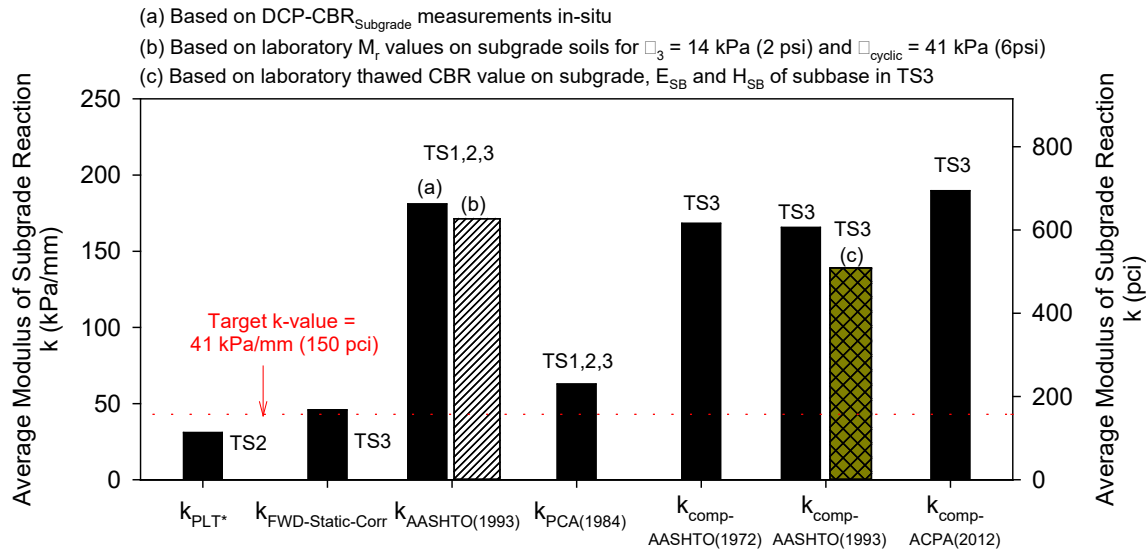


**Figure 8. Which is the correct  $k$  value? Date compares the design target  $k$  value with measured and estimated  $k$  values from various field and laboratory measurements – Wisconsin US 10 construction project**

The comparison shows that the  $k_{comp}$  values estimated from the empirical relationships and nomographs produced values that are about three to five times higher than the design  $k$  value and higher than the  $k$  values measured using PLT and FWD testing. This finding indicates that the  $k$  value determined from testing significantly depends on the test method and procedure followed. The  $k$  values determined from FWD testing and PLT are somewhat direct measurements, although some empirical corrections are needed. On the other hand, other methods (e.g., laboratory tests and in situ DCP tests) are indirect and rely solely on empirical relationships to determine the  $k$  and  $k_{comp}$  values. This difference in  $k$  values from somewhat direct versus indirect measurements is significant and calls into question the various methods listed in AASHTOWare Pavement ME Design that are solely based on empirical relationships between laboratory tests (e.g., soil classification and CBR) and in situ DCP tests.

The second project was completed in Michigan and involved reconstruction of I-96 in Clinton and Eaton Counties. The design included a 292 mm (11.5 in.) thick jointed PCC pavement to be supported over a 127 mm (5 in.) thick cement-treated base (CTB) layer with RPCC material and 279 mm (11 in.) of sand subbase over the existing subgrade. A geotextile separator was installed at the CTB/sand subbase interface. The rigid pavement design was performed using the AASHTO (1993) procedure. The pavement foundation input parameters included a  $k_{comp}$  value of 135 kPa/mm (500 pci) and a  $C_d$  value of 1.05, representing “good” drainage. The Michigan DOT estimated the target  $k_{comp}$  value using an empirical procedure described in AASHTO (1993) based on a target  $E_{SB}$  value of 413.7 MPa (60 ksi) for the CTB/sand subbase layer, a combined base/subbase layer thickness of 406 mm (16 in.), and a subgrade resilient modulus ( $M_r$ ) of 20.7 MPa (3 ksi).

FWD measurements on the CTB surface were used to backcalculate  $E_{SB}$  values representing the modulus of the top 406.4 mm (16 in.) of the base/subbase layer and the underlying subgrade  $M_r$  values. The results are presented in Figure 9 and Figure 10, respectively.

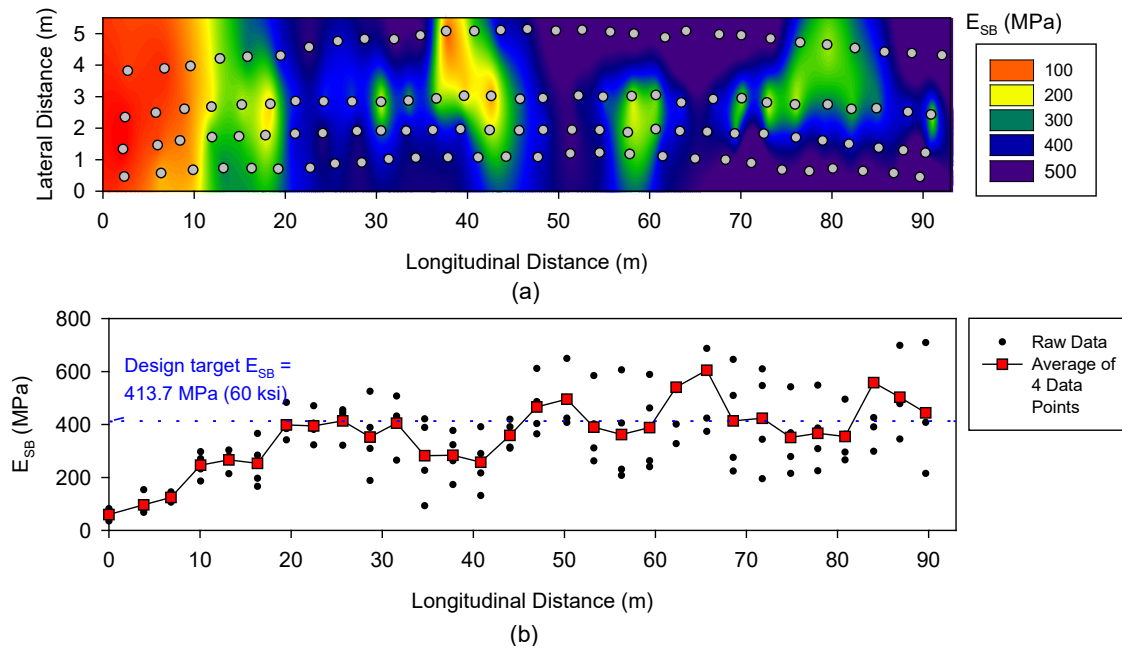


**Figure 9. Backcalculated  $E_{SB}$  values for the CTB/sand subbase layer from FWD tests over a 5.5 m wide x 92 m long area: (a) spatial contour map and (b) measurements longitudinally along the roadway – Michigan I-96 reconstruction project**

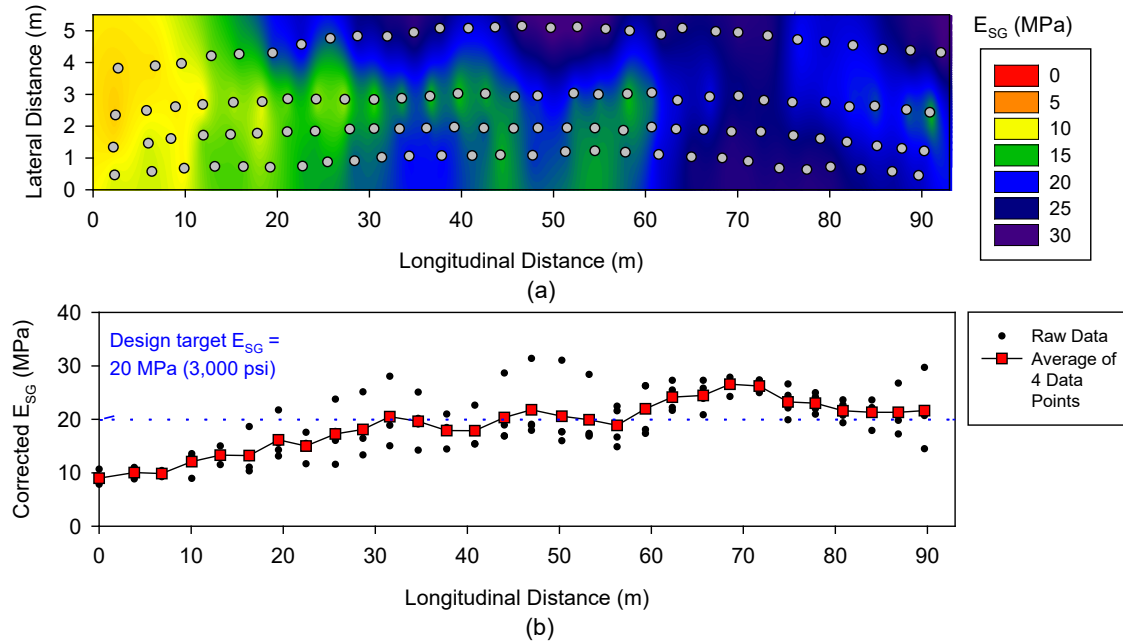


**Figure 10. Backcalculated subgrade modulus ( $E_{SG}$ ) values beneath the base/subbase layer from FWD tests over a 5.5 m wide x 92 m long area: (a) kriged spatial contour map and (b) measurements longitudinally along the roadway – Michigan I-96 reconstruction project**

The average  $E_{SB}$  was about 362 MPa (52 ksi), which was on average about 13% lower than the design  $E_{SB}$  with a coefficient of variation of about 50%. Of the 119 measurements from this section, 81 measurements were lower than the design  $E_{SB}$ . The in situ subgrade modulus values were backcalculated from FWD measurements and were multiplied by a correction factor of 0.33 per AASHTO (1993). The average corrected  $E_{SG}$  was about 18.9 MPa (2.7 ksi), which was slightly lower than the design  $M_r$ . Comparison of the color-coded spatial modulus value plots in Figure 9 and Figure 10 indicates that lower  $E_{SB}$  values between the 0 to 10 m mark are a reflection of lower  $E_{SG}$  values in the underlying layer.

The in situ measured values are compared with the design input parameter values for the foundation layers in **Error! Not a valid bookmark self-reference..**

**Table 3. Summary of design, in situ-measured, and laboratory-measured values – Michigan I-96 reconstruction project**

<b>Design Parameter</b>	<b>Design Value</b>	<b>In Situ Measurement (Average)</b>
Subgrade $M_r$	20.7 MPa (3.0 ksi)	Backcalculated corrected $E_{SG}$ from FWD measurements: 18.9 MPa (2.7 ksi)
Subbase elastic modulus ( $E_{SB}$ )	413.7 MPa (60 ksi)	Backcalculated $E_{SB}$ from FWD measurements: 361.5 MPa (52.4 ksi)
Composite modulus of subgrade reaction ( $k_{comp}$ )	135 kPa/mm (500 pci)	Using $E_{SB}$ and $E_{SG}$ from FWD and AASHTO (1993) nomographs: 100.9 kPa/mm (370pci)
Coefficient of drainage ( $C_d$ )	1.05 (Good)	“Excellent” for the full range of $K_{sat}$ measurements in situ on CTB layer

The in situ  $k_{comp}$  values were calculated based on FWD measurements ( $E_{SB}$  and corrected  $E_{SG}$ ) and the AASHTO (1993) nomograph procedure, which resulted in an average of about 101 kPa/mm (370 pci). This value was about 26% lower than the design  $k_{comp}$  value. In situ air permeability test results showed relatively high  $K_{sat}$  values, with the quality of drainage rated as “excellent” according to AASHTO (1993).

### **Spatial Nonuniformity of the Mechanistic Properties of the Foundation Layer**

According to the ACPA’s state-of-the-practice guidelines for the construction of foundation layers under PCC pavements, “[a]ny time a nonuniform support condition is created for a concrete pavement structure, the risk of premature failure is increased. Due to the high level of strength provided by concrete pavements, uniformity trumps strength for subgrades and subbases.” Further, “[b]ecause the concrete pavement provides high strength and load distribution characteristics at the surface, it does not necessarily require a strong foundation, but it is more important that the foundation provide uniform support conditions” (ACPA 2008). However, the extent to which nonuniformity in support conditions affects pavement performance is not well quantified. Measurement of nonuniformity was emphasized during this testing program.

All rigid pavement design guides, including AASHTOWare Pavement ME Design (AASHTO 2015), require a single modulus value for each of the foundation layers and do not address how to quantify and account for the nonuniform support conditions that exist in situ from a geospatial perspective. In this study, significant efforts were made at the field project sites to quantify the variability of the different foundation layer engineering properties using point tests and IC measurement values. Finite element models were developed and analyzed to assess the sensitivity of the design input values and nonuniform support conditions on mechanistically

predicted pavement performance characteristics. The subsections below highlight important and revealing findings that resulted from linking the field testing results with pavement stress-deflection behavior using finite element analysis.

### *Field Testing Results*

As part of the field testing conducted at multiple project sites, variability in the in situ engineering properties of the foundation layer materials was assessed through testing conducted over very small to large areas to characterize both short- and long-range nonuniformity for a given project.

One example of testing performed over a short area is from the US 30 highway construction project near Ames, Iowa, where testing was performed on the RPCC-modified subbase material (classified as A-1-a, GP). LWD tests were conducted at 32 test locations across the full pavement width on the subbase layer after the final compaction and trimming operations and just before paving. The results showed that  $E_{LWD}$  values varied between 19 MPa (2,756 psi) and 95 MPa (13,778 psi), with an average of about 56 MPa (8,122 psi) and a COV of 32% (Figure 11).

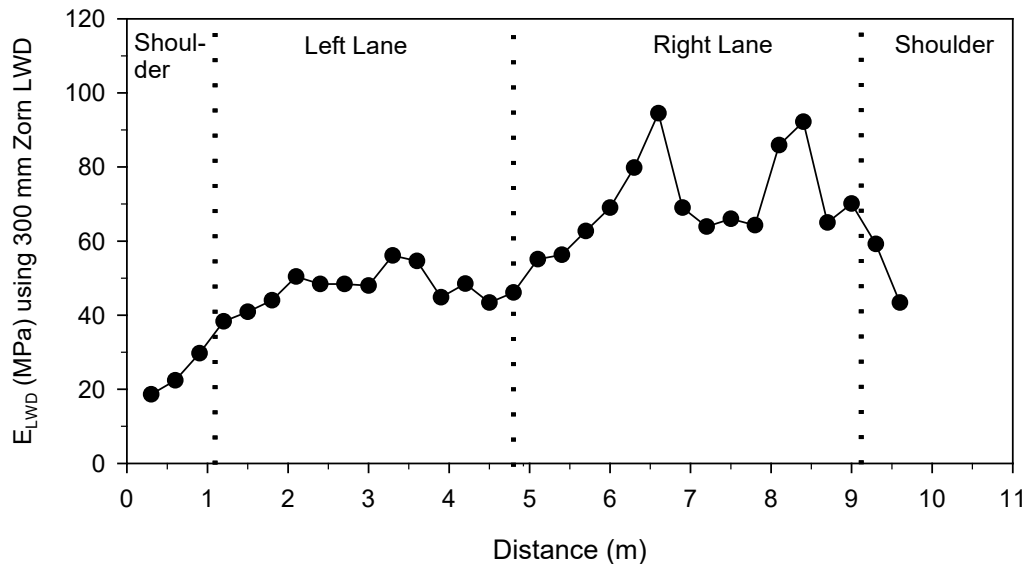


**Figure 11.  $E_{LWD}$  measurements across the pavement width near Sta. 1394+60 – Iowa US 30 construction project**

The  $E_{LWD}$  values in the right lane were comparatively higher than those in the left lane. Lower  $E_{LWD}$  values were found in areas with visually segregated larger particle sizes, as shown in a series of pictures taken across the pavement width (see Figure 12).



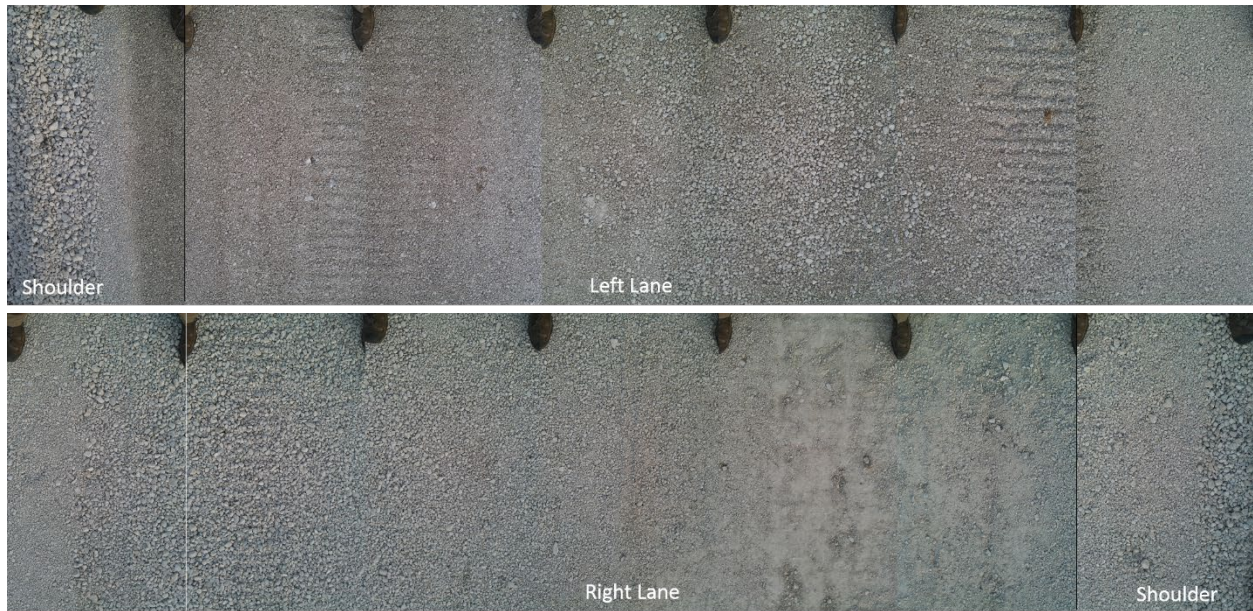


**Figure 12. Surface of the RPCC-modified subbase layer across the width of the pavement foundation layer near Sta. 1394+60 – Iowa US 30 construction project (photographs taken on August 8, 2011)**

A summary of univariate statistics showing the number of measurements, the statistical mean, and the COV of the  $E_{LWD}$ , DCP-CBR, dry unit weight ( $\gamma_d$ ), moisture content, and  $K_{sat}$  values obtained from multiple field projects are presented in Table 4.

**Table 4. Summary of mean and COV values of foundation layer properties from multiple sites**

Project	Layer	E <sub>LWD</sub>			DCP-CBR			$\gamma_d$			w			K <sub>sat</sub>		
		N	Mean (MPa)	COV (%)	N	Mean (%)	COV (%)	N	Mean (kN/m <sup>3</sup> )	COV (%)	N	Mean (%)	COV (%)	N	Mean (cm/s)	COV (%)
MI I-94	Steel slag base (A-1-a, GP)	121	58.5	12%	121	35.8	21%	121	20.01	3%	121	3.3	20%	119	3.4	119%
	Subgrade (A-4, ML)	—	—	—	121	3.8	53%	—	—	—	—	—	—	—	—	—
MI I-96	Sand subbase (A-1-b, SP-SM)	99	31.5	35%	79	12.2	34%	99	20.16	3%	99	7.4	15%	72	0.17	59%
	CTB with RPCC material (A-1-a, GP)	119	214.8	39%	—	—	—	118	14.56	6%	118	7.4	14%	62	2.5	76%
WI US10	Sand subbase (A-3, SP)	17	12.6	25%	17	5.6	22%	17	16.15	2%	17	3.7	13%	—	—	—
	Subgrade (A-7-6 (14), CL)	80	30.7	17%	79	15.4	32%	79	19.84	2%	79	7.5	13%	—	—	—
IA US 30	RPCC-modified subbase (A-1-a, GP-GM)	40	56.6	19%	20	67	27%	—	—	—	—	—	—	—	—	—
	Subgrade (A-6 (2), SC)	—	—	—	20	12.9	31%	—	—	—	—	—	—	—	—	—
PA SR-22	Subbase (A-1-a, GP-GM)	81	82.9	31%	—	—	—	44	21.44	2%	44	6.4	23%	28	0.92	86%
	Asphalt-treated base with crushed limestone (A-1-a, GP)	48	190.7	21%	—	—	—	—	—	—	—	—	—	99	4.6	42%
	CTB with crushed limestone (A-1-a, GP)	41	153.3	28%	—	—	—	42	17.01	6%	42	5.5	21%	49	7	45%
														23	0.2	101%
	Subgrade (A-6 (6), CL)	21	18.1	65%	—	—	—	21	17.53	3%	21	16.6	14%	—	—	—

The results demonstrate that of the engineering parameters measured,  $K_{sat}$  is the most variable, with COV values ranging between 42% and 119%, followed by the modulus/shear strength parameters ( $E_{LWD}$  and DCP-CBR), with COV values ranging between 12% and 65%; moisture content, with COV values ranging between 13% and 20%; and  $\gamma_d$ , with COV values of 6% or lower. These measurements are based on tests conducted over short (within about a 10 m x 10 m [32.8 ft x 32.8 ft] area) and long ranges (several 100s of meters) at a given project site. Interestingly, the parameter with the lowest COV, dry unit weight, is the single most widely chosen field test for quality acceptance testing of the placed pavement foundation materials.

The COV values presented in Table 4 provide a quantitative univariate measure of nonuniformity, but they do not address variability from a spatial perspective. Vennapusa et al. (2010) demonstrated the use of semivariogram analysis in combination with conventional statistical analysis to evaluate nonuniformity in QC/QA during earthwork construction. A semivariogram is a plot of the average squared differences among data values as a function of separation distance and is a common tool used in geostatistical studies to describe spatial variation. A typical semivariogram plot is presented in Figure 13.

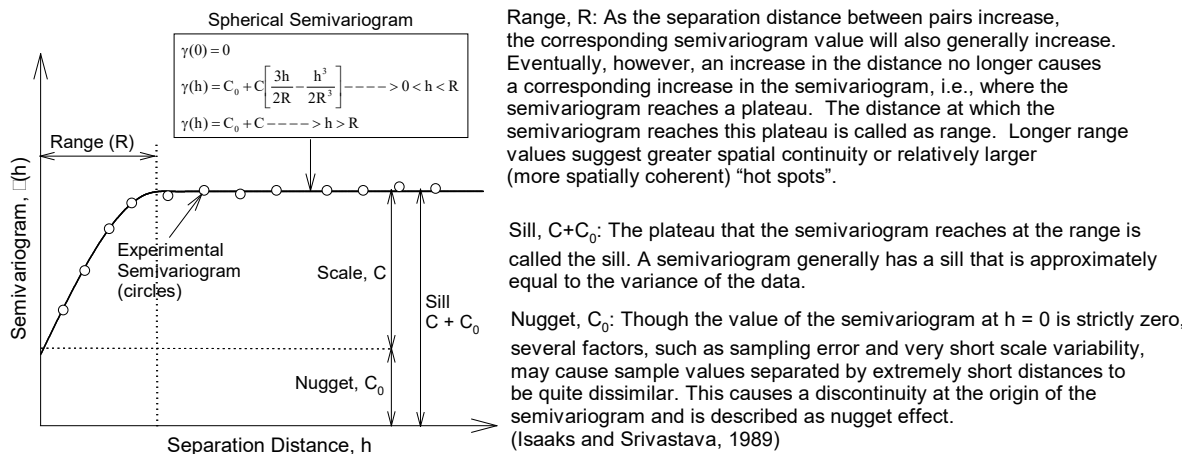


**Figure 13. Description of a typical experimental and spherical semivariogram and its parameters**

A semivariogram  $\gamma(h)$  is defined as one-half of the average squared differences among data values that are separated by a distance of  $h$  (Isaaks and Srivastava 1989). If this calculation is repeated for many different values of  $h$  (as the sample data support), the result can be graphically presented as an experimental semivariogram, shown by the circles in Figure 13. To obtain an algebraic expression for the relationship between separation distance and an experimental semivariogram, a theoretical model is fit to the data. Three parameters are used to construct a theoretical semivariogram: sill ( $C + C_0$ ), range ( $R$ ), and nugget ( $C_0$ ). These parameters are briefly described in Figure 13. In a theoretical semivariogram model, a low sill and long range of influence represent the best conditions for uniformity, while the opposite represents an increasingly nonuniform condition.

At several field project sites in this study, a detailed testing program was set up such that tests were conducted in a dense grid pattern over a small area and over a large area. One example of such testing was on the Michigan I-94 construction project, where dense grid testing was conducted by spacing each testing location about 0.6 m (2 ft) to 1.5 m (5 ft) apart (Figure 14) and long-range testing was conducted every 50 m (164 ft) over a 1,000 m (3,280 ft) area along the roadway alignment.



**Figure 14. Field testing in a dense grid pattern on an open-graded drainage course granular base layer consisting of recycled steel slag (classified as GP and A-1-a) – Michigan I-94 construction project (photograph taken on May 28, 2009)**

Testing was conducted on a final compacted aggregate base layer consisting of steel slag recycled material (classified as A-1-a, GP) with a nominal thickness of 0.41 m (16 in.). Semivariogram analysis was performed to analyze the point test data. The main goal of the semivariogram modeling was to understand the nature of the variability of the different measurements and to assess whether the current randomly selected QC/QA samples are adequate to provide a statistically valid data set on a given project. All test results from the Michigan I-94 project and a detailed analysis of the results are documented in White et al. (2016a).

A sample of the results showing the spatial variability of the  $\gamma_d$  and  $E_{LWD}$  values over an area of about 49 m<sup>2</sup> (527 ft<sup>2</sup>) is presented in Figure 15.

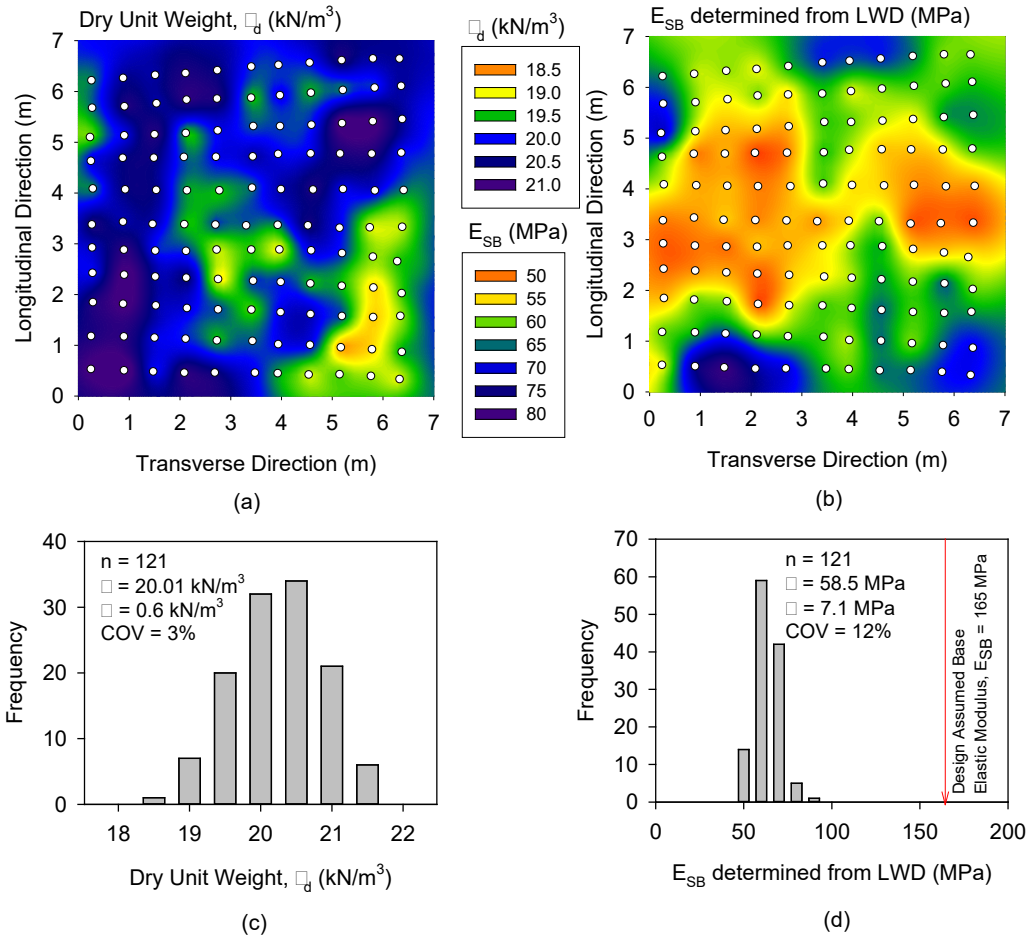


**Figure 15. Spatial contour maps of (a)  $\gamma_d$  and (b)  $E_{SB}$  values and histogram plots of (c)  $\gamma_d$  and (d)  $E_{SB}$  values based on LWD measurements on a compacted open-graded drainage course granular base layer – Michigan I-94 construction project**

Measurements obtained from the spatial grid were analyzed for patterns in different directions relative to the alignment of the roadway to check for anisotropy using geostatistical semivariogram modeling. The details of the analysis are provided in Li et al. (2018). In summary, the analysis on the dense-gridded test section showed that the transverse direction is more uniform than the longitudinal direction, as shown in Figure 16 (although results from other sites showed the opposite trend).

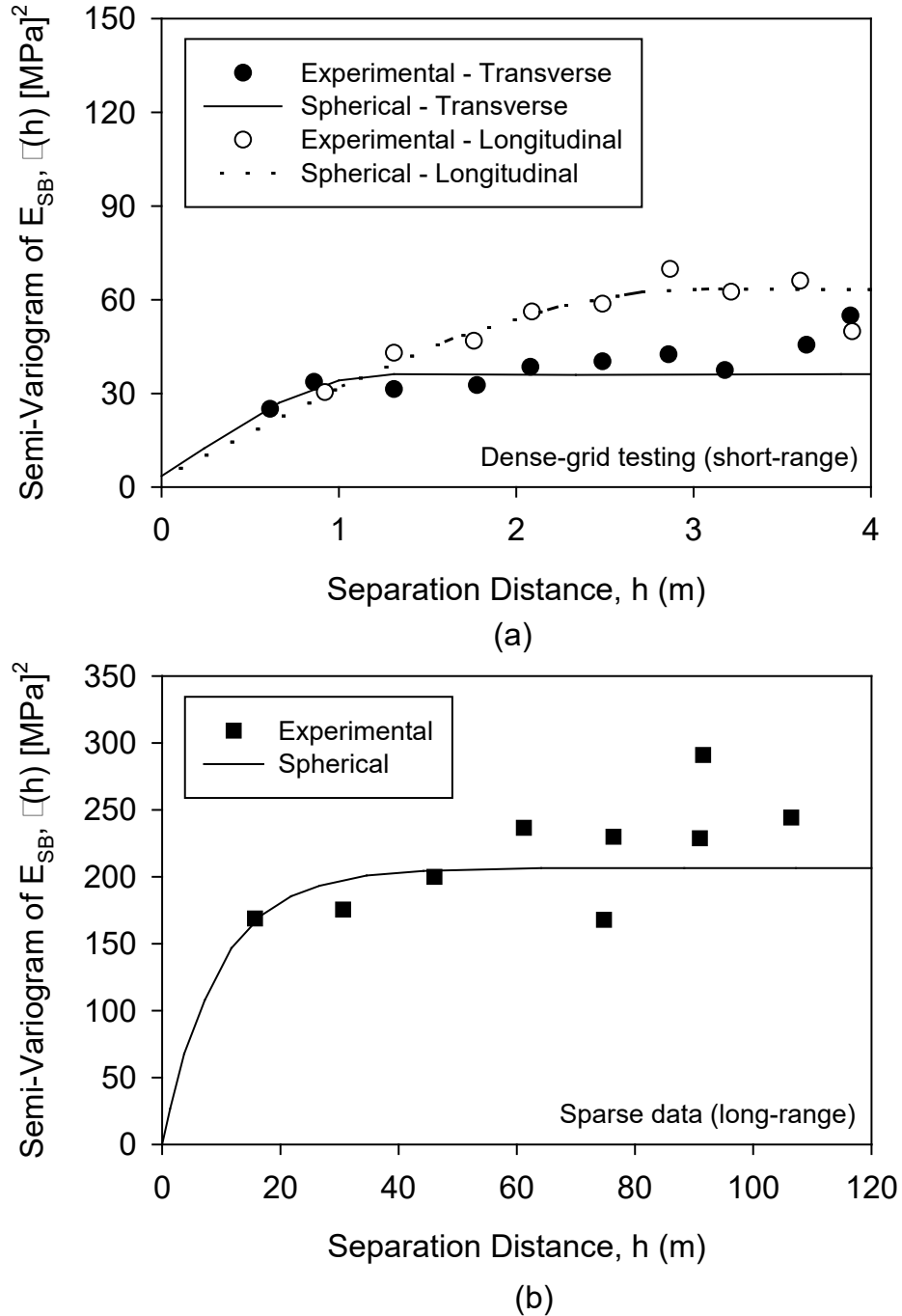


**Figure 16. Semivariograms of  $E_{SB}$  measurements from LWD testing: (a) from testing in a dense grid over a small area and (b) from sparse testing over a large area – Michigan I-94 construction project**

The results further showed that the semivariogram correlation lengths (which provide a measure of the spatial continuity in the data, with longer lengths representing more uniformity) were in the range of 2 to 3 m (6.6 to 9.8 ft) in the dense-gridded section. Semivariogram models for the measurements obtained over the larger test sections (Figure 16b) yielded larger correlation

lengths (27 to 38 m [89 to 125 ft]) than those found in the dense-gridded sections, suggesting that there is a nested structure in the data with both short- and long-range spatial continuities.

To obtain a statistically valid sample, there should be at least three to five measurements spaced at distances less than the correlation lengths determined from the semivariogram modeling. Based on the observed correlation lengths from this project (2 to 3 m [6.6 to 9.8 ft] for short-range variability and 27 to 38 m [89 to 125 ft] for long-range variability), it would be impractical to rely upon point testing methods to obtain statistically valid data sets for QC/QA. This indicates the need for continuous measurement systems such as IC or other near-continuous measurement technologies.

IC measurements were obtained at three project sites (Pennsylvania SR-22, Michigan I-94, and Iowa I-29) using Caterpillar and Volvo IC machines. IC operations involved mapping foundation layers that had been compacted using vibratory compaction with a smooth drum roller. The index parameters reported from the IC machines were obtained and compared with in situ point test measurements for the I-29 reconstruction project in Iowa. A more detailed discussion of the calibration/regression analyses with different in situ point measurements and the advantages and limitations of the different IC index value parameters is discussed elsewhere (e.g., Mooney et al. 2010, White et al. 2011). The IC measurement values are generally more strongly correlated to stiffness/modulus-based measurements ( $E_{LWD}$ ,  $E_{FWD}$ ,  $k_{PLT}$ , etc.) than shear strength measurements (e.g., CBR) and correlate poorly with volume-weight parameters such as dry unit weight or relative compaction.

Maps of the IC measurement values obtained on the special backfill subgrade treatment and the overlaid RPCC subbase layers from the I-29 project are shown in Figure 17.



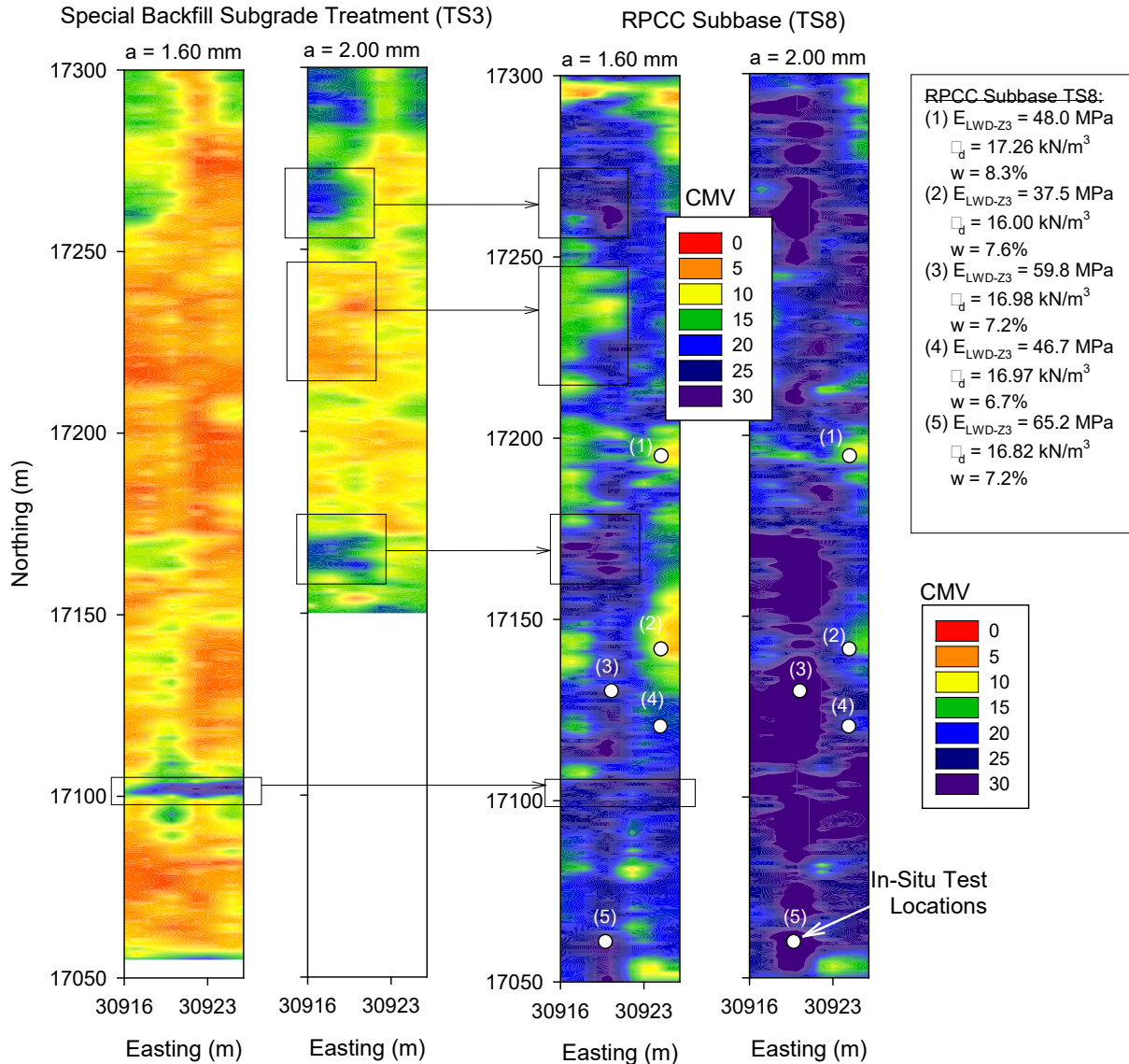


**Figure 17. IC measurement values obtained at different amplitude (a) settings on a special backfill subgrade treatment layer placed over the subgrade and on the overlaid RPCC subbase layer in the same area – Iowa I-29 reconstruction project**

The results show that “hard” and “soft” zones in the subgrade layer maps are reflected in the overlying RPCC subbase layer maps. This finding emphasizes that the level of nonuniform support in the subbase/base layers is strongly dependent on the uniformity of support in the underlying layers. When the underlying layer is “soft,” the overlying layer does not compact as well as when the underlying layer is “firm.”

#### *Influence of Foundation Input Properties on Design and Performance Predictions*

The foundation support  $k$  values obtained from the different field project sites tested in this study using PLT and FWD tests varied between 13.6 kPa/mm (50 pci) and 135.7 kPa/mm (500 pci). To



understand the sensitivity of the  $k$  input value on the principal stresses generated in the surface layer, two-dimensional (2D) finite element analysis was conducted using KENSLABS pavement analysis software. The analysis was set up with no temperature gradient on two jointed slabs with varying load transfer efficiency (LTE) values (greater than 85%, 25% to 40%, and 0% [no dowels]), for a standard 80 kN (18 kip) single-axle loading at the jointed corner. PCC layer thicknesses of 203 mm (8 in.), 254 mm (10 in.), and 305 mm (12 in.) were evaluated. The stress ratio (SR) values were calculated for each case as the ratio of the maximum principal stress in the pavement layer and the modulus of rupture of the concrete (assumed to be 4,550 kPa [660 psi]). Based on the SR values, the number of load repetitions for fatigue failure ( $N$ ) was calculated using the PCA (1984) fatigue model. For reference, an SR value of less than 0.45 results in a value of  $N$  that is greater than 100,000,000 cycles (“unlimited”).

The SR results from the 2D finite element analyses are presented in Figure 18, which shows that LTE and thickness have the largest influence on the SR values and that changing the  $k$  value from 13.6 kPa/mm (50 pci) to 135.7 kPa/mm (500 pci) has a minimal effect on the SR values.

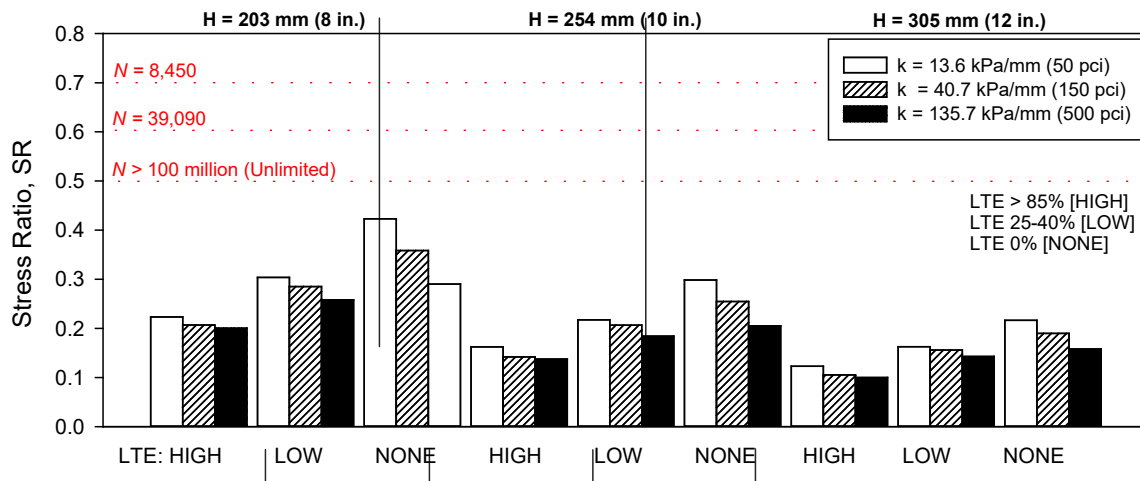


**Figure 18. Stress ratio values for different pavement joint LTE cases, foundation support  $k$  values, and pavement thicknesses for a standard 80 kN (18 kip) AASHTO single-axle dual-wheel loading near a corner**

Several studies have been conducted using AASHTOWare Pavement ME Design software to study the sensitivity of different input parameters on thickness design. Table 5 summarizes the findings from a study by Darter et al. (2014), which qualitatively compared the sensitivity of the different input parameters on the performance indicators predicted using AASHTOWare Pavement ME Design.

**Table 5. Sensitivity of AASHTOWare Pavement ME Design input variables on predicted performance indicators – jointed rigid pavement**

<b>Input Variable</b>	<b>Faulting</b>	<b>Transverse Cracking</b>	<b>IRI</b>
PCC thickness	M	L	M
PCC modulus of rupture and elasticity	N	L	S
PCC coefficient of thermal expansion	L	L	L
Joint spacing	M	L	M
Lane to PCC shoulder long-term LTE	L	N	L
Edge support	M	L	M
Permanent curl/warp	L	L	L
Base type and modulus	L	L	S
Climate	L	L	L
Subgrade type/modulus	S	M	S
Truck axle load distribution	S	L	S
Truck volume	L	L	L
Tire pressure	N	S	N
Truck lateral offset	M	L	M
Truck wander	N	M	N
Initial IRI	N	N	L

L – Large effect on predicted distress/smoothness

M – Moderate effect on predicted distress/smoothness

S – Small effect on predicted distress/smoothness

N – Little to No effect on predicted distress/smoothness

Source: Modified from Darter et al. 2014

The level of effect (i.e., large, moderate, small, and no effect) of each input parameter on the different performance indicators are shown in Table 5. The input variables related to the foundation layer are highlighted in gray. Depending on the distress type, the base and subgrade layer material type and modulus have a small to large effect on the predicted distresses.

A detailed parametric sensitivity analysis was conducted as part of the present study (see Brand and Roesler 2014) to quantitatively assess the different input parameters on the thickness design of the PCC layer. The parameters considered were traffic level (5 million to 100 million equivalent single-axle loads [ESALs]), base material type (granular or stabilized), climatic conditions (Des Moines, Iowa, or Atlanta, Georgia), subgrade soil type (A-1-a, A-3, or A-7-6) and  $M_r$  (27.5 to 124 MPa [4 to 18 ksi]), and joint spacing (3.7 m [12 ft] or 4.6 m [15 ft]).

The results of the sensitivity analysis showed that traffic level and joint spacing had the most impact, with a maximum change of 95 mm (3.75 in.) and 76 mm (3.0 in.), respectively, in slab design thickness. The effect of climate was not as critical, requiring only a 12.7 mm (0.5 in.) change in slab thickness between Des Moines, Iowa, and Atlanta, Georgia. The subgrade soil type or  $M_r$  of the subgrade showed minimal impact on the thickness design (less than 6.3 mm [0.25 in.]). AASHTOWare Pavement ME Design does not allow the user to account for the nonuniformity of support conditions. Other researchers using AASHTOWare Pavement ME Design have similarly reported that varying the  $M_r$  values and does not have a significant effect

on the thickness design (Velasquez et al. 2009, Khanum 2005, Kannekanti and Harvey 2005, Haider et al. 2009, Hoerner et al. 2007).

### *Impact of Nonuniform Support Conditions on Mechanistic Pavement Responses*

As part of an Iowa DOT-sponsored field study, White et al. (2005) documented the effects of nonuniform subgrade support on critical pavement responses. With in situ-measured subgrade stiffness values obtained in a spatial grid pattern used as spring supports, pavement responses were analyzed using ISLAB2000, a two-dimensional finite element program. The analysis showed that the maximum principal stresses and deflections were reduced in pavements with uniform subgrade support, thereby increasing slab fatigue life. Nonuniform support conditions resulted in a decrease in the predicted fatigue life of the pavement compared to the assumed uniform support. This study demonstrated the connection between subgrade nonuniformity and the potential for reduced fatigue life in the pavement layer.

A more detailed 2D and 3D finite element analysis was conducted as part of the present study to further evaluate the impacts of nonuniform support conditions on the tensile stresses developed in the pavement. The results from the detailed analyses are documented in Brand et al. (2014). In summary, multiple loading and support conditions were analyzed, along with temperature differentials in the pavement layer. The  $k$  values in the analysis varied from 8.4 to 54.8 kPa/mm (31 to 202 pci) based on the results obtained from the field testing sites, and each was compared with an average  $k$  value of 17 kPa/mm (63 pci).

No significant differences were found between the peak tensile stresses calculated for the uniform and nonuniform cases. The field data were then statistically reassigned by normal and beta distributions to predefined area sizes, which demonstrated that a normal distribution increased the probability of having low  $k$  values along the pavement edge, thereby raising the probability of higher peak tensile stresses. Overall, the results showed that certain nonuniform support conditions under concrete slabs can produce much higher tensile stresses than a uniform support condition, particularly when considering different loading positions and curling conditions, soft support along the pavement edge, and preexisting cracks (Brand et al. 2014). This study is further confirmation that nonuniformity is an important parameter and its impact on pavement stress is complex. Building pavement foundations with uniform support, to the extent possible, should improve long-term performance.

### *Impacts of Loss of Support on Mechanistic Pavement Responses*

Beyond the inherent nonuniform support conditions that exist with variable  $k$  values, nonuniform support can develop beneath the pavement layers due to LOS. Darter et al. (1995) defined LOS as “any gap or void that may occur between the base and the slab, or between a stabilized base and the subgrade, causing increased deflection of the slab surface.” The authors identified three main causes of LOS: (1) erosion of base/subgrade, (2) settlement or consolidation (or irrecoverable differential permanent deformations) of the foundation layers, and (3) temperature curling/moisture warping of the slab.

The curling/warping issue is typically addressed in design through reduced joint spacing. Significant research efforts have been undertaken to study the erosion potential of pavement foundation materials and to model its effects on pavement performance (e.g., Wijk 1985, Rauhut et al. 1982, Markow and Brademeyer 1984, Larralde 1984, Jeong and Zollinger 2001, Jung et al. 2010). However, the impacts of irrecoverable permanent deformation caused by repeated loading have not been well studied or addressed in design. Irrecoverable deformation was considered herein through in situ testing and modeling.

The AASHTO (1986) rigid pavement design procedure addresses LOS by defining the void as a percentage of area relative to the slab size and using an LOS factor to reduce the value of the design modulus of subgrade reaction ( $k$ ). Since direct measurement of void size has not been incorporated into pavement foundation verification or stabilization design practices, AASHTO (1993) and AASHTOWare Pavement ME Design provide suggested LOS and erosion index factors based only on material types. When LOS develops beneath a rigid pavement slab, the result is localized stress concentration within the pavement layer and localized higher stresses on the foundation support layers. According to Birkhoff and McCullough (1979), the presence of a void larger than 1.27 mm (0.05 in.) beneath the pavement is defined as an LOS condition. Corner breaking is the most common distress associated with LOS conditions (FAA 2016). Figure 19 shows simulation results created using EverFE software that illustrate tensile stresses and deformations in the pavement layer due to a single-axle loading near the corner.

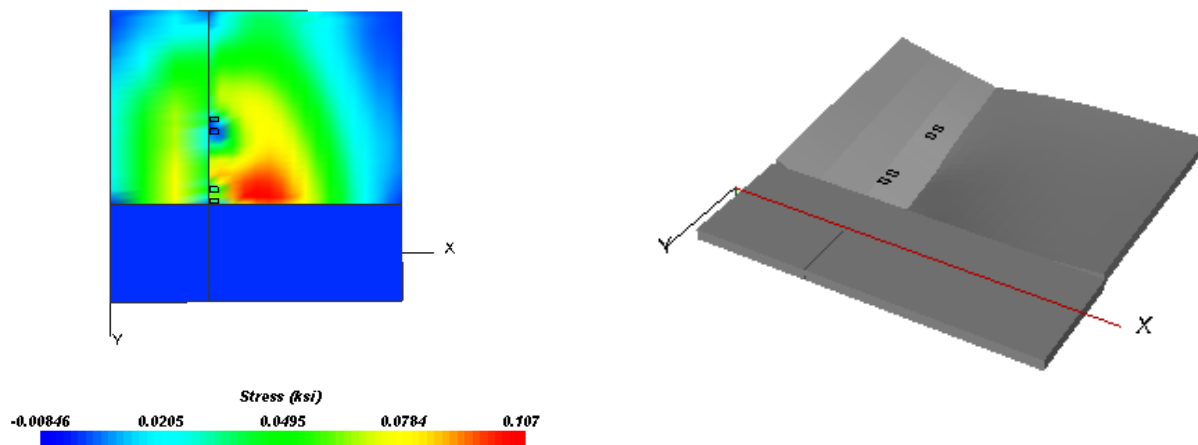


**Figure 19. EverFE simulation results depicting principal stresses in the pavement layer (left) and surface deflections (right)**

The figure depicts 80 kN (18 kip) AASHTO single-axle dual-wheel loading over a 254 mm (10 in.) thick PCC pavement on a foundation layer with a  $k$  value of 13.6 kPa/mm (50 pci). The simulation assumes no LOS and a uniform support condition. The maximum tensile stress for the presented case is low (118 kPa [171 psi]), but the stress contours highlight the potential for corner breaking as the tensile stresses increase, as expected.

To quantify and demonstrate the influence of the LOS conditions that can develop due to irrecoverable permanent deformations under cyclic traffic loading, 2D FE analysis was

conducted on a jointed pavement slab, as shown in Figure 20, using KENSLABS pavement analysis software (Huang 2004).

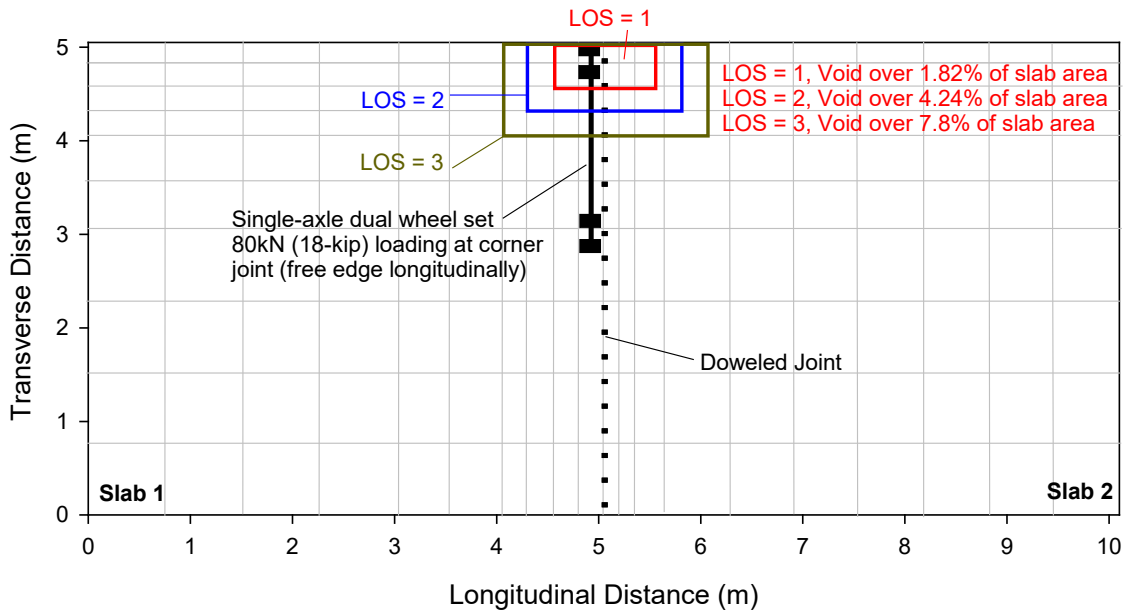


**Figure 20. FE model with two jointed slabs and 80 kN standard single-axle loading (with dual-wheel sets) near the joint/corner and an area of void beneath the slab for different LOS conditions**

KENSLABS was selected over other pavement analysis software programs because of its unique ability to model LOS with a defined magnitude of gap (developed through permanent deformation,  $\delta_p$ ) at each node. The different LOS factors were modeled with an area of void that is equivalent to the area of the slab, as defined in AASHTO (1986). An LOS factor of 1 corresponds to a void size of 1.59% of the area of the slab, an LOS factor of 2 corresponds to a void size of 4.59%, and an LOS factor of 3 corresponds to a void size of 8.16% (see AASHTO 1986).

The lowest (2 mm [0.08 in.]) and the highest (6 mm [0.24 in.])  $\delta_p$  values measured in situ from PLTs conducted on different projects as part of this study were used in these analyses to define the magnitude of the LOS gap. Analyses were conducted for the standard 80 kN (18 kip) single-axle loading case at the jointed corner and pavement thicknesses of 203 mm (8 in.), 254 mm (10 in.), and 305 mm (12 in.). The SR values were calculated for each case as the ratio of the maximum principal stress in the pavement layer and the modulus of rupture of the concrete (assumed to be 4,550 kPa [660 psi]). Based on the SR values, the number of load repetitions for fatigue failure ( $N$ ) were calculated using the PCA (1984) fatigue model. The foundation support  $k$  value (41 kPa/mm [150 pci]) and the joint properties were the same for all cases.

The SR values calculated from the peak stresses for each loading case are presented in the bar charts in Figure 21.

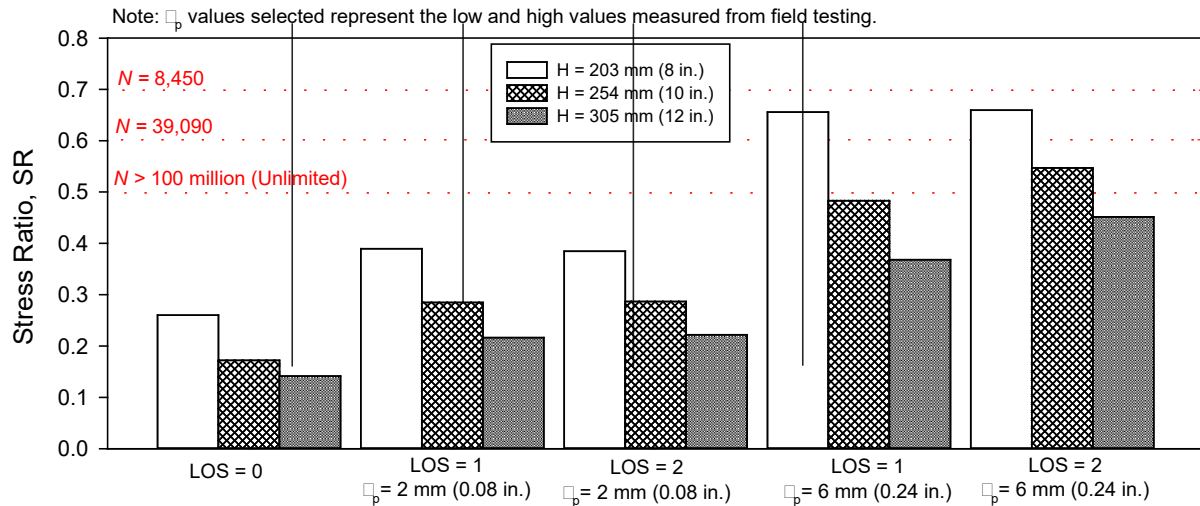


**Figure 21. Influence of LOS and magnitude of gap on SR values for LOS for different pavement thickness cases**

For an LOS of 0, the SR values were less than 0.45 for all three thicknesses evaluated. With an LOS of 1 or 2, the SR values increased and the associated number of load repetitions decreased. The results indicated that the magnitude of  $\delta_p$  has a significant impact, with SR values less than 0.45 for a  $\delta_p$  value of 2 mm and SR values greater than 0.45 value for a  $\delta_p$  value of 6 mm. These findings indicate that irrecoverable deformation of the pavement foundation can severely reduce the fatigue life of the pavement layer.

## In Situ Assessment of Distressed Pavement Sections

### *Assessment of Frost Heave and Joint Deterioration on US 30 near Ames, Iowa*

This project involved evaluation of distresses in the existing pavement, specifically to assess frost heave at the joints. It is well known that frost heave of foundation materials can cause severe joint deterioration in concrete pavements. A sufficient freezing depth, a continuous water supply, and frost susceptible geomaterials are the factors required to trigger frost heave-related issues in pavements. Field measurements of heave and temperature profile measurements were obtained on US 30 near Ames, Iowa, on the eastbound (EB) and westbound (WB) lanes near selected deteriorated joints in February and March 2010, when the air temperatures were between  $-4^{\circ}\text{C}$  and  $-12^{\circ}\text{C}$  ( $-24.8^{\circ}\text{F}$  and  $10.4^{\circ}\text{F}$ ). The results are documented in detail in Zhang et al. (2018) and White et al. (2016b).

The pavement consisted of an asphalt concrete (AC) overlay with a nominal thickness of 76 mm (3 in.) on aged PCC with a nominal thickness of 229 mm (9 in.). The pavement layers were underlain by asphalt-treated base (ATB) with a nominal thickness of 102 mm (4 in.). At the time of this field evaluation, the pavement displayed severe pavement distresses, with reflective cracking and vertical upheave near joints (Figure 22), especially during winter.





Vertical heave at the joint (air temperature -4°C)



Coring operation performed with 254 mm drill bit using air as drilling medium



Broken dowel bar and trapped water near bottom of pavement after extracting the core



Ice lenses within the pavement inter layers

**Figure 22. Heave near joints and drilling, coring, and sampling in February and March 2010 on an existing pavement with severe joint distresses – Iowa US 30 existing pavement evaluation project**

The Iowa DOT also reported incidents of damage to vehicle tires and problems with snowplow blade contact. Initial field investigations by the Iowa DOT rated the ride quality of the pavement section as “poor” based on pavement condition index (PCI) values that ranged from 54 to 56 on a scale of 0 to 100 scale (with 100 indicating good and 0 indicating failed condition). Later, this section of US 30 was rebuilt.

Core samples of the existing pavement were obtained near the joints using 254 mm (10 in.) and 100 mm (4 in.) diameter diamond rotary bits. Air was used as a drilling medium instead of water lubrication during coring to preserve the in situ moisture content of the cored specimens. The core samples showed that the PCC and the ATB layers were severely deteriorated, with the PCC layer samples obtained from the joints showing very little structural integrity. Ice lenses and trapped water were present at the interface of the hot-mix asphalt (HMA) overlay and PCC layer and at the interface of the PCC and ATB layers. The ATB layer was virtually impermeable. The coring operation, ice lenses within the pavement interlayers, and trapped water near the bottom

of the pavement are shown in Figure 22. The gravimetric moisture contents of the PCC layer samples ranged between 12.5% and 20.4%, which are very high compared to typical moisture contents in PCC pavements (Figure 23).

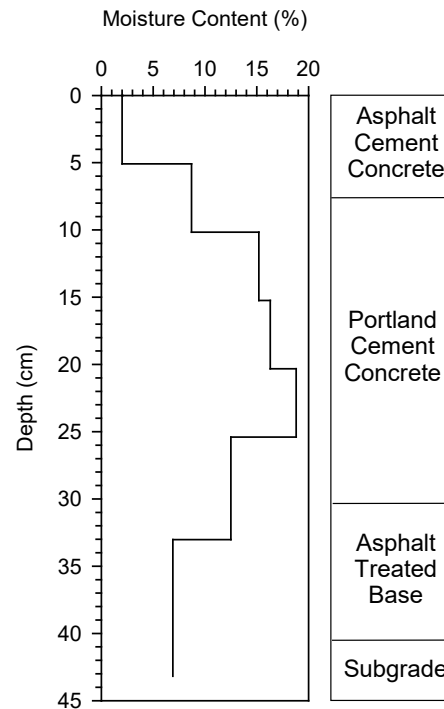


**Figure 23. Average moisture contents of core specimens at various depths – Iowa US 30 existing pavement evaluation project**

Vertical heave was measured at four selected joints in a spatial grid pattern. The measurements are shown as color-coded contour plots in Figure 24.



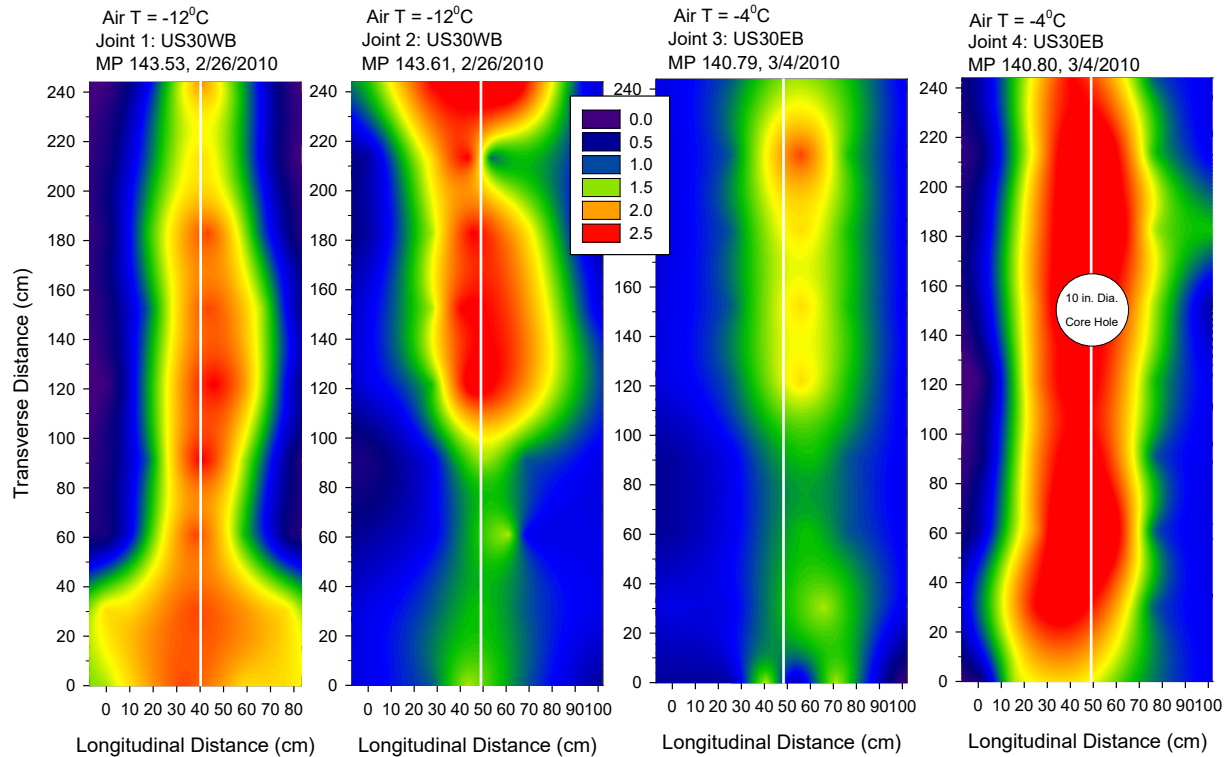


**Figure 24. Spatial contour plots of vertical heave near four selected joints – Iowa US 30 existing pavement evaluation project**

At deteriorated joint locations, the vertical heave reached up to 38 mm (1.5 in.), with nonuniform heave along the transverse direction. The longitudinal width of the heave bulges reached up to 76 mm (3.0 in.) near the shoulder.

The results and observations from this project present a classic case of cracks on the pavement surface contributing to water infiltration and the underlying undrainable base layer trapping water and allowing for the formation of ice lenses and frost heave at low temperatures.

#### *Assessment of Joint Deterioration on Urbandale Drive in Urbandale, Iowa*

This project was located on NW Urbandale Drive in Urbandale, Iowa. The site consisted of a four-lane divided roadway constructed in 1997 with a 260 mm (10.2 in.) thick jointed PCC pavement supported by a nominally 150 mm (5.9 in.) thick special backfill subgrade treatment (per Iowa DOT specifications) and compacted subgrade. The pavement experienced significant transverse joint failures along the corridor, with more severe failures along the southbound (SB) lanes than in the northbound (NB) lanes. Some longitudinal joint failures were also present. As part of the field study, a forensic investigation was conducted on the NB and SB lanes to assess the causes of the joint distresses (Figure 25).



**Figure 25. Joint deterioration (left) and CHP test in a drilled core hole at a joint obtained on November 7, 2013 (right) – Iowa Urbandale Drive project**

Field testing involved obtaining core samples for field distress evaluation and petrographic analysis and conducting FWD, DCP, and core hole permeameter (CHP) testing along selected pavement panels on the NB and SB lanes. The objectives of the field study were to assess the causes of premature joint failure on the roadway and investigate whether there were any differences in the support conditions between the NB and SB lanes that contributed to the greater distresses observed in the SB lanes compared to the NB lanes. FWD tests were conducted to assess the LTE of the pavement joints, peak plate deflections under dynamic loading ( $D_0$ ), voids beneath pavement (the FWD intercept [I] value), and the backcalculated  $k$  value ( $k_{\text{FWD-Static-Corr}}$ ). CHP tests were conducted to assess in situ drainage conditions (Figure 25, right). The results are documented in Vennapusa et al. (2015).

Field testing was conducted on three test sections. Two sections (TS1 and TS2) were in the NB lanes and one section (TS4) was in the SB lane. The field test results are summarized in Table 6.

**Table 6. Summary of in situ test results – Iowa Urbandale Drive project**

Measurement	TS1	TS2	TS4
Avg. $D_0$ (mm)	0.112	0.097	0.104
Avg. $k_{FWD-Static-Corr}$ (kPa/mm)	38.3	40.6	31.0
CBR of granular subbase layer (%)	21	27	34
CBR of subgrade (%)	3.7	5.1	12
$K_{CHP}$ (cm/s)	1.8E-04	2.5E-04	2.8E-04
Time to 50% drainage (days)	69	40	37
Estimated $C_d$	0.70	0.70	0.70
Support quality rating based on $k_{FWD-Static-Corr}$ (AASHTO 1993)	Very Poor	Very Poor	Very Poor
Drainage quality rating (AASHTO 1993)	Very Poor	Very Poor	Very Poor

$D_0$  = Peak deformation beneath the plate under loading from FWD test

$k_{FWD-Static-Corr}$  =  $k$  value determined from the FWD test and corrected for slab size and static conditions

$K_{CHP}$  = Coefficient of permeability determined from the CHP test device

CBR = CBR measured using the DCP test

$C_d$  = Coefficient of drainage

The FWD tests indicated that the average  $k$  value in each test section was lower than 41 kPa/mm (150 pci), which is considered “very poor” according to the AASHTO (1993) design guide. The values in the SB lane were on average about 1.3 times lower than those in the NB lane. The LTE values were greater than 85% at most of the joints (except one), indicating good load transfer conditions. The zero-load intercept values were all lower than 0.05 mm (2 mils), which indicated no apparent voids beneath the pavements. The CHP test results indicated that the hydraulic conductivity of the subbase layer varied from about 1.7E-04 to 2.8E-04 cm/s (0.5 to 0.8 ft/day) at the three test locations. No significant difference was observed between the results obtained from the NB and SB lanes. The time to 50% drainage was estimated to vary from about 37 to 69 days, which, according to AASHTO (1993), indicates “very poor” drainage.

Field observations of the core samples and petrographic analyses indicated that there were no significant differences between the cores obtained from NB and SB lanes. All cores showed water-cement ratio (w/cm) values ranging from about 0.45 to 0.55; air void contents ranging from 4% to 7%, which was not ideal (typically less than 5% is recommended); and some signs of ettringite in the air voids, pointing to abundant water. The distress observed in all cores is consistent with freeze-thaw damage. Figure 26 shows a core sample from a distressed joint, which exhibits distresses at the bottom of the sawcut, typically a result of trapped water below the sawcut and freeze-thaw cycles.



**Figure 26. Extracted core from a joint (with the right side representing the top of the pavement) showing freeze-thaw-related damage near the bottom of the sawcut (photograph taken on November 7, 2013) – Iowa Urbandale Drive project**

Further, it was also determined that damage was the worst in samples in which the backer rod stayed where it was intended, leaving a void that was then filled with water, leading to saturation and freeze-thaw distress.

In brief, the main cause of premature joint deterioration at this site was determined to be freeze-thaw distress that occurred due to poor drainage in the joints and subsurface. Increased saturation because of trapped water combined with a marginal air void system at the surface and an elevated w/cm ratio significantly increased the risk of damage. However, the results obtained from the NB and SB lanes did not provide conclusive evidence that there was a difference in terms of support conditions.

#### *Evaluation of Premature Pavement Distresses on US 34 near Mount Pleasant, Iowa*

The Iowa DOT identified sections of pavement on US 34 near Mount Pleasant, Iowa, that showed early deterioration in ride quality due to faulting, differential settlement, and longitudinal and transverse cracking (Figure 27).





**Figure 27. (a) Corner cracking on concrete panel, (b) longitudinal cracking, and (c) cracks observed on embankment fill slope near mile post 194 on US 34 WB, photograph taken on July 27, 2012 – Iowa US 34 pavement evaluation project**

The section was built in 2006 and consisted of PCC pavement with a nominal thickness of 260 mm (10 in.) placed over a 150 to 260 mm (6 to 10 in.) thick granular subbase layer. The PCC slab was sawcut to create transverse joints every 6.0 m (20 ft) with no dowel bars. Project drawings showed that crushed limestone was used for the granular subbase and a subdrain was installed near the pavement edge. Grading in the tested area required fills of up to 10 m (33 ft) and cuts of 3 m (10 ft). In the test area, a length of about 300 m (984 ft) consisted of subgrade constructed with embankment fill materials, with some areas next to 2% to 3% side slopes, and a length of about 530 m (1,740 ft) consisted of natural subgrade constructed in cuts. A  $k$  value of 41 kPa/mm (150 pci) was assumed during pavement design, following the PCA (1984) design method.

Field testing was conducted using FWD tests near the center and joints of 140 slab panels. The data obtained from the FWD tests were analyzed to determine  $k_{\text{FWD-Static-Corr}}$  and calculate different deflection basin index parameters that provided a relative measure of the support conditions provided by the foundation layer. The different index parameters are summarized in Table 7.

**Table 7. Summary of Student's *t*-test results on FWD deflection basin parameters near mid-panel on cracked and uncracked slabs – Iowa US 34 pavement evaluation project**

Parameter	Not cracked or cracked	Mean	COV (%)	t-value	P <sub>r</sub>
D <sub>0</sub> (μm)	Not Cracked	99	20	-4.07	< 0.001
	Cracked	135	32		
I (μm)	Not Cracked	< 1	760	-8.1	0.212
	Cracked	1	473		
Backcalculated <i>k</i> value (kPa/mm)	Not Cracked	29	23	4.06	< 0.001
	Cracked	22	38		
SCI (μm)	Not Cracked	6	23	-2.82	0.005
	Cracked	8	41		
BDI (μm)	Not Cracked	9	14	-3.71	< 0.001
	Cracked	12	31		
BCI (μm)	Not Cracked	9	109	-1.99	0.025
	Cracked	11	41		
AF (mm)	Not Cracked	808	2	-0.93	0.18
	Cracked	812	3		

Note: Highlighted cells indicate a statistically significant difference at a 95% confidence level between the cracked and uncracked slabs; COV indicates coefficient of variation.

D<sub>0</sub> = peak deflection measured directly beneath the FWD plate

I = zero-load intercept value determined by plotting the applied load on the x-axis and peak deflections on the y-axis; I > 5 μm (2 mils) indicates a void beneath the slab.

SCI = surface curvature index determined using deflection basin measurements

BCI = base curvature index determined using deflection basin measurements

BDI = base damage index determined using deflection basin measurements

AF = area factor determined using deflection basin measurements

A detailed description of these index parameters is provided in Vennapusa et al. (2018). In brief, lower index values represent better support conditions. Of the 140 slabs tested, 25 slabs showed distresses, including longitudinal and transverse cracking, mid-panel cracking, corner cracking, and faulting. Some of the cracked slabs had been patched with asphalt before the time of testing. All tests were conducted along the center of the outside (right) lane, where the distresses were predominant. All test results and analyses are documented in White et al. (2016c) and Vennapusa et al. (2018).

A Student's *t*-test analysis was conducted on the FWD measurements to assess whether there were statistically significant differences in the support conditions beneath cracked versus uncracked pavement slabs. The results of the statistical analyses for different FWD measurements are summarized in Table 7. Box jitter plots were developed for each of the measurement values, and example plots showing D<sub>0</sub> and backcalculated *k* values are shown in Figure 28.

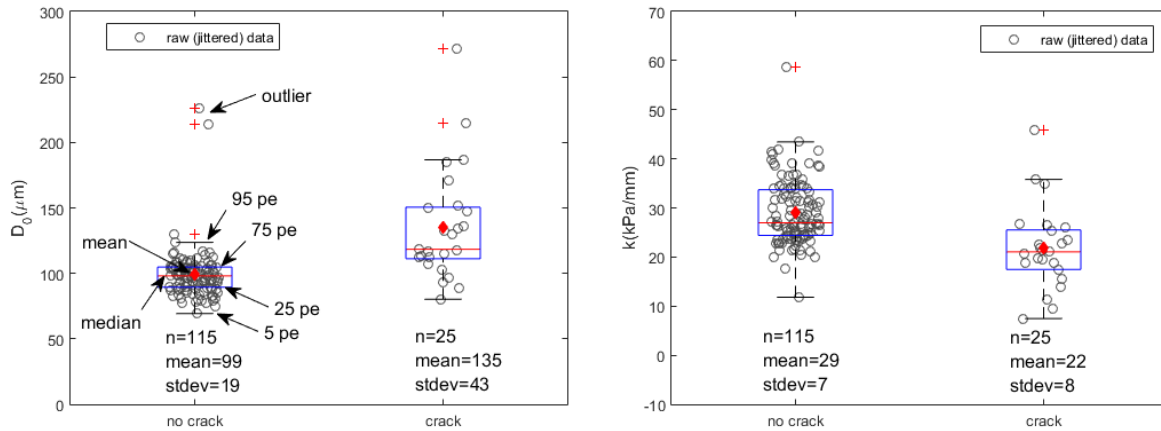


**Figure 28. Box plots comparing FWD test results at locations with and without cracking: (a) peak deformations beneath the plate under an applied load of 40 kN and (b) backcalculated  $k$  value – Iowa US 34 pavement evaluation project**

The results revealed that the foundation layers under uncracked slabs provided better support conditions than those under cracked slabs, with statistically significant differences. Tension cracks were evident along the side slope in the fill section, suggesting potential lateral movements in the embankment, which was another factor contributing to the surface cracking observed at this site (see Figure 27).

The  $k_{\text{FWD-Static-Corr}}$  values in both the cracked and uncracked panels were lower than those assumed during design at most of the test locations. There was no loss of support conditions as indicated by the FWD intercept (I) value at mid-panel or at the joints for any of the test locations.

Based on the field test results, statistical analyses, and observations at this site, it was concluded that a combination of embankment movements and comparatively weaker support conditions had contributed to the cracks observed at the pavement surface. However, given that most test measurements showed backcalculated  $k$  values below the  $k$  value assumed during design, it was unclear what level of support or FWD  $k$  value should have been considered adequate from a design perspective for this project site. Because of the empirical nature of the process for determining the backcalculated  $k$  value using the AREA method and the limited empirical evidence for correcting dynamic measurements to static values, it may not be appropriate to use the backcalculated  $k$  values directly in design. Some recent field studies have provided empirical evidence that the backcalculated  $k$  values from FWD tests are strongly related to the weakest layer properties in the top 1.5 m (4.92 ft) of the pavement foundation layer (White et al. 2014). More direct measurements of  $k$  values per AASHTO T 222 are needed to make comparisons with design assumptions.

Overall, this project provided information suggesting that the embankment fill and pavement foundation support layers contributed to the early ride quality issues and structural failure. If the embankment fill is not sufficiently stable to support the pavement foundation layers and the

foundation layers provide poor pavement support, the likelihood of early pavement distress is expected to be high.

### **In Situ Assessment of Rehabilitated Pavement Sections**

Many highway agencies are interested in understanding and evaluating different cost-effective and rapid rehabilitation techniques as an alternative to the full-depth repair of distressed in-service pavements. It is well understood that it is very expensive to fix poor pavement foundation conditions because doing so normally requires the removal of the pavement layer.

As part of this study, two project sites provided opportunities to conduct field testing to assess foundation layer properties and pavement performance following rehabilitation. One of the projects was in Pennsylvania on SR-422 and involved injecting high-density polyurethane (HDP) foam into the underlying base to rehabilitate the existing pavement, which had been exhibiting mid-panel transverse cracks. The study also included a small section where cementitious grout injection was used for comparison. The second project was in California on I-15 and involved the use of precast concrete pavement (PCP) systems, which consist of prefabricated concrete panels that are transported and placed on the prepared foundation after removal of the existing pavement. Summaries of the projects and the field testing highlights are provided below.

#### *Pennsylvania SR-422 Pavement Rehabilitation Project*

This project was on SR-422 in Indiana, Pennsylvania. The 9.7 km (6 mile) highway section was built in 1995 with a 280 mm (11 in.) thick PCC layer over a nominally 100 mm (4 in.) thick open-graded stone (OGS) base layer, a nominally 100 mm (4 in.) thick well-graded subbase layer, and a variable subgrade with a mix of clay/shale/sandstone rock. The PCC slabs were about 3.7 m (12 ft) wide by 6.1 m (20 ft) long and were jointed using dowel bars. The slabs showed significant distresses, with mid-panel cracking and faulting.

Based on preliminary International Roughness Index (IRI) and FWD testing, the Pennsylvania DOT (PennDOT) surmised that the observed surface distresses were related to the support conditions provided by the OGS base layer. Similar surface distresses have been documented on jointed PCC sections on I-80 in Pennsylvania that are supported by an OGS base layer (Beckemeyer et al. 2002). PennDOT initiated a rehabilitation strategy that involved injecting HDP foam. The purpose of the foam injection was to (1) stabilize the subbase aggregate layer, (2) mitigate faulting, and (3) improve joint LTE. Pictures of the HDP stabilization process are shown in Figure 29.



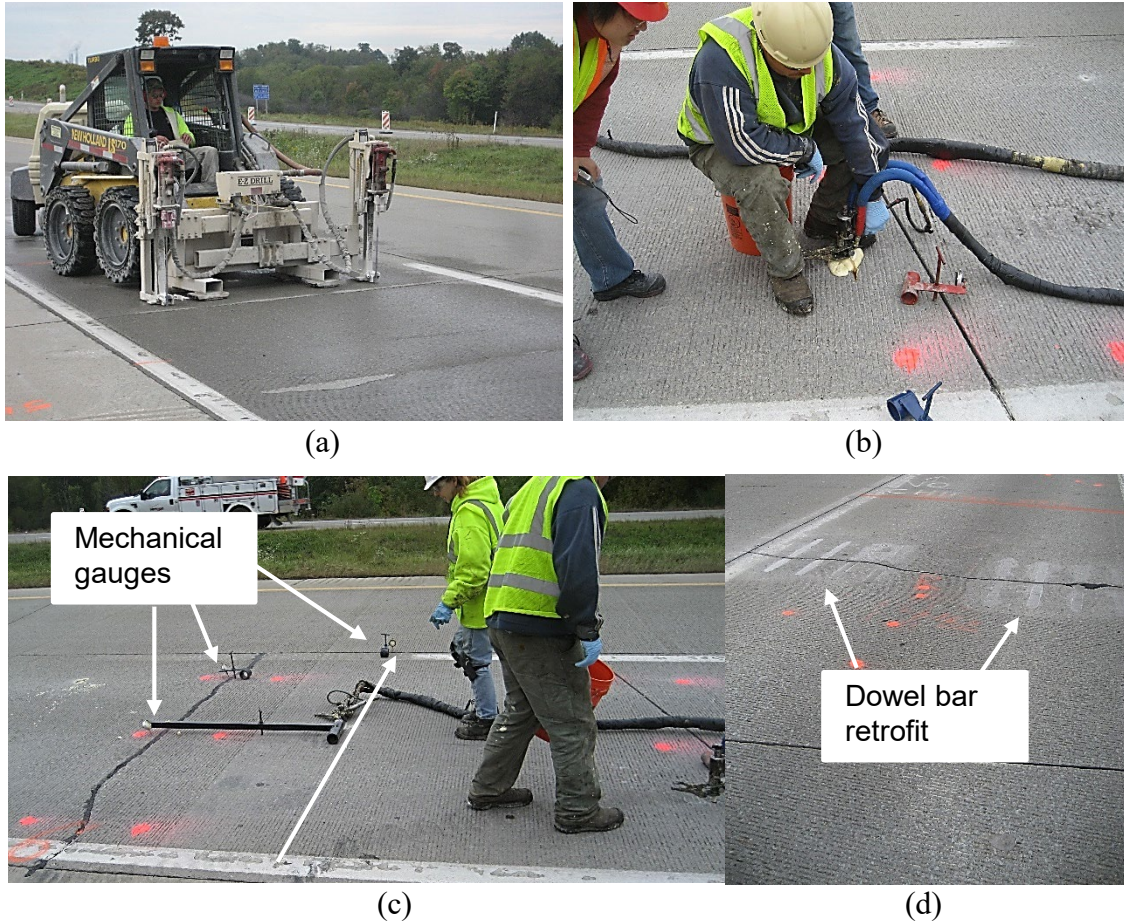


**Figure 29. Foam injection process: (a) drilling equipment used to drill injection holes, (b) foam injection, (c) mechanical gauges used to monitor pavement panel rise, and (d) dowel bar retrofitting performed at selected crack locations (photographs taken in October 2009) – Pennsylvania SR-422 rehabilitation project**

At selected locations, full-depth patching and dowel bar retrofitting was performed after the foam injection. A separate 160 m (500 ft) long control was stabilized using cementitious grout for a performance comparison.

In situ tests were performed during and after the rehabilitation work to evaluate improvements in the foundation and pavement layers. Testing involved characterizing the spatial propagation of the injected foam below the pavement; the strength, stiffness, and permeability of the treated subbase layer; changes in pavement surface elevation before and after treatment; joint LTE; potential voids beneath the pavement; and pavement ride quality. Tests were conducted in a concrete patch area, where the PCC surface was removed after HDP injection into the base layer (Figure 30).

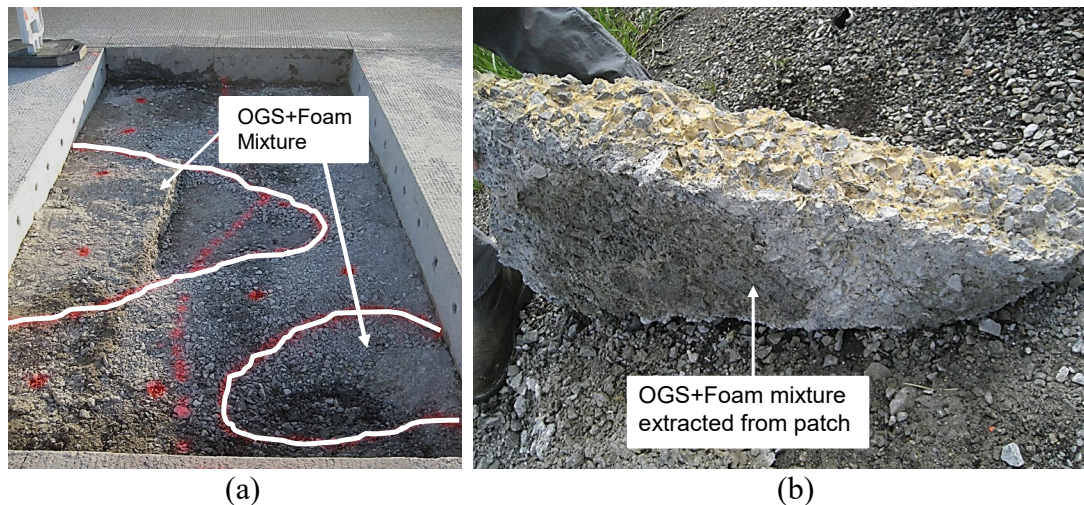


**Figure 30. (a) Patch area showing OGS and HDP mixture boundary and (b) close-up view of the OGS and HDP mixture sample extracted from the patch area (photograph taken in October 2009) – Pennsylvania SR-422 rehabilitation project**

The tests showed that the spatial extent of foam propagation in the base layer ranged from 0.3 to 1.0 m (1 to 3.3 ft) from the injection points. The foam injection process resulted in concentrated zones of foam mixed with subbase. Compared to the untreated areas, the HDP injection locations showed lower permeability, lower stiffness, and higher shear strength. Detailed results and analyses from this project are documented in White et al. (2015).

Pavement surface elevations were monitored by obtaining robotic total station measurements shortly before and after foam treatment on a 60 m (197 ft) long test section. The results were compared to the maximum allowed upward movement of 1.3 mm (0.05 in.) specified by PennDOT (2009). The test section consisted of nine pavement panels. Robotic total station pavement elevation profiles were obtained along three lines over the width of the driving lane: (a) line A-A located next to the passing lane, (b) line B-B located in the center of the driving lane, and (c) line C-C located next to the shoulder. Four of the nine panels did not have cracks before treatment. The other five panels had mid-panel cracks. Test points were located on either side of each crack and joint, and if no crack was present, a measurement was obtained at the middle of the panel. The difference in elevation ( $\Delta$ Elevation) was calculated as the elevation after treatment minus the elevation before treatment. The  $\Delta$ Elevation profiles along the A-A, B-B, and C-C lines are presented in Figure 31.

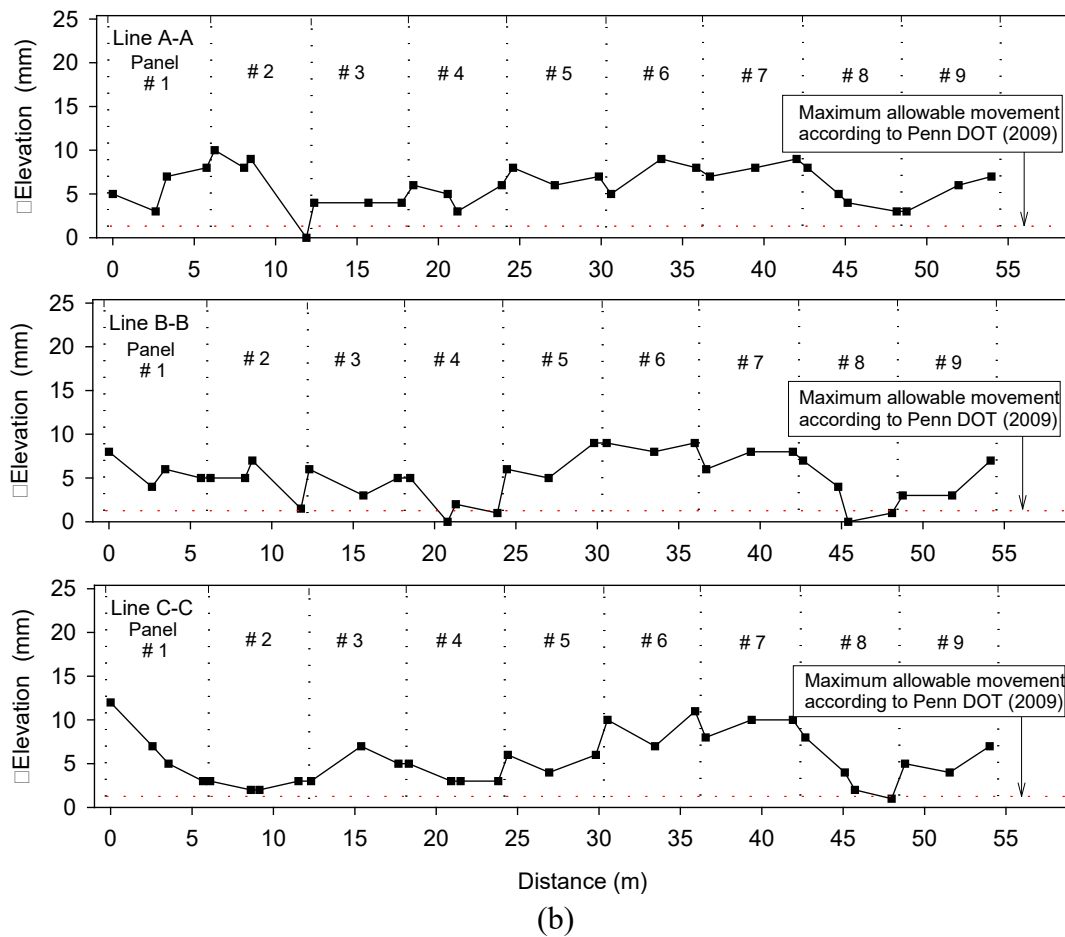
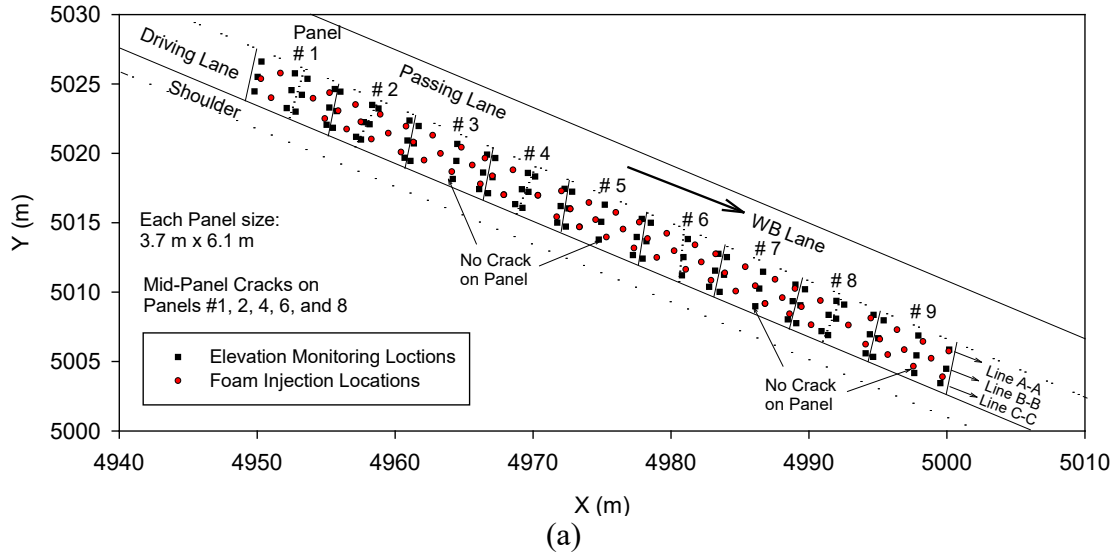


**Figure 31. Results of elevation monitoring near joints and cracks on nine panels: (a) plan view of elevation monitoring locations, foam injection locations, and A-A, B-B, and C-C survey lines and (b) change in elevation ( $\Delta$ Elevation) shortly after HDP foam injection along A-A, B-B, and C-C survey lines**

The elevation monitoring results indicated that the pavement panels were raised after treatment by an average of about 6 mm (0.24 in.), with a standard deviation of 3 mm (0.12 in.), across the test section. The upward movement measured at all locations was greater than the 1.3 mm (0.05 in.) maximum limit per the project specification. This suggests that improved injection control systems may be needed to limit panel heave. However, no faulting was observed at the cracks shortly after treatment in this section. The survey results in the cementitious grout section showed an average vertical rise of about 0.5 mm (0.02 in.) near the cracks and about 2.2 mm (0.09 in.) elsewhere.

FWD tests were conducted on the pavement before and after treatment to determine three critical parameters: LTE,  $D_0$ , and I. A comparison of the results for the HDP- and grout-treated sections is presented in Figure 32 and Figure 33.

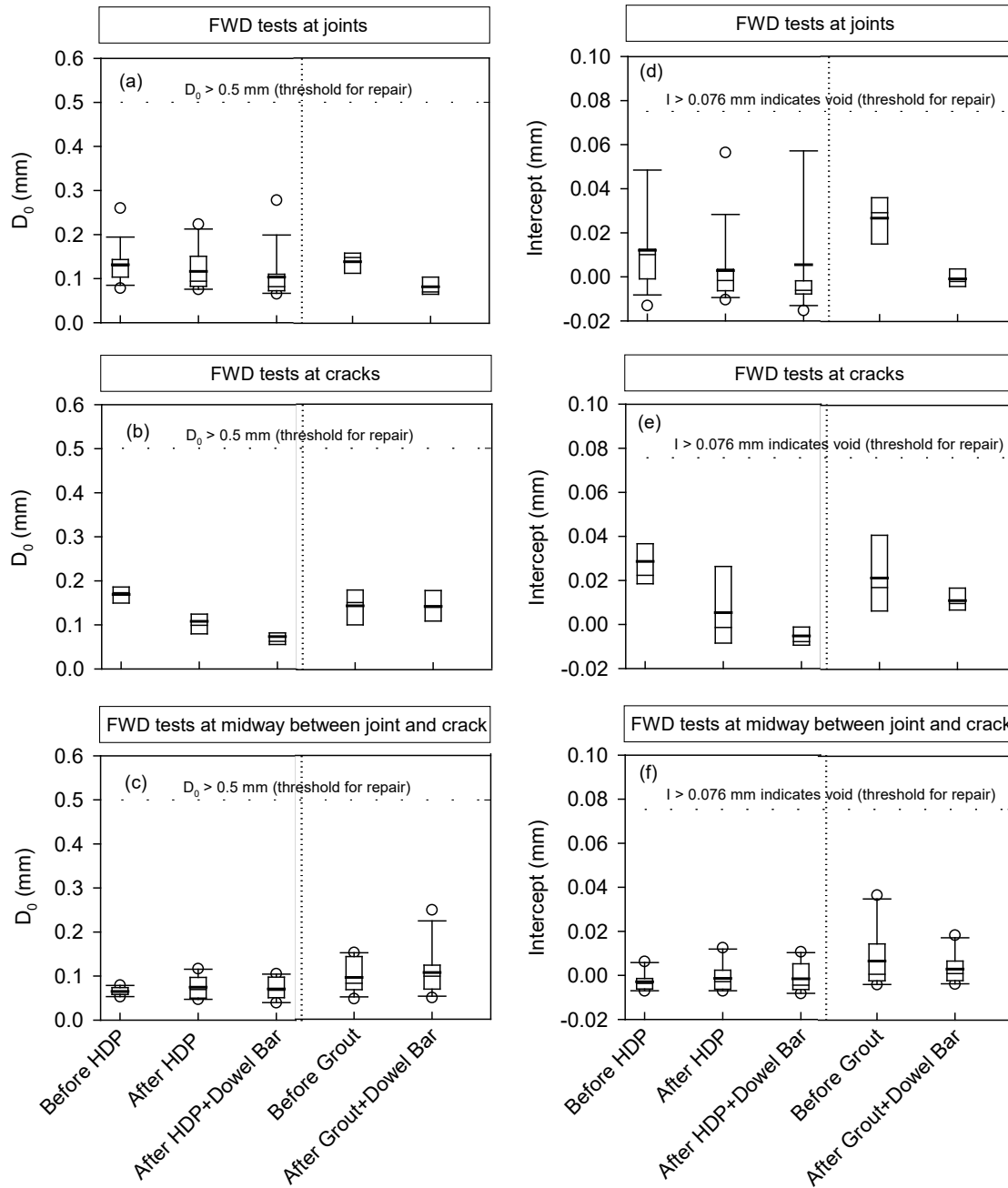


**Figure 32. (a)  $D_0$  at the joints, (b)  $D_0$  at the cracks, (c)  $D_0$  midway between the joint and the crack, (d) intercept at the joints, (e) intercept at the cracks, (f) intercept midway between the joint and the crack, before and after HDP/grout stabilization and dowel bar retrofitting at the cracks – Pennsylvania SR-422 rehabilitation project**



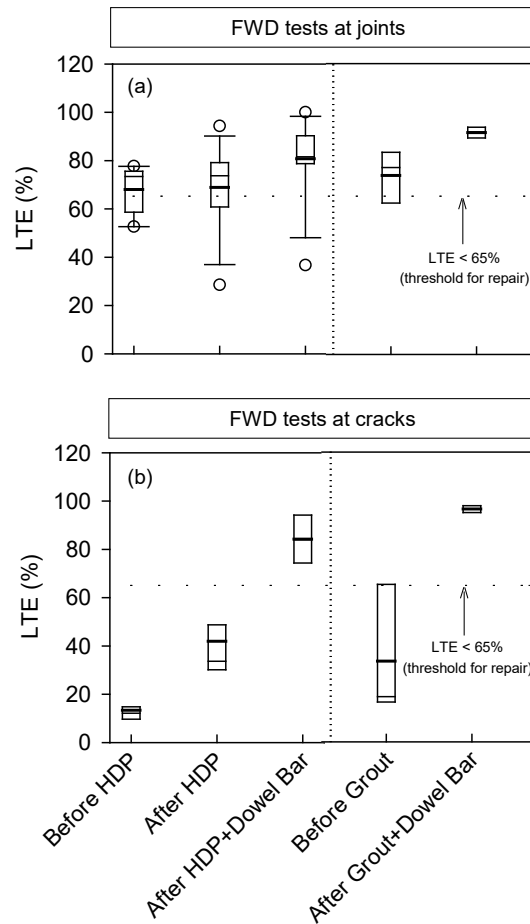


**Figure 33. (a) LTE at the joints and (b) LTE at the cracks, before and after HDP/grout stabilization and dowel bar retrofitting at the cracks – Pennsylvania SR-422 rehabilitation project**

The LTE values showed statistically significant improvement near the cracks and joints in both the cementitious grout and HDP foam sections. The LTE measurements at the cracks, although improved after HDP stabilization, did not meet the targeted criteria (>65%) until after dowel bar retrofitting. The  $D_0$  and  $I$  values showed statistically significant improvement only near the cracks (and not near the joints) in the HDP foam section and only near the joints (and not near the cracks) in the cementitious grout section.

The findings obtained from this project improve the understanding of the benefits and limitations of using HDP foam technology to rehabilitate concrete pavements. Additional field studies that characterize the long-term durability of foam-treated materials and a life-cycle cost analysis of the rehabilitation method are needed to fully evaluate the benefits of this technology. Based on the lack of control in setting the final panel elevation, improved control systems may be needed to leverage the full potential of HDP foam technology. Further, this study suggests that the OGS layer, though highly permeable, does not provide sufficient uniform support while limiting irrecoverable deformations.

## *California I-15 Pavement Rehabilitation Using Precast Concrete Panels*

This project was located on I-15 near Ontario, California, where Caltrans opted for PCP rehabilitation over a four-mile section of pavement. The PCP rehabilitation alternative was selected over a cast-in-place pavement because the highway was in an urban area with high traffic volumes, making lane closures a significant challenge. A total of 730 panels were installed. The unit cost of the PCP for the winning bid was about \$418/panel. The total bid cost of the project was about \$51.9 million. PCP systems constituted approximately \$4.6 million of the total construction cost. The existing pavement was originally constructed in the 1970s with approximately 213 mm (8.4 in.) of PCC over 122 mm (4.8 in.) of CTB. The existing pavement was removed, a new thin bedding sand layer was placed, and new 203 mm (8 in.) thick PCP panels were placed as part of the rehabilitation work. Bedding grout was pumped into precast ports for undersealing, and dowel grout was injected into the dowel slots. White et al. (2016d) details the results of field testing and observations made by the Caltrans and Second Strategic Highway Research Program (SHRP2) R05 project teams and field testing conducted as a part of the present project by the Iowa State University (ISU) research team.

The following are some key findings from the work performed by Caltrans and the SHRP2 R05 research team:

- The FWD test results showed that deflections were considerably smaller (0.076 to 0.127 mm [3 to 5 mils]) on panels where bedding grout was used.
- The panels with only dowel slot grouting showed more variability in surface deflections.
- Field monitoring for several months after construction revealed thin hairline cracks on several panels. A detailed survey was conducted on 696 panels, of which 24% were cracked.
- Based on crack survey mapping and field notes made during construction, it was concluded that the contractor's grading practices contributed to the cracking. It was determined that the stringline approach used to place the bedding material sometimes created high and low spots, resulting in nonuniform support conditions. Cracks at some locations were attributed to opening the lane to traffic before grouting.

Field testing conducted by the ISU research team included FWD and DCP tests on the CTB layer and FWD tests on adjacent test sections consisting of existing pavement and new PCP panels. The following are some of the key findings from this round of field testing:

- Tests on the CTB layer indicated that the average composite modulus was about 357 MPa (51.8 ksi) with a COV of about 17%. The average CTB layer modulus was about 7,200 MPa (1,044 ksi) with a COV of about 42%. The average subgrade layer modulus was about 105 MPa (15.2 ksi) with a COV of about 10%, which represented relatively stiff subgrade conditions.

- The CBR values estimated in the subgrade from the DCP tests showed relatively high values (ranging between 30 and 100), confirming the relatively high subgrade moduli values measured from the FWD testing. The average R-value of the subgrade (empirically estimated from backcalculated subgrade moduli values) was about 45 with a COV of about 5%. Statistical analyses of the FWD measurement values (Table 8) obtained from the existing and new pavements indicated that there was a statistically significant difference in the surface deflection ( $D_0$ ) and zero-load intercept (I) values near mid-panel, but no statistically significant difference was found in any of the other deflection basin parameters and the modulus of subgrade reaction ( $k$ ) values.

**Table 8. Summary of t-test analyses on FWD deflection basin parameters near mid-panel on new versus old pavement – California I-15 rehabilitation project**

Parameter	New or old pavement	Mean	COV (%)	t-value	P <sub>r</sub>
$D_0$ (μm)	New	118	9	-2.45	0.025
	Old	150	23		
I (μm)	New	-16	-192	-2.56	0.010
	Old	11	174		
$k_{\text{FWD-Static-Corr}}$ (kPa/mm)	New	47	21	1.30	0.11
	Old	41	25		
SCI (μm)	New	15	21	-0.48	0.32
	Old	18	99		
BDI (μm)	New	18	11	-0.49	0.32
	Old	20	54		
BCI (μm)	New	17	9	-0.86	0.21
	Old	19	43		
AF (mm)	New	725	4	-0.72	0.25
	Old	751	12		

Note: Highlighted cells indicate a statistically significant difference at a 95% confidence level between the new and old pavements.

The  $D_0$  and I values were lower in the new pavement than in the existing pavement. This suggested that the deflection response improved near the surface, which reflected better support conditions directly beneath the new pavement. This result was also confirmed in the SHRP2 R05 testing. Deeper improvements are not expected as reflected in the deflection basin parameters.

- There were no statistically significant differences in any of the measurement values obtained at the joints. The LTE values were relatively high (> 85%) at all locations.

In summary, the results indicated that the sections with PCP panels showed lower peak surface deflections under FWD loading than the sections with the existing pavement. The presence of bedding grout beneath the PCP panels reduced the surface deflections under FWD loading and resulted in less variability. The PCP panels showed thin hairline cracks several months after placement, and the cracked panels correlated well with areas that had problems with placement and leveling of the bedding material. Overall, the placement of the precast panels was a



remarkable engineering accomplishment, and it created an option for paving in high-volume traffic systems with reduced closure times.

## Impact of Seasonal Variation on Pavement Foundations and Performance

### *Seasonal Temperature Variation and Frost Depth*

In cold climates, pavement surfaces and foundation layers are subjected to seasonal temperature variation and freeze-thaw cycles. The number and duration of freeze-thaw cycles in the foundation layers can influence pavement performance. To better understand and document frost penetration depths and the number of freeze-thaw cycles occurring in the pavement cross-section, a pavement section on US 30 near Ames, Iowa, was instrumented to measure temperatures every minute from the pavement surface to a depth of about 1.6 m (5.2 ft) below the surface.

Using the temperature data, 0°C (32°F) frost isotherms, which form the boundaries of zones of frozen layers, were estimated for four winters, as presented in Figure 34.

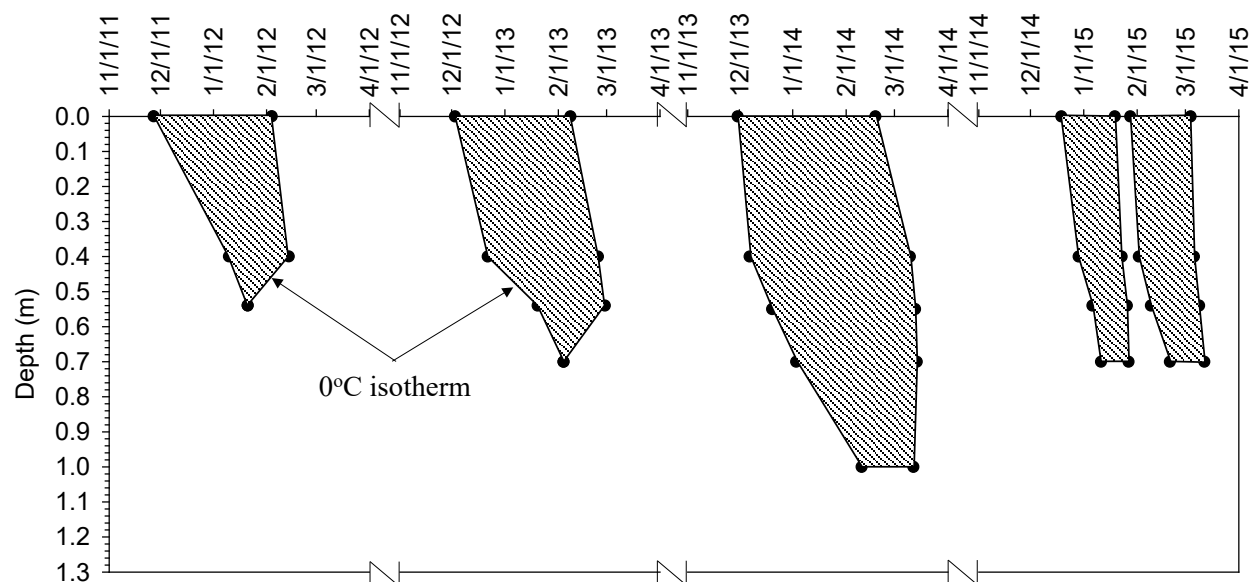


**Figure 34. Estimated frozen zones (shaded areas) at mile post 143.68 from 2011 to 2015 – Iowa US 30 reconstruction project**

The results indicated that the freezing periods in the 2011–2012 and 2012–2013 seasons lasted for about 2.2 to 2.4 months and in the 2013–2014 season lasted for about 2.6 months. Two separate freezing periods were observed during the 2014–2015 winter season, with each period lasting about 1 month. The thawing periods for the four seasons showed slight variations and lasted for about 10 to 25 days. The maximum frost penetration depth based on the isotherms ranged between 0.54 and 0.73 m (1.8 and 2.4 ft) for the 2011–2012, 2012–2013, and 2014–2015

seasons. The deepest frost penetration, which reached to 1.02 m (3.3 ft), was observed during the 2013–2014 winter season.

The number of freeze-thaw cycles at various depths calculated for each year from 2011 to 2015 at the US 30 project site are presented in Figure 35.

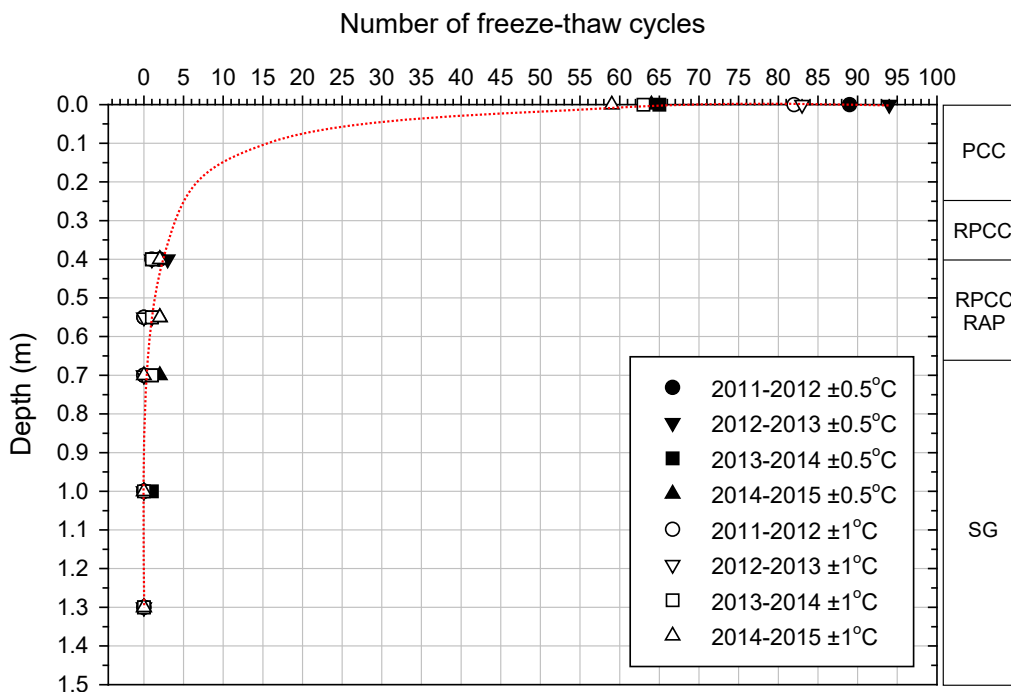


**Figure 35. Freeze-thaw cycles at various depths from 2011 to 2015 using  $\pm 0.5^\circ\text{C}$  and  $\pm 1^\circ\text{C}$  as cycle boundary values – Iowa US 30 reconstruction project**

The cycles were determined using both  $\pm 1^\circ\text{C}$  and  $\pm 0.5^\circ\text{C}$  as boundary values. The number of freeze-thaw cycles decreased with depth, as expected. The number of freeze-thaw cycles at the surface ranged between 59 and 94 cycles and decreased to about 5 to 10 cycles near the bottom of the pavement. The number of cycles decreased to less than 3 at a depth of about 0.7 m (2.3 ft) below the surface, and no freeze-thaw cycles were observed at depths greater than 1.1 m (3.6 ft) below the surface during the monitoring period.

#### *Seasonal Variations in In Situ Foundation Layer Properties*

Seasonal variations in the foundation layers are accounted for in pavement design via empirical adjustment of the foundation layers' modulus values. Variations in the in situ properties were captured using multiple rounds of FWD and DCP testing over a two-year period to capture the impact of seasonal variations at five different sites in Iowa (Table 9), and pavement temperature was also continuously monitored at one site (Plainfield, Iowa) during the testing period.

**Table 9. Summary of project sites in Iowa selected for seasonal variation testing**

<b>Project site</b>	<b>Year pavement built</b>	<b>Pavement thickness</b>	<b>Granular subbase material and thickness</b>	<b>PCI (ride quality rating)</b>
Fort Dodge	2005	254 mm	CLS, 254 mm	87 (Good)
Denison	1971	203 mm	CLS, 254 mm	55 (Fair)
Moville	1958	254 mm	Information on material type not available, 254 mm	18 (Very Poor to Serious)
Nevada	1992 (west)	254 mm	CLS, 254 mm	82 (Satisfactory)
	1998 (east)			91 (Good)
Plainfield*	2002	241 mm	CLS, 254 mm	94 (Good)

\* pavement temperature monitored at the site  
CLS = crushed limestone

As summarized in Table 9, the pavement test sections varied in age from 6 to 56 years, with different levels of distress and ride quality (poor to good) measured using the PCI values obtained at the time of testing. Testing was conducted eight times between July 2010 and July 2012.

Testing was conducted when the foundation layers were in a frozen condition (winter), thawed condition, and equilibrium condition (summer). DCP testing was conducted in the foundation layers by drilling a 25.4 mm (1 in.) diameter hole in the pavement layer down to the foundation layer.

Example results from the one of the test sites (Plainfield, Iowa) are presented in Figure 36, with the zero-degree isotherms, peak surface deflections ( $D_0$ ) under FWD loading, and  $k_{\text{FWD-Static-Corr}}$  values over a two-year testing period.

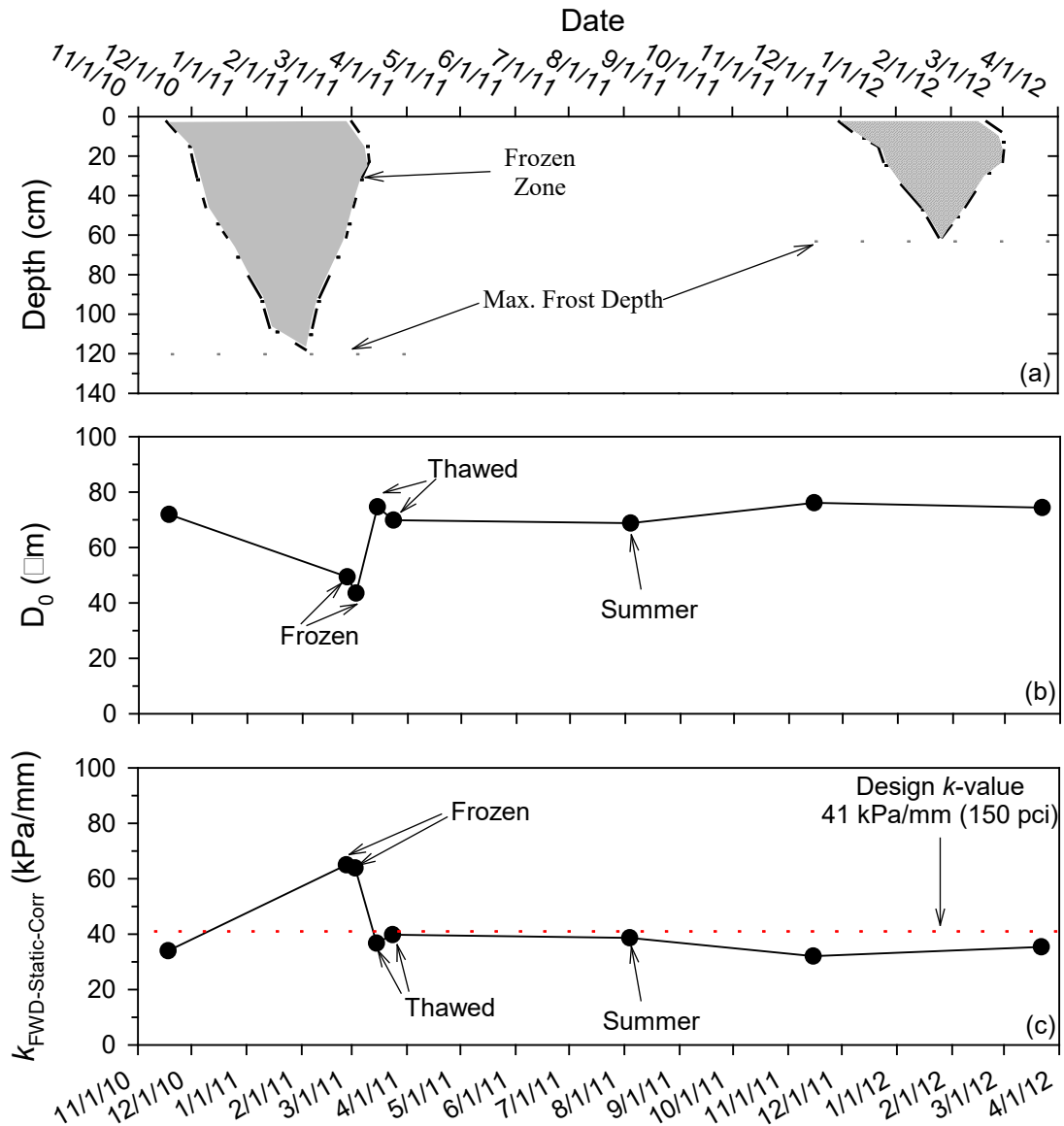


**Figure 36. Testing results from Plainfield, Iowa, test site: (a) zero-degree isotherm with time, (b) seasonal variations in  $D_0$ , and (c) seasonal variations in  $k_{FWD-Static-Corr}$**

The  $D_0$  and  $k_{FWD-Static-Corr}$  values varied with changes in ground temperature, as expected. During frozen conditions, the  $D_0$  values were about 45% lower than those observed before freezing. During the thawing period, the  $D_0$  values were about the same as those measured before freezing. After the thawing period, the  $D_0$  values recovered to levels similar to those observed before freezing and remained relatively constant throughout the summer.

During frozen conditions, the  $k_{FWD-Static-Corr}$  values were nearly twice as high as those before freezing. During the thawing period, the  $k_{FWD-Static-Corr}$  values dropped to the same level as those before freezing and remained relatively constant during the summer. Under thawing and summer conditions, the measured  $k_{FWD-Static-Corr}$  values were slightly lower than the Iowa DOT's design  $k$  value (41 kPa/mm [150 pci]).

The results from all of the test sites are detailed in Zhang (2016). In brief, for the five sections tested in this study, there were no significant differences in the  $k$  values obtained from FWD testing in thawed conditions and in the summer. The  $k$  values obtained from FWD testing in frozen conditions were about 10% to 56% higher than in summer at four of the five sites. At one test site, the values were about the same at all testing times. At two of the five sites, the  $k$  values obtained from FWD testing in thawed conditions and in the summer were about 1.5 to 2 times lower than the  $k$  value assumed during design (41 kPa/mm).

The PCI data available for each test section are compared with pavement age in Figure 37.

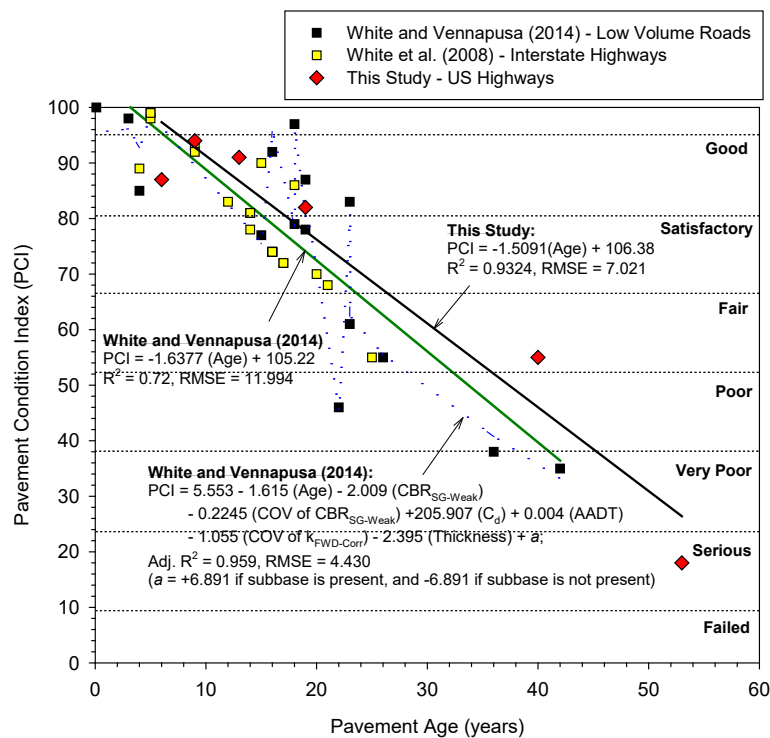


**Figure 37. PCI versus pavement age in the present study compared to results presented in White and Vennapusa (2014) and White et al. (2008)**

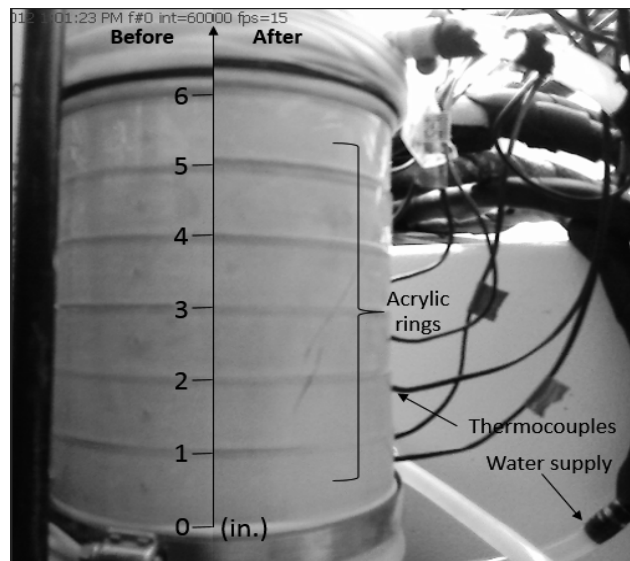
The relationships between pavement age and PCI showed a strong linear trend, with an  $R^2$  greater than 0.93. A similar statistical regression relationship was documented by White and Vennapusa (2014) based on testing at low-volume jointed PCC pavement sites. Based on multivariate parametric analyses conducted by White and Vennapusa (2014) and Zhang (2016), pavement age was determined to be the most significant factor in predicting PCI, followed by pavement thickness, with other influencing factors being foundation layer stiffness or strength, variability in the strength/stiffness properties, and drainage.

### *Laboratory Characterization of Frost Heave and Thaw Weakening Susceptibility*

Frost heave and thaw weakening laboratory tests were performed on disturbed samples of three pavement foundation materials to classify the materials according to their frost susceptibility. The materials included recycled subbase (classified as SM, A-1-a) and lean clay subgrade (classified as CL, A-6(5)), both collected from Boone County, Iowa, and Loess (classified as ML, A-4) collected from western Iowa. Testing was also performed on stabilized materials to determine whether they can reduce the frost susceptibility of a naturally highly frost-susceptible material. The stabilizers were Class C fly ash (from three different sources in Iowa) and portland cement for chemical stabilization and two types of fibers: polypropylene (PP) and monofilament (MF) fibers. The testing resulted in a matrix of 36 different materials.

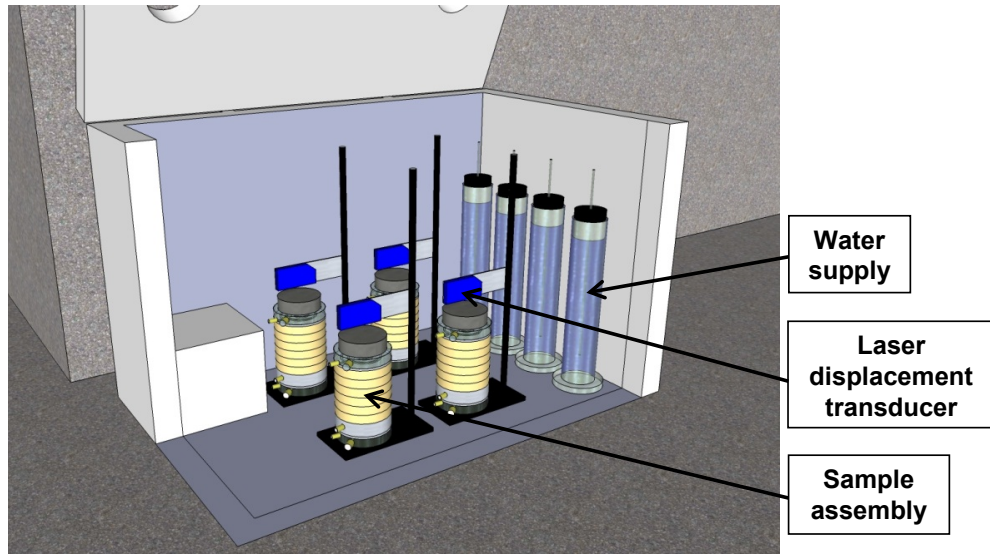
The testing details and results are presented in Johnson (2012), Zhang (2013), and Zhang et al. (2016). A brief overview of the testing procedure and a summary of the results and conclusions are provided below.

Frost heave and thaw weakening laboratory tests were performed according to ASTM D5918-06, which specifies two freeze-thaw cycles and recommends that four samples be tested for each material. The test setup is shown in Figure 38 and Figure 39.



Zhang et al. 2016

**Figure 38. Side-by-side specimen assembly before/after freeze-thaw testing (1 in. = 25.4 mm)**



Johnson 2012

**Figure 39. Idealized view of the temperature control chamber**

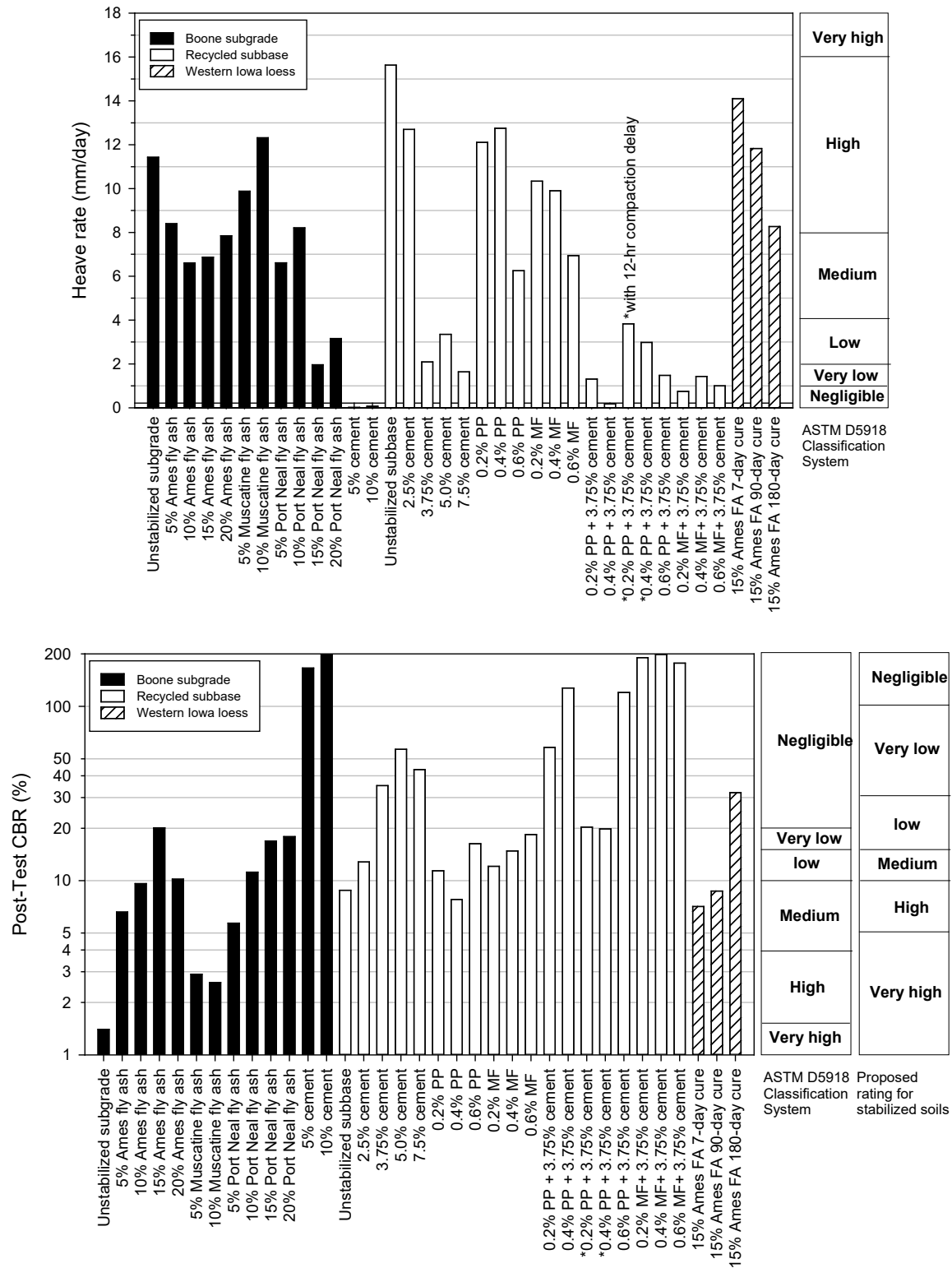
ASTM D5918-06 outlines frost susceptibility criteria that classify materials based on the heave rate and post-test CBR (**Error! Not a valid bookmark self-reference.**).

**Table 10. Frost susceptibility classification**

<b>Frost susceptibility classification</b>	<b>8-hour heave rate (mm/day)</b>	<b>CBR after thaw (%)</b>
Negligible	<1	>20
Very low	1 to 2	20 to 15
Low	2 to 4	15 to 10
Medium	4 to 8	10 to 5
High	8 to 16	5 to 2
Very High	>16	<2

Source: ASTM D5918-06

The frost heave and post-test CBR results are summarized in Figure 40, along with the frost heave and thaw weakening susceptibility ratings.



Reproduced from Zhang et al. 2016

**Figure 40. Comparison of frost heave rates and post-test CBR values for all stabilized and unstabilized material samples**

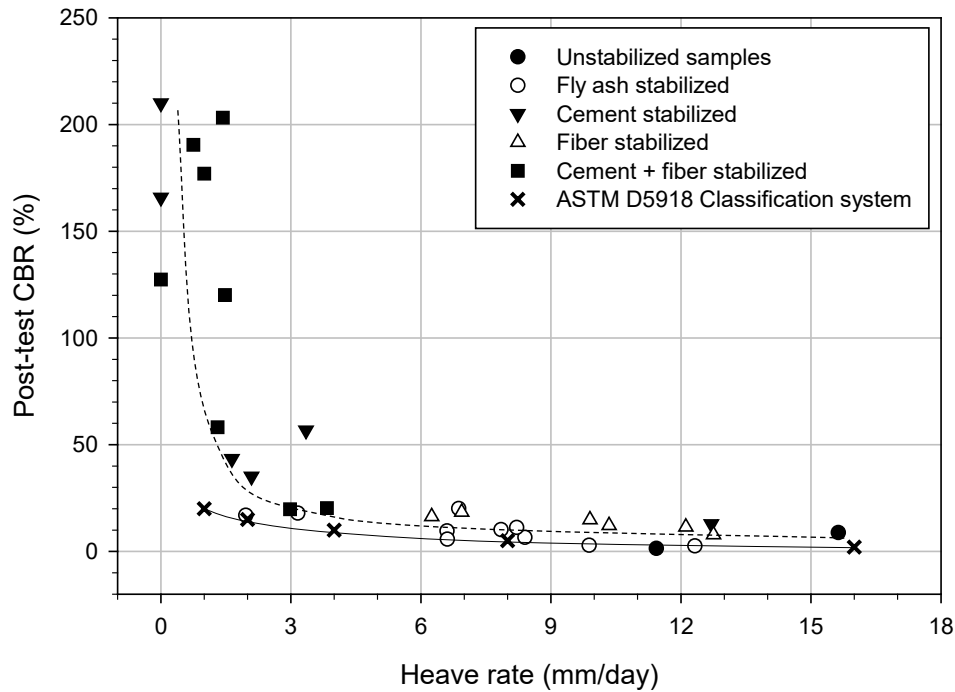


The unstabilized materials (SM, CL, and ML) exhibited frost heaves of 11.4 to 19.1 mm/day and post-test CBR values of less than 1 to 8.8, indicating high to very high frost susceptibility and medium to very high thaw weakening susceptibility.

Testing on the subgrade stabilized with fly ash yielded variable results but generally indicated an improvement in post-test CBR values. Lower heave rates were also observed with an increase in fly ash content. The set times of the fly ash stabilizers from the different sources were different. The results showed that shorter set times resulted in reduced frost heave and thaw weakening (Zhang et al. 2016). Both of the subgrades stabilized with cement (5% and 10%) showed heave rates close to 0 mm/day. For the recycled subbase, the frost susceptibility decreased as the cement content increased.

The recycled subbase stabilized with fibers showed an improvement in terms of reduced heave rate and increased post-test CBR values. The results indicated that the post-test CBR values were all higher than the pre-test CBR values. This finding suggests that the freeze-thaw action and associated stress development in the fibers contributes to an increase in the CBR values. The frost susceptibility ratings based on heave ranged from medium to high for the fiber-stabilized specimens. Adding cement to the recycled subbase-fiber mixtures significantly reduced the heave rates. The frost susceptibility classifications of all of the cement- and fiber-stabilized recycled subbase (with no compaction delay) specimens ranged from very low to negligible.

Figure 41 presents frost heave rates versus CBR values for all specimens.



Reproduced from Zhang et al. 2016

**Figure 41. Relationships between post-test CBR values and measured heave rates with a comparison to the ASTM D5918 criteria**

Very low thaw weakening susceptibility was achieved when the heave rate was less than 4 mm/day. Frost susceptibility based on frost heave, using the ASTM D5918 criteria, cannot predict thaw weakening susceptibility, especially for stabilized materials. An alternative thaw weakening susceptibility classification rating, shown in Table 11, was developed based on data obtained from the present study and ASTM D5918.

**Table 11. Proposed frost heave and thaw weakening susceptibility classification for stabilized soils based on data from this study**

Frost/thaw weakening susceptibility classification	2nd 8-hour heave rate (mm/day)	CBR after thaw (%)
Negligible	<1	>100
Very low	1 to 2	100 to 30
Low	2 to 4	30 to 15
Medium	4 to 8	15 to 10
High	8 to 16	10 to 5
Very high	>16	<5

The boundary values were adjusted to reflect differences in the post-test CBR values and heave rates for stabilized materials. The current ASTM classification does not distinguish classifications for materials with CBR values greater than 20. The alternative classification system proposed herein identifies thaw susceptibility as negligible for materials with post-test CBR values of 100 or more. The advantage of the proposed rating system is that it allows for a more refined classification of stabilized soils used in pavement foundation layers.

## **CHAPTER 3: MECHANISTIC CHARACTERIZATION OF PAVEMENT FOUNDATION LAYERS**

This chapter provides a brief history of the evolution of rigid pavement design, the key pavement foundation input parameters, and the ways these parameters have been measured by different agencies in the development of their design equations. This discussion highlights the importance of testing methods and can aid designers in the selection of the appropriate testing devices/methods for verifying design input parameters. Much of the background information is difficult to find and is likely often overlooked, which has resulted in the widespread use of empirical equations without an understanding of the uncertainties associated with those equations.

The different methods for measuring the foundation layer input parameters are discussed in terms of direct and indirect methods. Indirect methods include surrogate field test measurements and empirical relationships used to estimate the input parameters. A quantitative approach to assess the reliability of an empirical prediction method is provided near the end of this chapter. This approach provides guidance to engineers by offering a prediction equation to make an informed decision about the reliability of the approach for establishing the design input parameters. Although convenient, empirical equations for assessing pavement foundations in practice often come with a false sense of security when it comes to representing the actual field conditions. Empiricism is considered a major limitation in the advancement of pavement foundation engineering practice.

### **A Brief History of the Evolution of Rigid Pavement Design**

Pavement design methods and procedures have evolved over time from being purely experience-based in the early 1900s to becoming a science with a much more refined understanding of the behavior of the materials involved. Even with the improved understanding of the behavior of materials in the present day, empiricism still plays a necessary role in designing pavements. With experience, agencies have developed and refined their procedures. The purpose of this review is not to comprehensively describe the history of these methods and developments but to provide a brief overview of the historical developments in rigid pavement design in the context of the key foundation layer parameters that affect pavement performance.

The structural design of rigid pavement has long been based on the relationship between the flexural strength of the concrete and the stresses developed in the concrete under loading (Huang 2004). Closed-form solutions to complex derivations have been developed since the 1920s to estimate the stresses and deflections in rigid pavements under loading.

Goldbeck (1919) first published an analytical closed-form solution for a corner loading case to calculate stresses in a pavement for given loading and subgrade support conditions. Goldbeck's corner loading formula was assessed in the Bates Road Test in 1923 by the Illinois State Highway Department (Older 1924). The results from that road test demonstrated corner breaks on concrete slabs in general agreement with Goldbeck's analytical solution, although some of the inherent assumptions behind the solution were not present at the test road (Kher et al. 1971).

In 1925, Harold Westergaard at the University of Illinois performed the most extensive theoretical studies on stresses and deflections in concrete pavements for various loading cases applied near the corner, in the interior, and near the edge of a large slab. His work was later published in a series of papers (Westergaard 1926a, 1926b, 1927, 1948). The U.S. Bureau of Public Roads (which later became the Federal Highway Administration) conducted extensive field testing at the Arlington Experimental Farm in Virginia to validate Westergaard's solutions. The results from those studies were published in a series of papers by Teller and Sutherland (1935–1943). The rigid pavement design procedures provided in AASHTO (1972, 1986, and 1993) are based on Westergaard's analytical solutions. The U.S. Department of Defense (DOD) pavement design procedure currently uses Westergaard's edge-loaded model for heavily loaded pavements and his interior-loaded model for lightly loaded pavements (U.S. Department of Defense 2018).

Pickett et al. (1951) provided an extension to Westergaard's formulae based on field performance measurements for the corner loading case; this extension was later incorporated into the PCA design procedure (PCA 1984). Pickett's theoretical solutions for concrete slabs are based on elastic half-space theory, which assumes that the subgrade behaves more like an elastic solid than a dense liquid.

The new ME design method, which is used in AASHTOWare Pavement ME Design (AASHTO 2015), is a significant leap forward in pavement design. The “mechanistic” part of the design method relates the input parameters (i.e., wheel loading, number of loading cycles, material properties, and environmental conditions) and pavement responses such as stresses, strains, and deflections. The “empirical” part of the design method predicts distresses over time using empirical relationships developed based on observed field performance or laboratory testing. Empirical relationships are essential because theoretical relationships alone have not been proven to be sufficient for the realistic design of pavements (Huang 2004). The performance criteria used in rigid pavement ME design are mean joint faulting, percent transverse slab cracking, and IRI.

A component of the ME design method is the calibration of the empirical equations. AASHTO (2010) provides step-by-step guidance on how local agencies can perform the calibration process. Detailed procedures for developing an experimental plan, estimating the sample size, selecting the roadway segments, collecting the required field data, and assessing bias/standard error in the global calibration factors for local conditions are discussed in AASHTO (2010). The primary objectives of the calibration process are to reduce bias and increase the precision of the empirical models used in the design software for predicting performance indicators (i.e., distresses, ride quality). The end result of the calibration process is local calibration-based regression factors that can be updated in the design software. Many early adopter state agencies have invested in developing local calibrations (e.g., Kim et al. 2011, Ceylan et al. 2013, Darter et al. 2014, Mallela et al. 2013).

A sensitivity analysis using AASHTOWare Pavement ME Design software was performed as part of the present study to quantify the influence of pavement foundation support on the required slab thickness (see the detailed analysis in Brand and Roesler 2014). The analysis

results indicate that the required slab thickness is not sensitive to changes in soil type or unbound layer stiffness properties. This finding confirms what others have reported in the past (Velasquez 2009, Haider et al. 2009, Hoerner et al. 2007).

A recent National Cooperative Highway Research Program (NCHRP) study by Lytton et al. (2019) noted that the performance of pavements (both rigid and flexible) is known to be closely related to the properties of the unbound layers and proposed several enhancements to the ME design procedures. The proposed enhancements are made with increased consideration of the influence of the subgrade and unbound layers on pavement performance. Using the proposed new models, Lytton et al. (2019) concluded that the base and subgrade layer properties (stiffness and thickness) and moisture variations within those layers over the design life of the pavement (due to freezing-thawing or wetting-drying) have a significant impact on the performance indicators. To our knowledge, the proposed enhancements from Lytton et al. (2019) have not yet been evaluated in the field or incorporated into the pavement ME design procedure, but the findings are encouraging in terms of better accounting for important pavement foundation properties during the design process.

Regardless of the chosen design procedure, it is critically important that the design equations be calibrated to or developed using mechanistic geotechnical input parameters that have been measured properly. Further, it is important to study the pavement foundation parameters carefully so that verification tests align with field acceptance testing procedures.

### **Geotechnical Input Parameters in Rigid Pavement Design**

The deflections and stresses introduced by external loading (traffic or environmental) into a concrete pavement slab are influenced by the performance of the underlying foundation layers. The stresses and deflections in the slab are related to the distresses in the slab, which affect pavement rideability. Christopher et al. (2006) summarized the influences of different foundation layer properties on the typically observed rigid pavement layer distresses. A modified version of that summary is provided in Table 12. The dominant geotechnical parameter that causes distresses in rigid pavements is the modulus of the foundation layers (Christopher et al. 2006). The other factors listed in Table 12—moisture/drainage-related problems, volumetric deformations (e.g., shrink-swell, freeze-thaw), contamination, and erosion—all contribute to a loss of strength/stiffness in the support layers.

**Table 12. Influence of foundation layer properties on rigid pavement layer distresses**

<b>Rigid Pavement Distress</b>	<b>Inefficient base stiffness/strength</b>	<b>Inefficient subgrade stiffness/strength</b>	<b>Moisture/Drainage Problems</b>	<b>Freeze-thaw</b>	<b>Swelling</b>	<b>Contamination</b>	<b>Erosion</b>	<b>Spatial Variability</b>	<b>Permanent deformation</b>
Fatigue Cracking	✓	✓	✓	✓		✓	✓	✓ <sup>b</sup>	✓
Punchouts (CRCP <sup>a</sup> )	✓	✓	✓	✓		✓	✓		
Pumping			✓				✓		✓
Faulting	✓		✓	✓	✓	✓	✓		✓
Roughness	✓		✓	✓	✓	✓	✓	✓	✓

<sup>a</sup> CRCP – continuously reinforced concrete pavement

<sup>b</sup> Fatigue cracking is not identified as a distress type related to spatial variability in Christopher et al. (2006) but is added herein to reflect the effects it has on the stress concentrations it can generate, as discussed in Chapter 2, and the resulting reduction in the fatigue life of the pavement.

Source: Modified from Christopher et al. 2006

Permanent deformation is another important factor that is directly linked to the development of distresses due to the development of voids beneath the pavement, especially if the deformation occurs near the joint, as demonstrated in the FE analysis results in Chapter 2. The strength and stiffness properties, drainage, erosion, and volumetric movements all contribute to permanent deformation.

In rigid pavement design procedures, the foundation support is characterized by the modulus of subgrade reaction ( $k$ ). An alternative to this is the use of  $M_r$  in recent years (AASHTO 2008, 2015), which is converted to a  $k$  value internally in the design equations for convenience only. The different design procedures commonly used in the US, AASHTO (1972) to AASHTO (2015), PCA (1984), U.S. Department of Defense (2018), and FAA (2016), define and interpret input parameters differently. Table 13 provides a summary of these design guides and the input parameters used in each, along with notes on the direct and indirect test measurements/methods for these parameters.

**Table 13. Summary of rigid pavement design procedures and foundation layer input parameters**

Design Procedure	Input parameter(s)	Comments
PCA (1984)	Modulus of subgrade reaction ( $k$ )	<ul style="list-style-type: none"> <li>• <u>Direct Test Measurement</u>: Static 762 mm diameter plate load test per ASTM D1196 (nonrepetitive test).</li> <li>• <u>Indirect Test Measurement</u>: Empirical correlations with CBR or R-value tests.</li> </ul>
	Composite modulus of subgrade reaction ( $k_{comp}$ )	<ul style="list-style-type: none"> <li>• <math>k_{comp}</math> values are provided in the design guide to account for any addition of aggregate base/subbase layer, based on the <math>k</math> value and thickness of the aggregate base/subbase (treated/untreated) layer.</li> <li>• Design equations are calibrated for a <math>k</math> value determined at 1.27 mm (0.05 in.) of deflection and the corresponding applied load (Darter et al. 1995).</li> </ul>
	Drainage	<ul style="list-style-type: none"> <li>• Acknowledged to be a significant factor affecting performance but not addressed using a specific design factor.</li> <li>• A subsequent publication by ACPA (1995) provides guidance on drainage factors: “free-draining and daylighted subbases are reasonable alternatives to rapidly draining permeable subbases with edge drainage systems that often lack stability for long-term performance or cause other performance problems.” The ACPA publication suggests target permeability values for free-draining materials of 15 to 46 m/day [50 to 150 ft/day].</li> </ul>
	Uniformity	<ul style="list-style-type: none"> <li>• The design guide cross-references another PCA publication (later revised as ACPA 1995) for provisions on uniform support, which states that uniformity of the foundation is of utmost importance for performance.</li> <li>• ACPA (1995) provides guidance on achieving uniform support conditions through construction process control measures for expansive soils, frost-susceptible soils, pumping, and wet soils. The reference document also acknowledges that “providing uniformity” is “one of the largest challenges in the design and construction of any pavement structure.”</li> </ul>
AASHTO (1972)	Modulus of subgrade reaction ( $k$ )	<ul style="list-style-type: none"> <li>• <u>Direct Test Measurement</u>: Static 762 mm diameter plate load test per AASHTO T 221 (repetitive test).</li> <li>• <u>Indirect Test Measurement</u>: Local experience and correlations with other tests (the types of other tests are not specified).</li> <li>• Design equations are calibrated for gross <math>k</math> value (<math>k_G</math>) calculated from American Association of State Highway Officials (AASHTO) field plate load tests (Highway Research Board 1962) using total deformations at three different applied stress levels with three cycles at each level.</li> </ul>
	Drainage	<ul style="list-style-type: none"> <li>• The guide states that the design procedure assumes that provisions will be made for surface and subsurface drainage and that some situations may require special attention regarding the design and construction of drainage systems. No specific drainage design factor is used or target permeability values provided.</li> </ul>
	Uniformity	<ul style="list-style-type: none"> <li>• No specific design- or construction-related guidance is provided.</li> <li>• The guide states that the inclusion of subbases above the subgrade is to provide “uniform, stable, and permanent support.” It also states that the design equations assume “that uniform and high-quality construction will be obtained, particularly with respect to density, gradation, and quality of materials.”</li> </ul>



Design Procedure	Input parameter(s)	Comments
AASHTO (1986, 1993)	Effective modulus of subgrade reaction ( $k_{eff}$ ) corrected for LOS	<ul style="list-style-type: none"> <li><math>k_{eff}</math> is calculated using the following steps:               <ol style="list-style-type: none"> <li>Determine composite <math>k</math> value<sup>1</sup> using the subgrade resilient modulus (<math>M_r</math>), subbase layer modulus (<math>E_{SB}</math>), and the thickness of the subbase layer (<math>D_{SB}</math>) for each month of the year.</li> <li>Adjust <math>k_{comp}</math> for depth to the rigid foundation (if &lt; 3.3 m).</li> <li>Determine the relative damage based on projected pavement thickness and determine the yearly average <math>k_{eff}</math>.</li> <li>Adjust <math>k_{eff}</math> for potential LOS beneath the pavement.</li> </ol> </li> <li><u>Direct Test Measurement</u>: Subgrade <math>M_r</math> per AASHTO T 274<sup>2</sup> to convert to <math>k</math> value or static 762 mm diameter plate load test per ASTM D1196 or AASHTO T 222 or a similar procedure. <math>E_{SB}</math> determined per AASHTO T 274<sup>2</sup> with confinement control for unbound granular materials and per ASTM D4123 for stabilized materials with high strength/stiffness.</li> <li><u>Indirect Test Measurement</u>: Empirical correlations with CBR or R-value tests.</li> <li>The potential for LOS due to erosion, pumping, repetitive loading (settlement), and freeze-thaw effects is considered using the LOS factor (varying from 0 to 3) to adjust the <math>k</math> value. The value is selected by the designer based on the subbase layer type and the anticipated area of void beneath a slab area.</li> </ul>
	Drainage coefficient ( $C_d$ )	<ul style="list-style-type: none"> <li><math>C_d</math> is an index value selected based on the quality of drainage (i.e., time required for the water to drain) and the percent of time the pavement structure is exposed to moisture levels approaching saturation.</li> <li>The time required for the water to drain is calculated based on the pavement geometry, type of drainage features (daylighted or subdrain), the thickness of the base, and the saturated hydraulic conductivity of the material (<math>K_{sat}</math>).</li> <li><u>Direct Test Measurement</u>: No guidance is provided on direct measurement of <math>K_{sat}</math>.</li> <li><u>Indirect Test Measurement</u>: Estimated using gradation parameters.</li> </ul>
	Uniformity	<ul style="list-style-type: none"> <li>No specific design- or construction-related guidance is provided. The guide states that the inclusion of subbases above the subgrade is to provide “uniform, stable, and permanent support.”</li> </ul>
U.S. Department of Defense (2018)	Modulus of subgrade reaction ( $k$ )	<ul style="list-style-type: none"> <li><u>Direct Test Measurement</u>: Static 762 mm diameter plate load test per CRD-C 655 (USACE 1995) at 10 psi applied stress. The design method requires performing a large enough number of tests (at least two per subgrade type and condition) to determine an average value that provides confidence that the selected value is representative of in-place conditions. Field correction of saturation, per CRD-C 655 (USACE 1995) is required for soils that are subject to saturation and can be disregarded in areas where high saturation levels and erosion/pumping is not an issue in the pavements within the vicinity.</li> <li><u>Indirect Test Measurement</u>: Empirical correlations with CBR or R-value tests.</li> <li>For cases where a base layer is present, two options are provided. One is to perform static plate load tests directly on the base layer, and the other is to use a graphical procedure presented in the design guide to estimate a composite <math>k</math> value based on the subgrade <math>k</math> value and the thickness of the base layer.</li> </ul>
	Drainage	<ul style="list-style-type: none"> <li>Drainage is considered using base layers that meet the minimum gradation requirements and other drainage features included (e.g., subdrains).</li> </ul>
	Uniformity	<ul style="list-style-type: none"> <li>No specific design- or construction-related guidance is provided.</li> <li>Regarding subgrade support, the guide states that “[t]he subgrade should be compacted to provide uniformity of conditions and a working platform for placement and compaction of the subbase.”</li> <li>The design guide states that an important purpose of the aggregate base course layers is “to provide uniform long-term support to the slab with adequate drainage to prevent pumping and loss of support.”</li> </ul>

Design Procedure	Input parameter(s)	Comments
FAA (2016)	Elastic modulus ( $E$ ) of subgrade	<ul style="list-style-type: none"> <li>• <u>Direct Test Measurement:</u> Static 762 mm diameter plate load test per AASHTO T 222 (nonrepetitive test) to determine <math>k</math> value and calculate <math>E</math> (in units of psi) using <math>20.15 \times k^{1.284}</math> (<math>k</math> in units of psi/in.). The field <math>k</math> value must be corrected for future subgrade saturation.</li> <li>• <u>Indirect Test Measurement:</u> Empirical relationship with CBR.</li> </ul>
	Drainage (FAA 2013)	<ul style="list-style-type: none"> <li>• No drainage input parameter is needed. A minimum <math>K_{sat}</math> value of 305 m/day (1,000 ft/day) is recommended as a requirement where permeable base layers are used. Similarly, target <math>K_{sat}</math> values of 1,500 m/day (5,000 ft/day) for open-graded material and 300 to 1,500 m/day (1,000 to 5,000 ft/day) for rapid-draining material are recommended.</li> <li>• A minimum time requirement of 10 days to achieve 50% drainage is provided, with a provision to reduce the time to 24 hours with 85% drainage in areas with materials known to cause reduced pavement life.</li> </ul>
	Uniformity	<ul style="list-style-type: none"> <li>• No specific design- or construction-related guidance is provided.</li> <li>• The design guide assumes that “[t]he base layer provides a uniform, stable support for the rigid pavement slabs.”</li> </ul>
AASHTO (2008, 2015)	Resilient modulus ( $M_r$ )	<ul style="list-style-type: none"> <li>• Three levels of design inputs are suggested in AASHTO (2008, 2015). Level 1 includes direct measurement methods, while Levels 2 and 3 include indirect measurement methods or default values.</li> <li>• <u>Direct Test Measurement:</u> Selection of stress-dependent constitutive model parameters (<math>k_1</math>, <math>k_2</math>, and <math>k_3</math>) or determination of <math>M_r</math> at the anticipated field stresses. FWD is recommended for existing pavements, but the guide only provides a non-stress-dependent elastic modulus value (based on peak deformations and not resilient deformations) that is corrected to adjust for field conditions.</li> <li>• <u>Indirect Test Measurement:</u> Level 2 includes empirical correlations to estimate <math>M_r</math> from other test measurements such as CBR, DCP, and R-value. Level 3 includes using default or recommended <math>M_r</math> values based on the AASHTO soil classification.</li> <li>• <math>M_r</math> measurements selected during design using laboratory testing are obtained at optimal conditions (compacted to standard Proctor optimum moisture content and maximum dry density). Seasonal variations in <math>M_r</math> are analyzed within the design software using the Enhanced Integrated Climatic Model (EICM).</li> </ul>
	Drainage	<ul style="list-style-type: none"> <li>• A minimum drainage requirement of 305 m/day (1,000 ft/day) is recommended for the base layers. The same method to calculate time of drainage as discussed in AASHTO (1993) is provided as part of the drainage design documentation, but it is unclear how the information is used in the design process.</li> </ul>
	Uniformity	<ul style="list-style-type: none"> <li>• No specific design-related guidance is provided.</li> <li>• The design guide suggests considering use of thicker granular layers to “provide uniformity of support or act as a construction platform for paving.”</li> </ul>

<sup>1</sup> Darter et al. (1995) concluded that the top-of-the-base composite  $k$  value calculated using the nomograph procedure produces unrealistically high values and is not recommended for design. The authors noted that elastic  $k$  value ( $k_E$ ) determined in the AASHTO Road Test (Highway Research Board 1962) based on tests conducted directly on the subgrade are recommended for design input.

<sup>2</sup> Applicable only for subgrade (cohesive) materials. The test method was withdrawn from the AASHTO Standard Specifications in 1991 and was later replaced by AASHTO T 307, which is applicable for both cohesive and granular soils.

Another important foundation layer property that affects pavement performance is drainage. “Poor” drainage conditions can contribute to cracking and faulting distresses due to pumping,

erosion, and concrete durability problems. Drainage is generally addressed during design by specifying a minimum level of permeability/hydraulic conductivity of the base material along with drainage features (e.g., slopes, subdrains), except in AASHTO (1986, 1993), where a coefficient of drainage ( $C_d$ ) is used as the drainage design input parameter.

In the subsections that follow, an overview of the important geotechnical input parameters is provided, along with different direct and indirect measurement methods used in practice.

### *Modulus of Subgrade Reaction ( $k$ ) Value*

The modulus of subgrade reaction ( $k$ ) value is the key foundation layer input parameter in rigid pavement design (AASHTO 1972, 1986, 1993, 2008; PCA 1984). Selection of a particular subgrade modulus can have effects on the design of a pavement, and ensuring the selected value is achieved in the field during construction can have significant impacts on the costs associated with the future performance and maintenance of the roadway. Figure 42 illustrates how variability in the value of  $k$  affects the design life of a pavement.

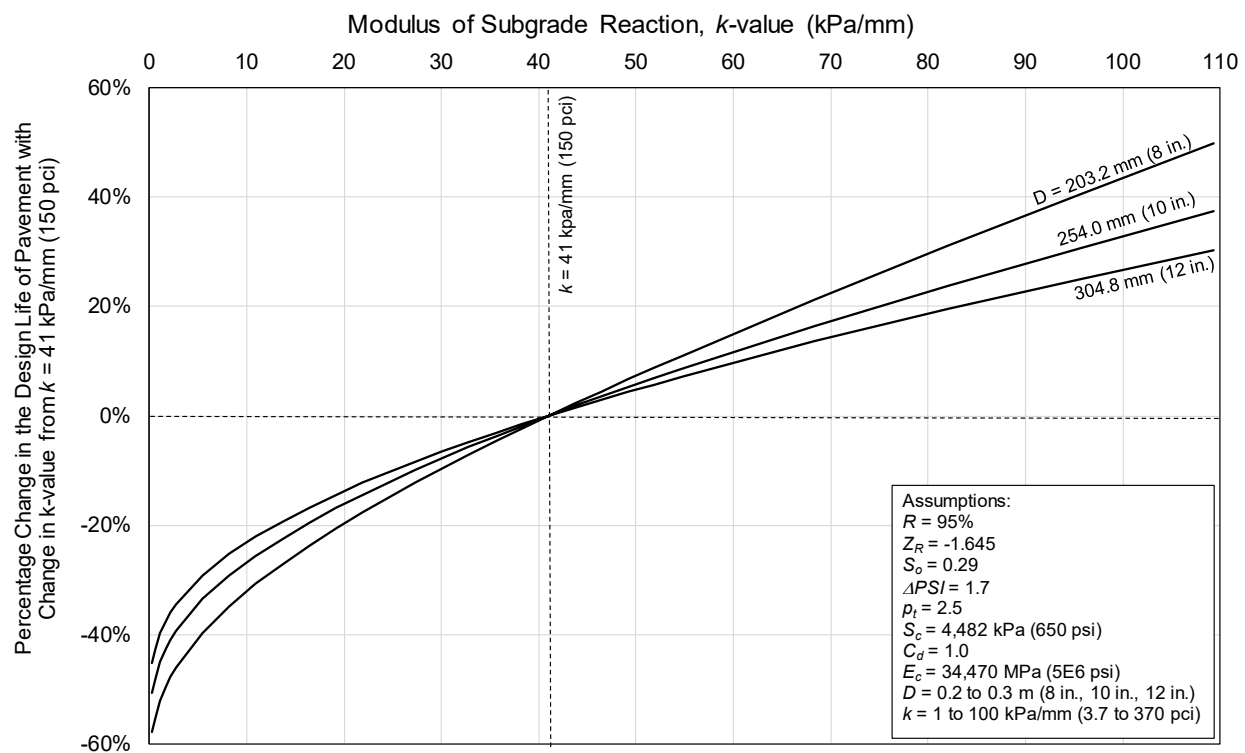


**Figure 42. Sensitivity of change in  $k$  value on the design life of a pavement using the AASHTO (1993) rigid pavement design procedure**

The design life presented in Figure 42 was calculated using the AASHTO (1993) rigid pavement design equation. A  $k$  value of 41 kPa/mm (150 psi/in.), which the Iowa DOT typically uses as the design input value in pavement design, was used as an arbitrary reference value to calculate the

percent change in design life while keeping all other input parameters constant. Clearly,  $k$  value is a significant factor in delivering long pavement life.

The AASHTO (1993) empirical expression that relates traffic volume, pavement structure, and pavement performance is shown in equation (1), and the input parameters used in the calculations are noted in Figure 42:

$$\log_{10}(W_{18}) = Z_R S_o + 7.35 \log_{10}(D + 1) - 0.06 + \frac{\log_{10}\left(\frac{\Delta PSI}{4.5-1.5}\right)}{1 + \frac{1.64 \times 10^7}{(D+1)^{8.46}}} + (4.22 - 0.32p_t) \log_{10} \left[ \frac{S_c C_d (D^{0.75} - 1.132)}{215.63 J \left( D^{0.75} - \frac{18.42}{(E_c/k)^{0.25}} \right)} \right] \quad (1)$$

where  $W_{18}$  = number of 18 kip ESALs,  $Z_R$  = standard normal deviate (function of design reliability level),  $S_o$  = overall standard deviation (function of overall design uncertainty),  $\Delta PSI$  = allowable serviceability loss at end of design life,  $p_t$  = terminal serviceability,  $k$  = modulus of subgrade reaction (pci),  $S_c$  = PCC modulus of rupture (psi),  $E_c$  = PCC modulus of elasticity (psi),  $J$  = empirical joint load transfer coefficient,  $C_d$  = empirical drainage coefficient, and  $D$  = PCC slab thickness (in.).

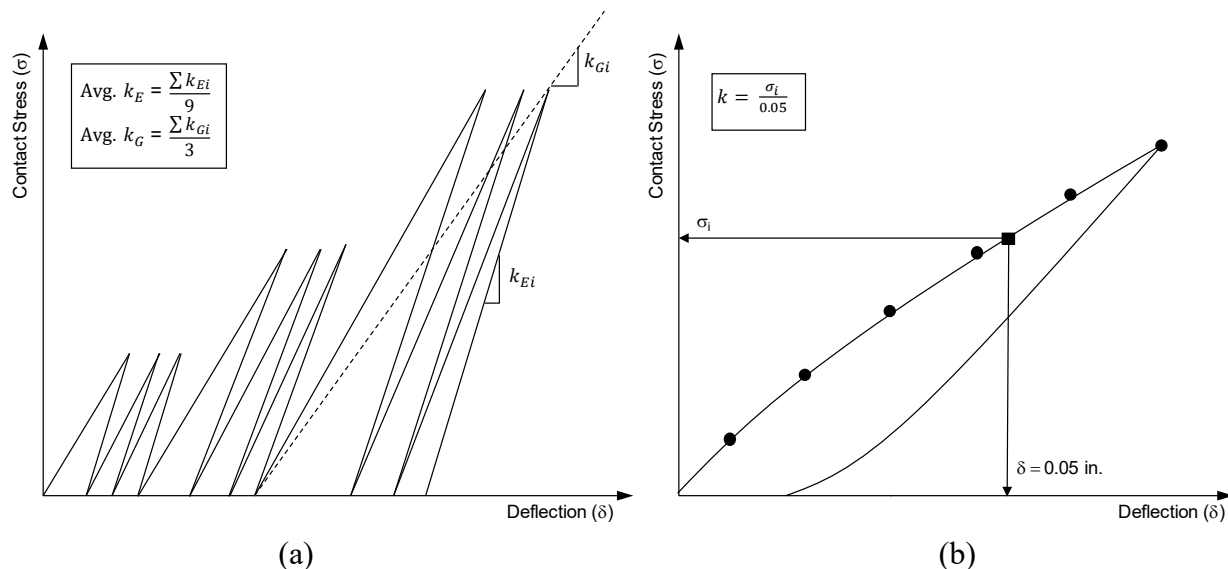
#### Direct Determination of $k$ Value on Foundation Layers

Plate load testing is considered the long-standing “gold standard” for measuring the  $k$  value. Its use has been well documented in the benchmark studies performed on airfields and highways from the 1930s to the 1980s by the Bureau of Public Roads, the U.S. Army Corps of Engineers, AASHTO, and several state agencies (Teller and Sutherland 1935a, 1935b, 1935c, 1936, 1943; USACE 1943, 1953; U.S. Departments of the Army and Air Force 1958; Highway Research Board 1962). These pioneering efforts from the 1930s to the 1980s established plate load testing as the primary method for determining the load-displacement relationship of the foundation layers and had a significant role in calibrating the pavement thickness design equations developed by AASHTO, PCA, and the U.S. Army Corps of Engineers.

Standardized test methods for direct measurement of the  $k$  value include the AASHTO T 222 or ASTM D1196 nonrepetitive static plate load test or the AASHTO T 221 or ASTM D1195 repetitive static plate load test, which are directly performed on the foundation layer. The AASHTO T 222 test setup requires the use of a 762 mm (30 in.) diameter loading plate that is stacked with a set of bearing plates arranged in a pyramid fashion that have diameters between 152 and 762 mm (6 to 30 in.).

Although the testing procedure has been standardized, the procedure for interpreting the results is mostly left to the user. When describing the  $k$  value, Terzaghi (1955) noted that “widespread among engineers” is the “erroneous conception” that the “numerical value of the coefficient of

subgrade reaction depends exclusively on the nature of the subgrade” and that without proper consideration of the test methods, “such values can be very misleading.” Therefore, it is important to understand the methods and interpretation procedures used in determining the  $k$  value and its role in the development of the original design equations. There are two main approaches to interpreting the  $k$  value, as illustrated in Figure 43, one per the AASHTO Road Test (Highway Research Board 1962) and the other per the U.S. Army Corps of Engineers method as used in the PCA (1984) design guide.



(a) Reproduced from Darter et al. 1995 and AASHTO 1972, 1986, and 1993 and (b) AASHTO T 222 and PCA 1984

**Figure 43. Interpretation of plate load testing results per (a) the AASHTO Road Test and AASHTO design procedures and (b) AASHTO and PCA design procedures**

The U.S. Army Corps of Engineers used a nonrepetitive incremental loading method to determine the  $k$  value, which was later standardized as the AASHTO T 222 procedure. The  $k$  value was defined using the applied stress corresponding to an average plate deformation of 1.27 mm (0.05 in.). This formed the basis of the PCA (1984) and the U.S. Army Corps of Engineers rigid pavement design procedures and has not changed much since the 1960s.

The AASHTO Road Test included repeated load-unload plate load testing. The testing included loading/unloading cycles at three stress levels (34.5 kPa [5 psi], 68.9 kPa [10 psi], and 103.4 kPa [15 psi]) using a 762 mm (30 in.) diameter loading plate (nine loading cycles in total). The  $k$  values were then determined using two procedures. The first procedure involved determining what is referred to as the elastic  $k$  value ( $k_E$ ) based on the rebound deformations for each loading cycle (excluding the permanent deformation) and then averaging the data for the nine cycles. The second procedure involved determining what is referred to as the gross  $k$  value ( $k_G$ ) based on the total deformation produced for each load level (at the end of the three loading cycles) and then averaging the data for the three load levels.

The AASHTO (1972) design guide states that the  $k_G$  value must be used during design. The later versions of the AASHTO design guide (AASHTO 1986, 1993) did not discuss whether to use  $k_E$

or  $k_G$ . The  $k_E$  value is higher than the  $k_G$  value. The magnitude of difference between these, however, depends on the stiffness of the material, degree of saturation, level of compaction, and stresses applied. It is not documented in the original AASHO reports (Highway Research Board 1962) or the AASHTO design guides published later (AASHTO 1972, 1986, 1993) whether the  $k_E$  or the  $k_G$  values were used in the correlations presented with other measurements such as CBR. As part of guidance provided with recommended revisions to the AASHTO (1993) design inputs, Darter et al. (1995) recommended the use of the  $k_E$  value as the design input.

Some design procedures provide guidance on increasing the  $k$  value for cases with a base layer placed above the subgrade layer and refer to the improved value as the composite  $k$  value. The composite  $k$  value is either experimentally determined (i.e., by directly measuring the  $k$  value over the base layer) or empirically estimated using procedures described in the pavement design guides (see PCA 1984 and AASHTO 1993). Darter et al. (1995) indicated that the top-of-the-base composite  $k$  value calculated using the nomograph procedure in AASHTO (1993) produced unrealistically high values and were not recommended for design. The results presented in Chapter 2 of this report also confirm this observation.

The manual methods of plate load testing are time consuming due to significant setup times, with heavy reaction loads often creating unsafe working conditions. Also, providing reproducible results from the manual methods can be difficult because of operator bias, i.e., lack of control in maintaining and applying loads. With advancements in automation, modern plate load testing methods have been developed. Recently, the Iowa DOT implemented an automated plate load test (APLT) to determine in situ  $k$  values as part of a statewide verification program (White et al. 2019b).

As an alternative to direct testing and simplification, several agencies have developed local empirical relationships between plate load test measurements and CBR values, R-values,  $M_r$  values, and other test results. Some of these empirical relationships are discussed in the following subsections.

#### Empirical Methods to Estimate $k$ Value

Three primary sources of empirical relationships are currently used in practice by pavement engineers:

- A web-based application tool provided by the ACPA, <http://apps.acpa.org/applibrary/KValue/>
- A regression relationship based on experimental data in U.S. Department of Defense (2018) and previously modified by Barker and Alexander (2012)
- A theoretical relationship using elastic analysis to convert  $M_r$  to  $k$  values developed by AASHTO (1993)

The ACPA's web-based application converts subgrade layer  $M_r$  values to  $k$  values and vice-versa. The ACPA's relationships were developed to estimate values that are considered

“expected or reasonable” in practice (personal communication, R. Rodden, December 6, 2012). The relationships are not based on independent experimental testing. The web-based application also calculates the composite  $k$  value (e.g., subbase aggregate layer over subgrade) if the subgrade layer  $M_r$  and the subbase layer thickness are provided. The calculation procedure is based on a nomograph and regression equations presented in the AASHTO (1993) pavement design manual. Some variations of this nomograph are included in the *Airfield Design Manual* published by the U.S. Departments of the Army and the Air Force (1979).

The *O&M Manual: Asphalt and Concrete Pavement Maintenance and Repair* (U.S. Department of Defense 2018) includes a figure showing a log-log relationship between the  $k$  value and subgrade  $M_r$  with some experimental data. There is no reference to the source of the relationship in the manual or other information related to (a) the stresses used in determining the  $k$  value and the  $M_r$  value, (b) how  $M_r$  was determined, or (c) what plate size(s) were used in the tests. These factors significantly affect the estimated  $k$  value. A report published by the U.S. Army Corps of Engineers (Barker and Alexander 2012) reported the power relationship shown in equation (2) for the experimental data published in U.S. Department of Defense (2018), where  $M_r$  is in units of psi and  $k$  value is in units of psi/in., with an  $R^2$  of 0.899 and no estimate reported for standard error in the prediction.

$$M_r = 26(k)^{1.284} \quad (2)$$

The AASHTO (1993) pavement design guide provides equation (3), which shows a linear relationship between  $M_r$  and  $k$  value. The relationship was developed using the results of an elastic layer program simulating loading from a 30 in. diameter flexible plate and determining the displaced volume (based on the deflection basin) of the soil directly beneath the plate (see AASHTO 1986 Vol. II). It was indicated therein that by measuring the volume of displaced soil instead of the plate deformations near the edge (as in the case of a static plate load test on a rigid plate), the calculated  $k$  values would be similar to what would result when loading using a rigid plate.

$$M_r = 19.4(k) \quad (3)$$

One can arrive at a similar relationship as that expressed in equation (3) by using the classical Boussinesq’s solution shown in equation (4). This equation relates plate deformations beneath a circular rigid footing to soil elastic modulus ( $E$ ) by assuming a Poisson’s ratio ( $\nu$ ) of 0.4, a shape factor ( $f$ ) of  $\pi/2$  (rigid plate over cohesive soils), and a loading plate radius ( $a$ ) of 15 in.

$$E = (1 - \nu^2) fak = 19.8 k \quad (4)$$

A difference to note between equations (3) and (4) is the use of  $E$  in equation (4) versus  $M_r$  in equation (3), which are often incorrectly assumed to be the same value.  $M_r$  is calculated using recoverable/resilient deformation, while  $E$  is typically calculated using total or peak deformation. Total or peak deformation includes both recoverable and permanent deformations. Permanent

deformation is almost always ignored in the selection of design input values, leading to the assumption that pavement foundations behave elastically, which is not exactly the case.

Field experience with in situ static and cyclic plate load testing suggests that achieving purely elastic behavior in situ is not achievable for natural/unstabilized geomaterials. Based on the authors' experience with repeated plate load tests in the field, a near-linear elastic behavior is achievable and is typically only observed after applying approximately 500 to 20,000 or more load-unload cycles, depending on the stress conditions and the compaction state of the materials.

The following are additional inherent assumptions behind the empirical relationships listed above that pavement design engineers should consider:

- The multiplication factor of 19.79 in equation (4) or 19.4 in equation (3) is valid only for a given set of  $\nu$ ,  $f$ , and  $a$  parameter values. Shape factor ( $f$ ) values vary between  $\pi/2$  (1.57) and  $8/3$  (2.67), depending on the type of material that is tested and the plate rigidity (see the discussion on factors in Ullidtz 1987 and Vennapusa and White 2009). Varying the  $f$  value alone changes the multiplication factor between 19.4 and 33.6.
- Unless both the  $M_r$  and  $k$  value tests are performed with the exact same plate size and under similar stress conditions and the tested soil profile is homogenous, comparisons of measurement values can be significantly affected by the differences in the influence depths of the two measurements. This difference can be exacerbated if the comparisons are made between the results of a field  $k$  value test and a laboratory  $M_r$  test because the laboratory test cannot truly simulate the in situ conditions, especially for layered materials.

The relationship between  $M_r$  and  $k$  value identified by Barker and Alexander (2012) for the data published in U.S. Department of Defense (2018), as shown in equation (2), is compared to the AASHTO (1993) relationship, shown in equation (3), and the relationship used by the ACPA web application in Figure 44.



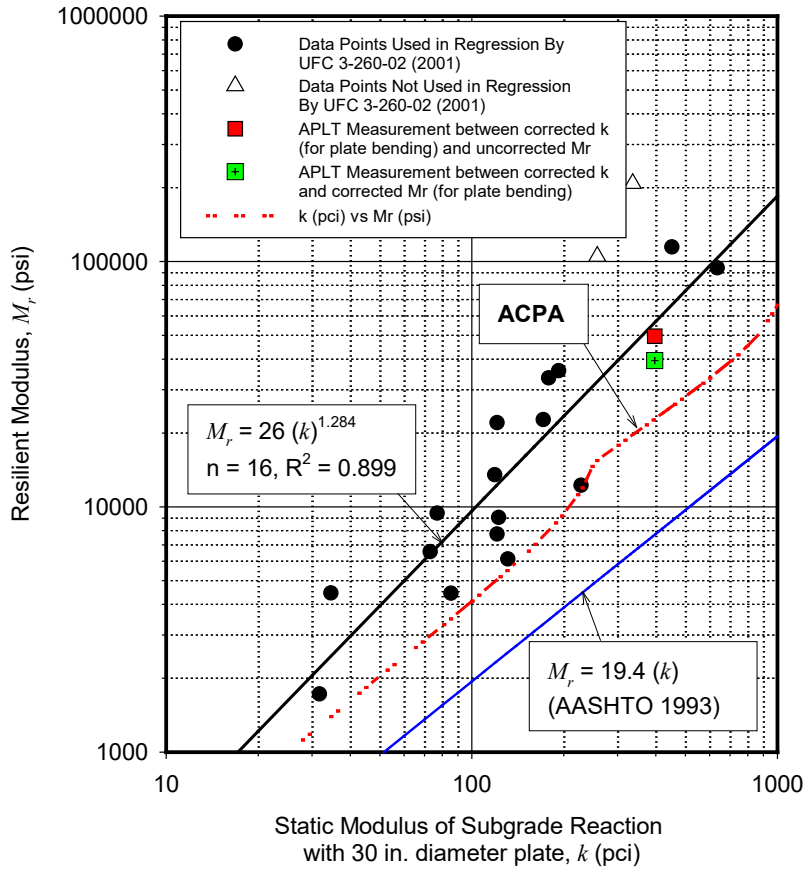


**Figure 44. Comparison of the relationships between  $M_r$  and  $k$  value obtained from U.S. Department of Defense (2018), AASHTO (1993), and the ACPA web-based prediction tool**

The relationship used by the ACPA web application is shown as the red dashed line in Figure 44. Since the relationship used in the ACPA web application has not been published, the line was generated using data points calculated for a range of selected  $M_r$  values. The relationship used in the ACPA web application predicts values that are in the range of values predicted using equation (2) and equation (3).

Various regression relationships between CBR and  $k$  values have been documented in the literature since the 1940s, mostly based on work performed by the U.S. military. Barker and Alexander (2012) and Darter et al. (1995) provide a historical overview of how and when the different relationships were derived. These relationships appeared in various technical manuals published by the U.S. Army Corps of Engineers (Barker and Alexander 2012 and USACE 1966) and in Packard (1973) and are shown in equations (5) through (8). The relationships are applicable for cohesive soils.

$$\text{Barker and Alexander (2012): } k = 20(\text{CBR}) \quad (5)$$

$$\text{USACE (1966): } k = 49.94(\text{CBR})^{0.7685} \text{ for soils with LL} > 50 \quad (6)$$

$$\text{USACE (1966): } k = 30.387(\text{CBR})^{0.7897} \text{ for soils with LL} < 50 \quad (7)$$

$$\text{Packard (1973): } k = 53.438(\text{CBR})^{0.5719} \quad (8)$$

Hall et al. (1997) presented guidelines for converting CBR to equivalent static  $k$  values backcalculated from FWD testing, which is a dynamic test developed to measure peak deflections under dynamic loading. Based on the data available from test sections studied under the nationwide Long-Term Pavement Performance (LTPP) program, Hall et al. (1997) presented midrange, upper bound, and lower bound values to predict the equivalent static  $k$  values from CBR measurements (Figure 45). It was not reported therein whether the CBR values were obtained directly from a field CBR test or estimated from other tests.

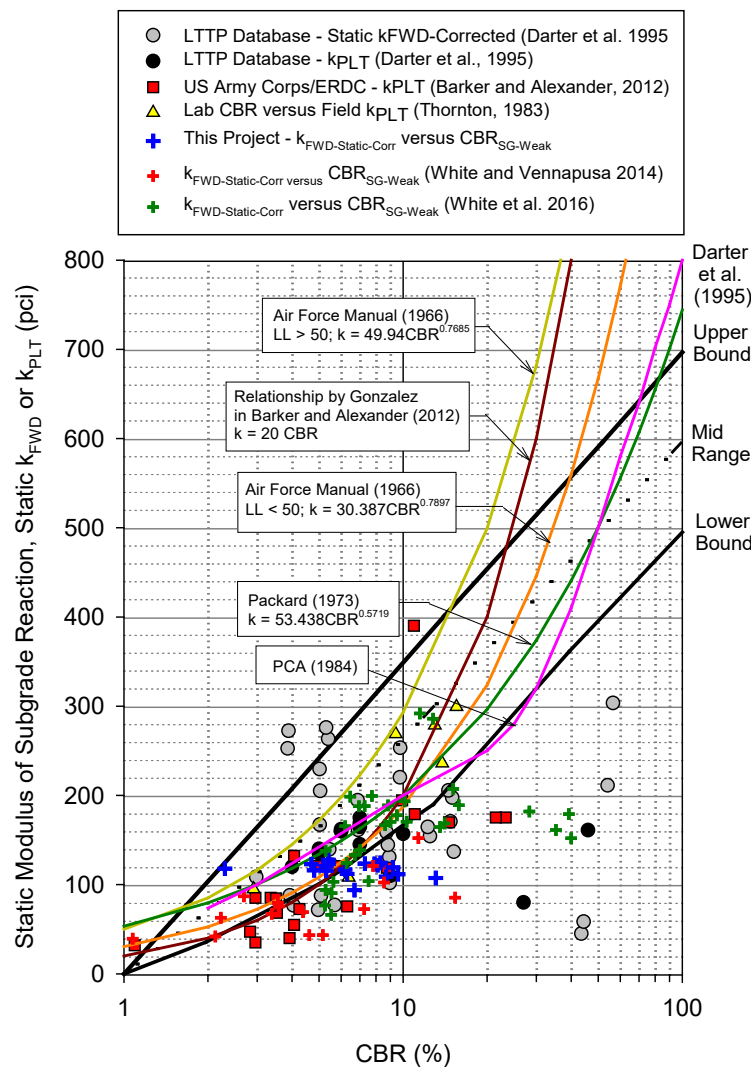


**Figure 45. Relationships between  $k$  and CBR published in the literature and data points from the present study and others (1 pci = 0.27 kPa/mm)**

Figure 45 shows a compilation of experimental test results available in the literature comparing CBR and  $k$  values determined from both static PLT and FWD testing. The CBR values in the plot were obtained using direct field CBR tests and DCP tests. The results from the different field project sites from the present study (PLT and DCP tests) are also included in Figure 45. The scatter in the experimental test results and the variations between the different relationships published over the years present a high degree of uncertainty associated with estimating the  $k$  values from CBR measurements.

Many factors contribute to the high degree of uncertainty and lack of correlations when it comes to the selection of pavement foundation parameters:

- High inherent variability between the different project conditions and materials
- Large differences in the stresses used to determine  $k$  values among the various studies and failure to account for stress dependencies in the interpretation
- Poor documentation of the differences in the CBR measurement/estimation for each study (e.g., direct field CBR measurement versus an estimated value from DCP test measurement)
- Limited empirical data that directly compare backcalculated equivalent static  $k$  values from FWD testing to the true static plate load testing used in many of the original pavement evaluation studies
- Failure to account for the large discrepancy in the volume of soil measured during a field CBR test versus a  $k$  value test. The 30 in. diameter plate used in  $k$  value testing represents a measurement influence depth of about 60 in. (two times the plate diameter). The measurement influence depth of a CBR test is on the order of a few inches.

#### Estimation of $k$ Value from FWD Testing on PCC Surface Layers

To estimate the  $k$  value of the foundation layer beneath an existing concrete pavement, FWD tests are often performed. An FWD test involves applying and measuring a dynamic load and the corresponding deflection basin via sensors placed at defined distances away from the loading plate. The load and deflection basin data are analyzed to estimate the foundation layer  $k$  value.

The commonly used analysis method to estimate the  $k$  value from FWD data is the AREA method, originally proposed by Hoffman and Thompson (1981) and described in AASHTO (1993). The AREA method in AASHTO (1993) uses deflection data from four sensors, while variations of the method use data from three, five, or seven sensors (see Substad et al. 2006, Smith et al. 2007, McPeak et al. 1998). This method assumes that the pavement slab and the subgrade are horizontally infinite. However, this assumption leads to an underestimation of the  $k$  values for jointed pavements. Theoretical corrections for a finite square slab are provided by Croveti (1994), and the approach has been further developed for a rectangular slab by Darter et al. (1995). Nevertheless, these procedures do not account for load transfer to adjacent slabs.

The  $k$  value estimated from FWD testing and the AREA method is referred to as the dynamic  $k$  value ( $k_{\text{FWD-Dynamic}}$ ). AASHTO (1993) suggests dividing the  $k_{\text{FWD-Dynamic}}$  value by a factor of 2 to determine the equivalent static  $k$  value ( $k_{\text{FWD-Static}}$ ). The origin of this factor of 2 dates to field testing results reported in Foxworthy (1985), wherein comparisons were reported between the

$k_{\text{FWD-Dynamic}}$  values obtained from a Dynatest Model 8000 FWD and  $k$  values ( $k_{\text{PLT}}$ ) obtained from static plate load tests using a 762 mm (30 in.) diameter plate. Foxworthy (1985) used the AREA-based method to calculate  $k_{\text{FWD-Dynamic}}$ , while the procedure followed to calculate  $k_{\text{PLT}}$  is not reported. The results obtained from Foxworthy's (1985) study (Figure 46) are based on seven FWD tests conducted on PCC pavements with slab thicknesses varying from about 254 to 648 mm (10 to 25.5 in.) and plate load tests conducted on the foundation layer immediately beneath the pavement.

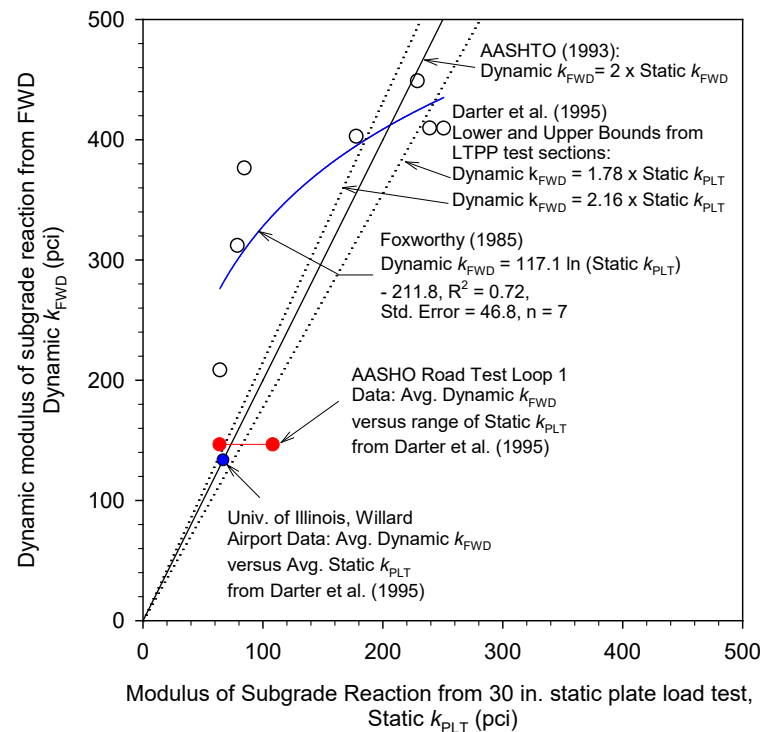


**Figure 46. Static  $k_{\text{PLT}}$  values versus  $k_{\text{FWD-Dynamic}}$  measurements reported in the literature**

A few of these sections consisted of a 127 to 305 mm (5 to 12 in.) thick base course layer and some did not. The subgrade layer material consisted of CL soil from Sheppard Air Force Base in Texas, SM soil from Seymour-Johnson Air Force Base in North Carolina, and an unspecified soil type from McDill Air Force Base in Florida. No slab size correction was performed. Data from Foxworthy (1985) yielded a logarithmic relationship between the dynamic and static  $k_{\text{PLT}}$  values, as shown in Figure 46. On average, the  $k_{\text{FWD-Dynamic}}$  values were about 2.4 times higher than the  $k_{\text{PLT}}$  values. Darter et al. (1995) compared the FWD test data and  $k_{\text{PLT}}$  values from eight LTPP test sections and reported factors ranging from 1.78 to 2.16, with an average of 1.91.

Recently, Jeffrey Roesler at the University of Illinois at Urbana-Champaign conducted FWD testing on two concrete pavement sections to estimate the  $k_{\text{FWD}}$  values and compare those to the  $k_{\text{PLT}}$  values measured using a 762 mm (30 in.) diameter plate directly on the foundation layers in the same sections. The  $k_{\text{PLT}}$  values were obtained in the sections prior to paving. The results, reported in White et al. (2019a), showed that the  $k_{\text{FWD}}$  values were about four times higher and were less variable than the  $k_{\text{PLT}}$  values. It was noted in White et al. (2019a) that “[s]ince FWD

tests were performed on the completed pavement structure, the larger load distribution and lower stress states on the foundation layers from FWD tests likely resulted in less measured foundation layer variability than what is present.” Thus, there is a disconnect between FWD backcalculation and true static k value tests performed on the subgrade.

### *Foundation Layer Resilient Modulus*

The use of the  $k$  value from static plate load tests is based on pavement responses to static loading. Several researchers as a part of the Arlington Road Test and AASHTO Road Test conducted repeated plate load tests with several load repetitions. Documenting the results of repetitive load testing from the Arlington Road Test, Teller and Sutherland (1936) reported that the goal of the test was to “reach a condition such that each succeeding application of a given load would produce the same vertical displacement of the bearing plate. This might be termed a state of approximate elastic equilibrium.” While at that time they did not refer to the modulus calculated using deformations in elastic equilibrium as the resilient modulus, their important work along with other contributions over the years focused on characterizing the resilient modulus of the subgrade, particularly for flexible pavements (Groeger et al. 2003). The initial work focused on measuring  $M_r$  from repeated field load tests, which was considered expensive and time consuming to perform, so the focus transitioned later to fast and inexpensive repeated loading triaxial tests in the laboratory (Vinson 1989).

The mechanistic analysis of pavements and characterization of the influence of the foundation layers, although these have improved over the years, are still based on layered elastic analysis theory. In elastic analysis, the layer modulus is characterized by considering only the elastic deformations, also referred to as the resilient deformations. Therefore, resilient modulus ( $M_r$ ) is considered the key input parameter in estimating the stresses, strains, and deflections in the pavement system, whether flexible or rigid. For this reason, the new procedure used by AASHTOWare Pavement ME Design considers  $M_r$  to be the primary input parameter, though the selection of the  $M_r$  value is mostly empirical and FWD testing has become the test of choice for estimation.

It is well known and understood that  $M_r$  is a highly stress-dependent parameter, and most soils exhibit the increasing stiffness with increasing bulk stress and decreasing stiffness with increasing shear stress. The results from a test that involves applying a series of cyclic deviator and confining stresses can be used to model behavior using the universal model (AASHTO 2015), shown in equation (9).

$$M_r = k_1^* P_a \left( \frac{\theta}{P_a} \right)^{k_2} \left( \frac{\tau_{oct}}{P_a} + 1 \right)^{k_3} \quad (9)$$

where  $M_r$  = resilient modulus (psi),  $P_a$  = atmospheric pressure (psi),  $\theta$  = bulk stress (psi) =  $\sigma_1 + \sigma_2 + \sigma_3$ ,  $\sigma_3 = \sigma_2$ ,  $\nu$  = Poisson’s ratio,  $\tau_{oct}$  = octahedral shear stress (psi) =  $\sqrt{(\sigma_1 - \sigma_2)^2 + (\sigma_2 - \sigma_3)^2 + (\sigma_3 - \sigma_1)^2} / 3$ , and  $k_1$ ,  $k_2$ , and  $k_3$  = regression coefficients.

The  $k_1$  coefficient is proportional to  $M_r$  and therefore is always  $> 0$ . The  $k_2^*$  coefficient explains the behavior of the material with changes in the bulk stresses. Increasing the bulk stress increases the  $M_r$  value, and therefore the  $k_2^*$  coefficient should be  $\geq 0$ . The  $k_3^*$  coefficient explains the behavior of the material with changes in the shear stresses. Increasing the shear stress softens the material and decreases the  $M_r$  value. Therefore, the  $k_3^*$  coefficient should be  $\leq 0$ . Many other forms of stress-dependent models are available in the literature.

In AASHTOWare Pavement ME Design (AASHTO 2015), it is recommended that  $M_r$  be determined using laboratory testing (AASHTO T 307) for new projects and estimated using FWD for rehabilitation projects. Laboratory testing provides a controlled set of data at different stress combinations to develop the regression parameters used in the universal model (equation 9). While laboratory testing can provide baseline measurements that can be used in design, the boundary conditions are typically nonrepresentative of the in situ conditions. As a simplification and alternative to laboratory testing,  $M_r$  is often obtained from empirical correlations with soil classification, CBR values, or Hveem R-values. AASHTO (2015) allows the use of empirical relationships as part of Level 2 and Level 3 design, which deviates from mechanistic solutions that involve using empiricism to select the inputs.

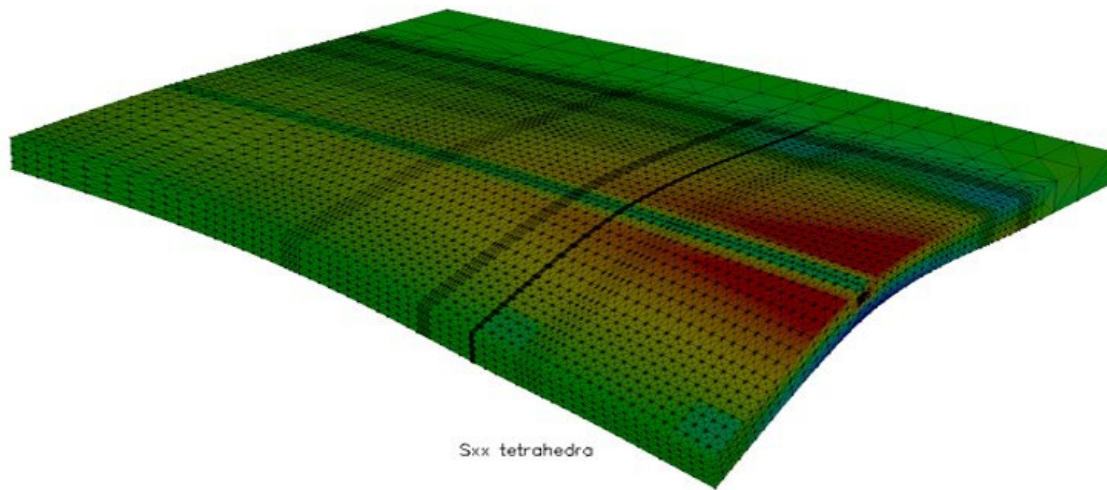
In situ  $M_r$  is often estimated from nondestructive tests, including FWD or LWD. As noted previously, in practice the elastic/deformation moduli values calculated from these test devices based on elastic (total) deformations are often confused with  $M_r$  values, which are based on resilient (i.e., recoverable) deformation. The limitations of these nondestructive tests for  $M_r$  include (1) the lack of a conditioning stage prior to testing and (2) a limited ability to maintain contact stress during unloading, which is considered critical during laboratory testing.

During pavement construction, pavement foundation materials are subjected to relatively high loads from construction traffic and compaction equipment. In response to these loads, aggregate particles rearrange themselves, resulting in greater density, greater stress, and greater stiffness. For this reason, it is important to apply conditioning load cycles prior to testing to determine in situ  $M_r$ , which is not possible with conventional FWD testing.

Once surface paving is complete, the pavement foundation below is confined by the overlying pavement layers. The response of the pavement foundation to subsequent repeated traffic loading is both nonlinear and stress dependent, and therefore the effect of confinement is an important condition to consider in a field-based  $M_r$  test. In a recent study, the Iowa DOT implemented the APLT as part of a statewide testing program to determine in situ  $M_r$  values and developed a database of in situ universal model parameters (per equation 9) for individual and composite layer systems (White et al. 2019b). In situ cyclic plate load tests overcome many of the recognized limitations of laboratory testing (e.g., boundary conditions, changes in particle packing from reconstituted samples, particle size limitations) in matching field conditions, especially for layered unbound layers (e.g., aggregate base over soft subgrade). Real-world field variability also creates a challenge for laboratory test results to be considered representative.

### *Nonuniformity and Loss of Support*

Pavement design procedures, even the modern AASHTOWare Pavement ME Design (AASHTO 2015), do not address how to quantify and account for the nonuniform support conditions that exist in situ. Cracks in the PCC pavement layer are formed due to excessive deformations under loading (see Figure 47), and those cracks are exacerbated if nonuniform conditions exist beneath the pavement.



Brand et al. 2014

**Figure 47. Deformed shape and stress contours for slabs with surface-initiated cracks and edge loading**

White et al. (2005) assessed the effect of nonuniform subgrade support on critical pavement responses. The results of the analysis showed that the maximum principal stresses and deflections were reduced in the pavement when a uniform subgrade was present, which thereby increased the fatigue life of the slab. Nonuniform support conditions resulted in a decrease in the predicted fatigue life of the pavement compared to the predicted fatigue life for the assumed uniform support. A more detailed 2D and 3D finite element analysis was conducted as part of the present study to further examine the impacts of nonuniform support conditions on the tensile stresses that develop in the pavement (Brand et al. 2014). Overall, the results showed that certain nonuniform support conditions under concrete slabs can produce much higher tensile stresses than uniform support conditions, particularly when considering different loading positions and curling conditions, soft support along the pavement edge, and preexisting cracks.

One of the early efforts to understand how nonuniform support conditions impact concrete pavements was documented by Leonards and Harr (1959). Their focus was on addressing the issue of LOS due to slab curling. Later, others published analytical solutions and finite element analyses to evaluate slabs over a void (Richart and Zia 1962, Hudson and Matlock 1966, Huang 1974). Their results showed that LOS greatly increases slab deflections. The LOS caused by curling/warping is typically addressed through joint spacing.

Other causes of LOS include erosion of the base/subgrade and settlement or consolidation (or irrecoverable differential permanent deformations) of the foundation layers. AASHTO (1986) addressed LOS due to erosion during design, and AASHTOWare Pavement ME Design also addresses the erosion issue, through the selection of appropriate materials beneath the pavement. However, the impacts of irrecoverable permanent deformations caused from repeated loading has not been well studied or addressed in terms of design. The results of FE analyses with different LOS conditions are documented in Chapter 2. Figure 48 shows an example case of a pavement experiencing LOS due to permanent deformation at the corner (a gap is modeled beneath the pavement); the pavement is subjected to 18 kip single-axle corner loading with two different support values ( $k = 41 \text{ kPa/mm}$  and  $136 \text{ kPa/mm}$ ).

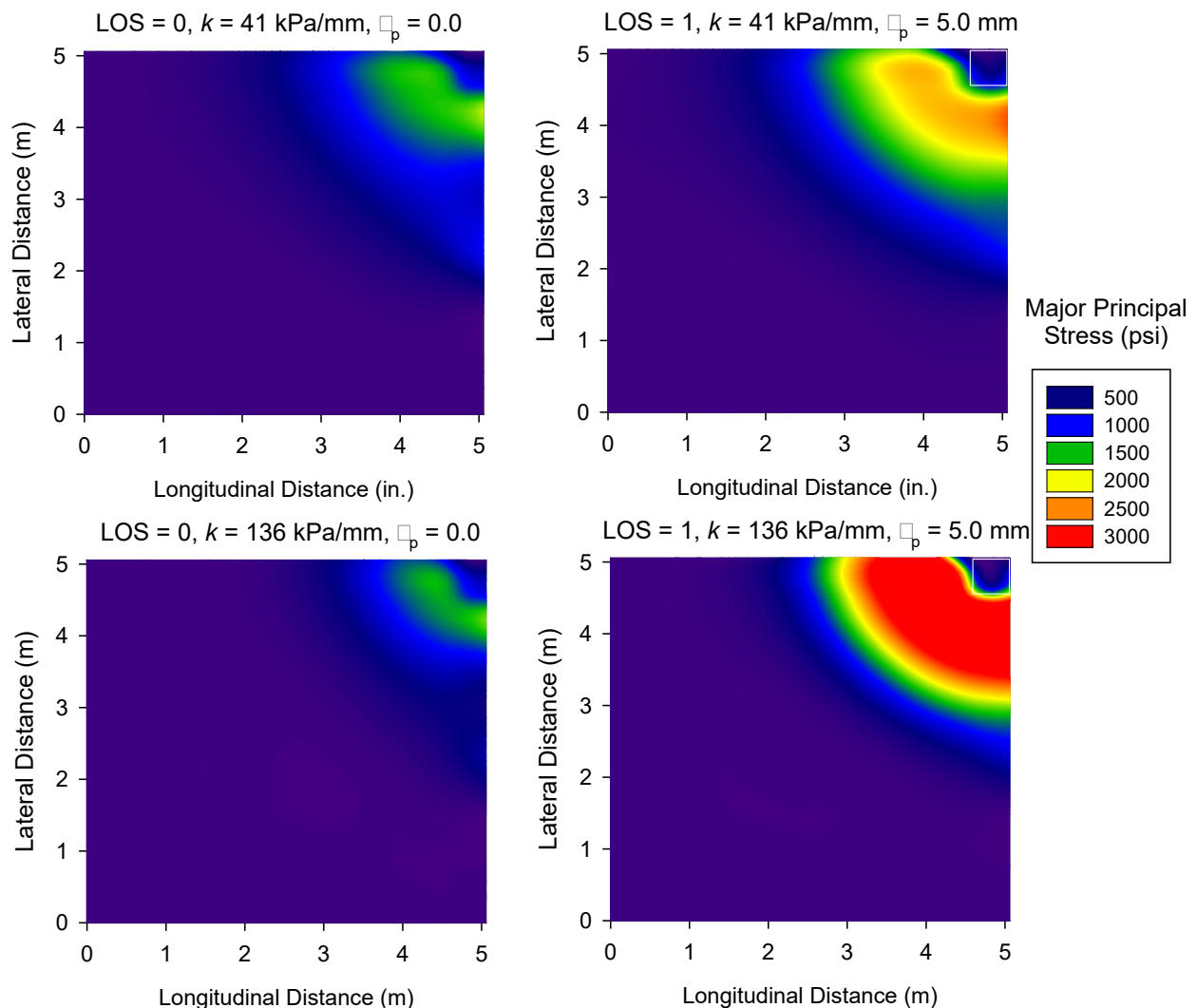


**Figure 48. Color contours of major principal stresses in a jointed concrete slab (200 mm [8 in.] thick) subjected to 80 kN (18 kip) AASHTO single-axle dual-wheel loading, with different  $k$  values and a gap modeled beneath the slab when LOS = 1**



The results show an increased concentration of high principal stresses near the corner, indicating the potential for corner cracking, which is a common type of distress in PCC pavements with poor foundation support.

Nonuniform support and localized irrecoverable permanent deformations leading to LOS can significantly reduce the fatigue life of the pavement. Currently, addressing these issues in design is complex and impractical. The issue of nonuniformity must be addressed during construction by establishing maximum levels of variability that are considered adequate for support and by avoiding localized areas with sharp transitions in support conditions.

### *Influence of Seasonal Variations*

Post-construction changes in saturation levels in the foundation layers are inevitable due to seasonal changes in wetting-drying or freezing-thawing. The level of variation depends on the geographic location, material type, layer boundary conditions, and depth of the layer in the pavement structure. AASHTO's Pavement ME Design currently addresses seasonal variations through the Enhanced Integrated Climatic Model (EICM), which incorporates regional databases of climatic changes and assumed moisture variations and their potential effects on moduli values through empirical equations (AASHTO 2015). The 1993 version of the AASHTO pavement design guide (AASHTO 1993) addresses seasonal variations by assigning a modulus value for each month. Some other pavement design procedures (e.g., FAA 2016, PCA 1984) conservatively assume design moduli values of materials in the saturated state.

Regardless of the design method chosen, it is well known that modulus/stiffness properties are significantly influenced by the degree of saturation. The value assumed during design is not a singular value but is a stress-dependent and moisture/saturation-dependent value. Therefore, any field modulus/stiffness measurements taken at the time of construction under in-place conditions must be adjusted according to the assumptions made during design for the anticipated saturation levels.

In the discussion below, four different methods cited in the literature to account for post-construction changes in moisture content are summarized.

#### 1-D Odometer Consolidation Test Method

The design input values for modulus in the FAA (2016) and the PCA (1984) procedures are based on a “saturated” subgrade condition. The justification provided in the FAA (2016) design guide for this assumption is that traffic must be supported during seasonal periods of high moisture (e.g., the spring season) and that most foundations tend to reach nearly complete saturation after about three years.

The use of static PLTs to determine  $k$  values is discussed in the FAA design guide, and these values are corrected for saturation using a 1-D odometer consolidation test procedure described in AASHTO T 222. The procedure involves conducting 1-D odometer tests on two soil samples

obtained from the field—one in a saturated and the other in an unsaturated condition—to determine the correction factor ( $F_{Saturation}$ ) for the  $k$  values.

$$F_{Saturation} = \frac{d}{d_s} + \frac{h}{75} \left( 1 - \frac{d}{d_s} \right) \quad (10)$$

where  $d$  = deformation of the odometer sample at the in situ moisture content under a unit load of 68.9 kPa (10 psi) (in.),  $d_s$  = deformation of the saturated odometer samples under a unit load of 68.9 kPa (10 psi) (in.), and  $h$  = thickness of base course material (in.).

Equation (10) was originally developed by the U.S. Army Corps of Engineers for use as a reference applied stress corresponding to 1.27 mm (0.05 in.) of plate deformation during in situ  $k$  tests (Barker and Alexander 2012). However, Barker and Alexander (2012) added that for a given material, the correction factors would not be significantly different if the ratio of applied pressures at a constant deformation is used instead of the ratio of deformations. The  $h/75$  portion of equation (10) concerns the thickness of the base material above the subgrade. When tests are conducted on the surface of a base, the  $F_{Saturation}$  value varies from the ratio of deformations ( $d/d_s$ ) when no base is present to no correction ( $F_{Saturation} = 1$ ) when the thickness of the base is 1.9 m (75 in.). This means that subgrade saturation does not influence the  $k$  values if the base layer is greater than 1.9 m (75 in.) thick, which is about 2.5 times the diameter of the plate (762 mm [30 in.]).

Based on in situ tests conducted at a Vicksburg, Mississippi, test facility by the U.S. Army Corps of Engineers, Barker and Alexander (2012) found that typical values of  $F_{Saturation}$  are 0.6 and 0.8 for clays and silts, respectively. This procedure is only applicable for cohesive materials, and, per AASHTO T 222 and Barker and Alexander (2012), corrections are not required for free-draining base/subbase materials. Other studies have shown that granular materials are also influenced by the degree of saturation. However, the level of influence depends on the gradation properties of the materials (Bilodeau and Dore 2011, Cary and Zapata 2010, Lytton et al. 2019).

This method is simple to implement when developing saturation correction factors. It can be applied to  $k$  values from static PLTs as well as resilient modulus ( $M_r$ ) values from cyclic PLTs. However, there are limitations with this test procedure: (a) it is applicable only for nongranular materials, (b) the correction factors represent only one set of stress conditions (10 psi applied load), (c) there is no control over the level of saturation that is achieved in the soaked sample, and (d) the correction factor can only be obtained for one change in saturation level per test. If field tests from a site show significant differences in the in situ moisture and dry density measurements, multiple sets of tests are needed to develop test location-specific correction factors.

#### Gradient Method Based on Laboratory $M_r$ Tests

The gradient method, described in Drumm et al. (1997) and defined in equation (11), is used to determine the  $M_r$  values after post-construction saturation.

$$M_{r(wet)} = M_{r(opt)} + \frac{dM_r}{dS} \Delta S \quad (11)$$

where  $M_{r(wet)}$  = resilient modulus at increased post-compaction saturation,  $M_{r(opt)}$  = resilient modulus at optimum moisture content and maximum dry density or alternatively at in situ moisture content and dry density ( $M_{r(insitu)}$ ),  $dM_r/dS$  = gradient of the resilient modulus with respect to the saturation or slope of  $M_r$  versus the degree of saturation curve, and  $\Delta S$  = change in post-compaction saturation expressed as a decimal.

Per the test procedure described in Drumm et al. (1997), three replicate samples that are prepared and compacted to a desired moisture content and dry density (described in the paper as optimum moisture content and maximum dry density) are needed. Two of the three samples are backsaturated using a triaxial cell by applying backpressure to two different target saturation levels. All three samples are then stored in a moist curing room for seven days and are tested for  $M_r$  at different stress cycle combinations (using the LTTP P46 procedure). The gradient ( $dM_r/dS$ ) value is determined by plotting the  $M_r$  results (for a given stress sequence) versus degree of saturation.

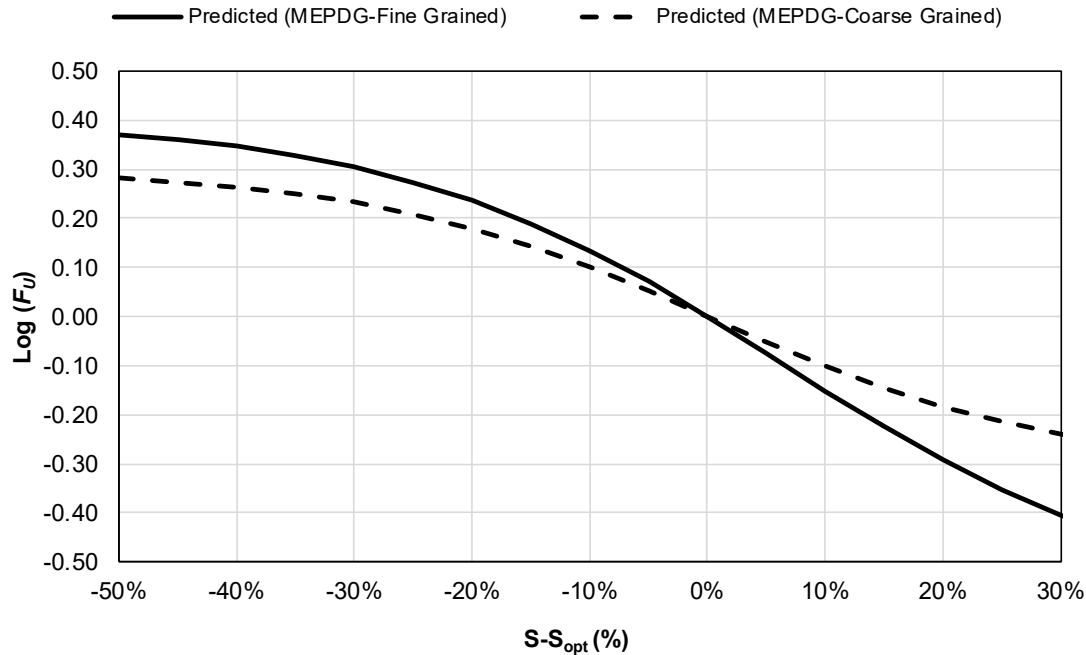
Drumm et al. (1997) described the results for nongranular materials, but the method can also be applied to granular materials. The correction factors developed from this procedure can be applied to both  $k$  values determined from static PLTs and  $M_r$  values determined from cyclic PLTs at a desired target stress level. An advantage in determining the gradient is that, from one data set for a given site, test location-specific correction factors can be calculated using the in situ moisture content and dry density at each location. One limitation with this procedure is that the rate of reduction in  $M_r$  as saturation increases is assumed to be linear. It has been documented in the literature that the relationship between changes in the degree of saturation and changes in  $M_r$  is a nonlinear sigmoid (see ARA, Inc. ERES Division 2000). The results presented in ARA, Inc. ERES Division (2000) indicated that the gradient is linear between -20% and +20% of the degree of saturation, corresponding to the standard Proctor optimum moisture content and maximum dry density. Changes in saturation above or below this range can lead to erroneous estimations in the corrected  $M_r$  values.

#### Enhanced Integrated Climatic Model Method (Without Matric Suction)

AASHTOWare Pavement ME Design uses the EICM to consider changes in the moisture content of a pavement's foundation layers over the pavement's design life. The corresponding changes in  $M_r$  values are determined using an environmental factor for unfrozen, unbound materials ( $F_U$ ). The  $F_U$  model is shown in equation (12) and was originally developed by Witczak et al. (2000).

$$\log F_U = a + \frac{b-a}{1+e^{\left(\ln \frac{-b}{a} + k_m(S-S_{opt})\right)}} \quad (12)$$

where  $F_U = M_r/M_{r-opt}$ , the ratio of  $M_r$  at a given time to  $M_r$  at optimum conditions ( $M_{r-opt}$ );  $a = -0.3123$  for coarse-grained materials and  $-0.5934$  for fine-grained materials;  $b = 0.3010$  for coarse-grained materials and  $0.3979$  for fine-grained materials;  $k_m = 6.8157$  for coarse-grained materials and  $6.1324$  for fine-grained materials;  $S$  = degree of saturation, expressed as a decimal, corresponding to the  $M_r$  value; and  $S_{opt}$  = degree of saturation, expressed as a decimal, corresponding to the  $M_{r-opt}$  value. A plot of  $S-S_{opt}$  versus  $F_U$  that illustrates the influence of changes in  $S$  on the  $F_U$  values using equation (12) for coarse- and fine-grained materials is shown in Figure 49.



ARA, Inc. ERES Division 2000

**Figure 49. Variation in  $F_U$  with changes in degree of saturation**

The regression parameters  $a$  and  $k_m$  in equation (12) are the best estimates for the data available at the time of the model's development, and parameter  $b$  is conservatively assumed to match an  $F_U$  value of 2 for coarse-grained materials and 2.5 for fine-grained materials (ARA, Inc. ERES Division 2000). It is noted in ARA, Inc. ERES Division (2000) that the model parameters were determined based on very small number of studies that reported the influence of moisture content on  $M_r$  along with post-compaction changes in moisture content/degree of saturation. Additionally, the influence of significant changes in dry density, different stress states, and a wide range of soil types could not be incorporated at the time of the model's development. The authors of ARA, Inc. ERES Division (2000) recommended an update to the model's parameters as more results become available.

In 2010, Cary and Zapata (2010) re-evaluated the EICM model developed by Witczak et al. (2000) through a data analysis involving 96 soils (967 data points) from multiple sources of data in the literature (Cary 2008, Fredlund et al. 1977, Edil and Motan 1979, Rada and Witczak 1981, Rada 1981, Santha 1994, Thadkamalla and George 1995, Mohammad et al. 1995, Drumm et al. 1997, Gehling et al. 1998, Parreira and Goncalves 2000, Andrei 2003, Khoury and Zaman 2004,

Ooi et al. 2004, Yang et al. 2005, Liang et al. 2008, and Khoury et al. 2009). Based on comparisons between the values predicted by the EICM and the measured values, Cary and Zapata (2010) determined that for fine-grained materials, the  $M_r$  values were often underestimated at dry of optimum conditions and overestimated at wet of optimum conditions. For coarse-grained materials, the authors determined that the  $b$  value developed assuming a maximum  $F_U$  of 2 underestimated the real values for dry of optimum conditions.

Based on their re-evaluation of the EICM parameters, Cary and Zapata (2010) proposed re-calculating the parameters in equation (12) using equations (13) through (15), which incorporate the index properties of the material as a product of the percent fines passing the No. 200 sieve ( $P_{200}$ ) and the plasticity index ( $PI$ ) of the material.

$$a = (\alpha + \beta \cdot e^{-P_{200} \cdot PI})^{-1} \quad (13)$$

$$b = \delta + \gamma \cdot (P_{200} \cdot PI)^{0.5} \quad (14)$$

$$k_m = (\rho + \omega \cdot e^{-P_{200} \cdot PI})^{0.5} \quad (15)$$

where  $\alpha = -0.600$ ,  $\beta = -1.87194$ ,  $\delta = 0.8$ ,  $\gamma = 0.08$ ,  $\rho = 11.96518$ , and  $\omega = -10.19111$ . Based on these updated regression parameters, Cary and Zapata (2010) reported that the coefficient of determination ( $R^2$ ) for the measured versus predicted  $F_U$  values was about 0.58, which was considered good for data collected from multiple sources.

#### Saturation Corrections as a Function of Matric Suction

Several researchers have presented models incorporating matric suction parameters into the constitutive universal model for  $M_r$  (e.g., Gupta et al. 2007, Liang et al. 2008, Cary 2011, Azam et al. 2013, Nokkaew et al. 2014). There are varying degrees of complexity in determining the properties of those models, the laboratory testing needed for those models, and the uncertainties involved in implementing those models. One of the simpler approaches, proposed by Liang et al. (2008), incorporates two suction parameters into the constitutive  $M_r$  model as follows:

$$M_r = k_1 P_a \left( \frac{\theta + \chi_w \psi_m}{P_a} \right)^{k_2} \left( \frac{\tau_{oct}}{P_a} + 1 \right)^{k_3} \quad (16)$$

$$\chi_w = \left( \frac{(\psi_m)_b}{\psi_m} \right)^{0.55} \quad (17)$$

where  $\chi_w$  = Bishop's parameter corresponding to a given moisture content or degree of saturation,  $\psi_m$  = matric suction at a given moisture content or degree of saturation, and  $(\psi_m)_b$  = air-entry value or matric suction where air starts to enter the largest pores in the soil.

Liang et al. (2008) evaluated the model (equation [16]) for matric suction values greater than the air-entry value (i.e.,  $\psi_m > (\psi_m)_b$ ) and therefore for  $\chi_w > 1$ . The suction parameters can be measured experimentally by developing soil water characteristics curves (SWCCs) for the material and measuring the in situ moisture content and dry density. The experimental procedure involves performing filter paper method tests (ASTM D5928) on reconstituted samples compacted to different moisture contents and dry densities. Alternatively, SWCCs can be estimated following the empirical relationships provided in Zapata and Houston (2008) based on soil index properties and using the model in Fredlund and Xing (1994).

### *Foundation Layer Drainage Properties*

Drainage is addressed using a drainage coefficient value in the AASHTO flexible and rigid pavement design procedures (AASHTO 1986, 1993). The coefficient values are referred to as  $m_i$  and  $c_d$  in flexible and rigid pavement design, respectively. The  $m_i$  and  $c_d$  values are determined based on the time and degree of drainage desired in the design and the anticipated duration that the layer is expected to be in a near-saturated condition. The time and degree of drainage calculations assume a near-saturated condition and are based on flow calculations using pavement geometry, drainage layer thickness, and the coefficient of permeability ( $K_{sat}$ ) of the drainage layer.

In the 2008 edition of AASHTO's *Mechanistic-Empirical Pavement Design Guide* (AASHTO 2008), a minimum  $K_{sat}$  value of 305 m/day (1,000 ft/day) is assumed for asphalt- and cement-treated drainable base layers. In the faulting prediction model used in the guide, a minimum  $K_{sat}$  value of 300 ft/day is used to classify the drainage layer as sufficiently permeable to avoid pumping under loading.

Although the PCA (1984) design procedure does not explicitly state the minimum drainage requirements, subsequent publications by the same organization (ACPA 2007) have established recommendations on drainage requirements. According to ACPA (2007), a good-quality free-draining base consists of a material that can provide adequate drainage while maintaining stability and that has a  $K_{sat}$  value of 15 to 46 m/day (50 to 150 ft/day) based on laboratory tests. ACPA (2007) also states that materials with  $K_{sat}$  values of up to 107 m/day (350 ft/day) based on laboratory tests may also provide long-term stability for foundations. The guide specifically states that unstabilized materials with a high degree of drainability, i.e., more than 107 m/day (350 ft/day), are no longer recommended by ACPA because they pose issues during construction and are no longer considered a cost-effective design element for concrete pavements due to their problematic history. ACPA (2007) reports that contractors have described paving over highly drainable unstabilized material as "paving on marbles."

The results from the present study (see Chapter 2) and field studies involving in situ permeability testing (White et al. 2004, 2007, 2013) have indicated that the coefficient of variation of in situ permeability is as high as 50% to 400%, making it the most variable engineering parameter in the pavement system. Some of the factors that contribute to the high level of variability include (a) inherent variations in the material gradation and morphology, (b) segregation caused by construction activities that deposit and spread the aggregate, and, to a lesser degree, (c) particle

breakdown due to compaction and construction traffic (White et al. 2007). The spatial variability of permeability has been documented through field studies (see Chapter 2), but the degree of its consequences is poorly understood.

In practice, most design engineers assume a  $K_{sat}$  value for the drainage layers based on marginally accurate empirical relationships or limited laboratory testing but with virtually no field verification. This lack of field measurement provides little confidence in the assumed design values and does not address the fact that permeability is a highly variable parameter. White et al. (2007) summarized the various in situ testing devices available to determine in situ permeability for pavement materials; the devices used air, water, and vacuum as the permeating medium. None of those testing devices are widely used in practice. A major hindrance to the widespread use of these devices is often the difficulties involved in conducting the tests: sealing, water transportation, fines migration, trapped air bubbles, lengthy testing times, verification of test measurements, and lack of clear benefits to construction quality control.

As part of an Iowa DOT research project in 2004, White et al. (2004) developed a gas permeameter testing (GPT) device that was then updated in 2010 as part of an NCHRP-IDEA project. The GPT device was used as a part of the present project, and the results are summarized in Chapter 2. The details of the testing device and the results of validation testing are documented in White et al. (2007, 2013). The device can be used to measure  $K_{sat}$  in situ in under 30 seconds and can be used on materials with a wide range of  $K_{sat}$  values (6 to 9140 m/day [20 to 30,000 ft/day]), which can be an effective QC/QA tool to verify design assumptions and assess the field segregation of fine/coarse materials (White et al. 2013). Additional tests with the GPT device have been undertaken in Minnesota and Indiana.

### **Empirical Relationships and Associated Uncertainties/Risks**

As documented in this chapter, the current state of the practice in determining design input parameters ( $k$  value,  $M_r$ , and  $K_{sat}$ ) is largely based on empirical relationships with minimal testing and surrogate measurement. Little progress will be made toward improving pavement foundations without investment in more exact and appropriate test protocols. The use of empirical relationships or indirect testing is convenient and offers much lower up-front costs than direct measurement options. However, empirical or indirect approaches introduce risk because of the uncertainties associated with the predicted values and thus the possibility that the predictions will not match the actual field conditions. Further, the baseline measurements provide limited documentation for improving future design and understanding.

It is often difficult to assess how reliable an empirically predicted value is. Often, engineers rely on historical comfort when choosing to use an empirical relationship. In this section, a statistical approach using a simple graphical procedure (Figure 50) is presented to quantify the reliability associated with using a prediction equation.

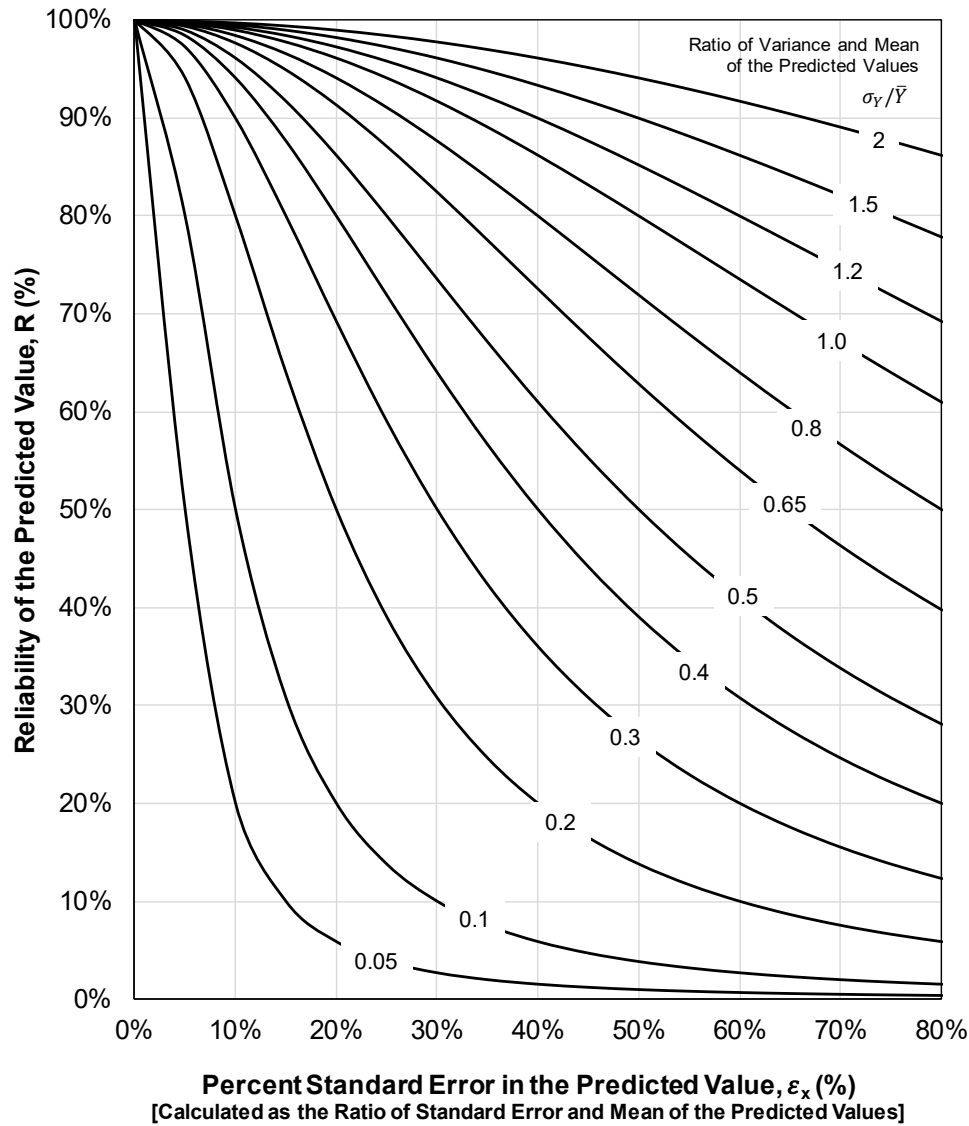


**Figure 50. Estimating the reliability of a predicted value based on the standard error of the estimates from empirical relationships**

To use this approach, the source of the prediction equation must be known to calculate the equation's reliability using two parameters from the data set: (a) the standard error of the predicted values and (b) the ratio of the variance and the mean of the predicted values used in developing the relationship (which provides a measure of the range over which the measurements were obtained). The calculations used in developing this graph assume a linear regression between the measured and predicted values. If the empirical equation represents a nonlinear or multivariate relationship, then the data will need to be reanalyzed to plot measured versus predicted values and fit a linear regression line to recalculate the standard error. The mathematical relationships linking the measurement reliability, variance, and standard error of the predicted values are provided below and are adapted from Dupont and Plummer (1998) and Devine (2003):



$$\sigma_e^2 = \sigma_y^2 - \rho^4 \lambda^2 \sigma_x^2 \quad (18)$$

$$\rho = \frac{\sigma_x}{\sqrt{\sigma_x^2 + \varepsilon_x^2}} \quad (19)$$

$$R = \rho^2 \times 100 \quad (20)$$

where  $\sigma_e^2$  = variance (square of the standard deviation) of the residuals of the fit (i.e., the difference between the predicted and measured values),  $\sigma_x^2$  = population variance of the X-variable (the indirect or predicted measurement value),  $\sigma_y^2$  = population variance of the Y-variable (the direct measurement value),  $\lambda$  = slope of the linear regression relationship between X and Y,  $\rho$  = measure of reliability/bias in the X-variable due to measurement error,  $R$  = reliability of the X-measurement (%),  $\varepsilon_x$  = measurement error or standard error of the estimate,  $\varepsilon_x/\bar{X}$  = percent standard error in the predicted value,  $\bar{X}$  = mean of the X values, and  $\bar{Y}$  = mean of the Y values.

Figure 50 presents the relationship between  $R$  and  $\varepsilon_x$  as a function of different variance-to-mean ratios of the predicted values ( $\sigma_Y/\bar{Y}$ ). The  $\sigma_Y/\bar{Y}$  provides a measure of the range of the values used in developing the prediction equation. Using Figure 50, to have a, an empirical relationship that makes predictions with a high reliability must demonstrate a low standard error and a wide range of values over which the equation was developed. Users of this information and Figure 50 are encouraged to plot their own testing results to estimate reliability and thereby consider data quality before the data are plugged into a design equation.

## **CHAPTER 4: MECHANISTIC PAVEMENT FOUNDATION SPECIFICATION FRAMEWORK**

Current specifications for pavement foundation layers are a combination of construction method requirements (e.g., lift thickness, roller passes) and end results requirements (e.g., minimum relative compaction). These processes serve a practical function but limit advancement in terms of pavement foundation improvement. In moving to a performance-based specification approach, the support conditions for the pavement foundation layer are specified in terms of the pavement designers' requirements (e.g., resilient modulus or modulus of subgrade reaction), including a new requirement for uniformity (e.g., COV of resilient modulus). Key features of a performance-based construction specification should include the following:

- Measurement technologies that provide near 100% sampling coverage
- Acceptance and verification testing procedures that measure the performance-related parameters that are relevant to the mechanistic design inputs
- Protocols for establishing target values for acceptance based on design
- Quality statements that require achievement of spatial uniformity
- Protocols for data analysis and reporting that ensure that the construction process is field-controlled in an efficient manner

The starting point for moving toward a performance-based specification is to develop an entirely new quality inspection workflow involving communication between the designer, engineer, contractor, and inspector. What follows is a review of current specifications and a description of the key elements of a performance-based workflow.

### **Review of the Current State of the Practice for Design and Construction QC/QA**

Table 14 summarizes the state of the practice for design and construction QC/QA for pavement foundations in the participating states (California, Iowa, Michigan, Minnesota, Wisconsin) and in two additional Midwestern states (Minnesota and North Dakota). The questions sent to each state and the states' responses are listed in the table.

**Table 14. Summary of the state of the practice for PCC pavement design, pavement foundation testing, and stabilization**

State	Response
<i>What design method is being followed for PCC pavement currently (e.g., AASHTO (2008), PCA, other)?</i>	
CA	Caltrans has prepared its own design catalog (set of design tables) for PCC that is based on both past empirical rigid pavement design and an early version of AASHTOWare Pavement ME Design (version 1). The design catalog considers traffic (in terms of traffic index [TI]), climate region, soil type, and lateral support. The design catalog is available in Caltrans (2018).
IA	Currently PCA (1984), but intent is to use AASHTOWare Pavement ME Design in the future.
MI	AASHTO (1993). Much effort has been put into switching to MEPDG for many years through statewide calibration research, but we're not there yet.
MN	MnPAVE Rigid 3.0 (compiled output from a calibrated MEPDG 1.1)
ND	AASHTOWare Pavement ME Design
PA	AASHTO (1993)
WI	AASHTO (1972)
<i>Does your state measure or has your state measured the in situ pavement foundation parameters as part of design calibration/verification? Y/N. If yes, what parameters (e.g., resilient modulus)?</i>	
CA	No. Caltrans originally used the subgrade R-value for preparing its design catalog. Later a correlation was made between R-value and Unified Soil Classification System (USCS), which is now available in design tables.
IA	We currently have a research project underway to measure some in situ foundation parameters. Limited laboratory testing of material was done previously.
MI	Yes. There was statewide research to assign an $M_r$ threshold based on soil classification. FWD is collected on most large project for comparison at this point.
MN	No foundation testing after construction. Yes, there is foundation testing for design using laboratory R-values or backcalculated R-values from FWD data on the HMA shoulders using the TONN 2010 program.
ND	No.
PA	Yes, resilient modulus.
WI	Sometimes FWD (resilient modulus).

State	Response
<b><i>What QC/QA testing is required for embankments, subgrades, and aggregate bases (e.g., percent relative compaction)?</i></b>	
CA	For subgrade and embankment, it is relative compaction. For soil stabilization, it is relative compaction and stabilization agent application rate. For aggregate subbase, it is gradation, R-value, sand equivalent, and percent relative compaction.
IA	New embankment or subgrade soil: moisture (typical) or moisture and density (infrequent). Aggregate: typically no testing.
MI	Nuclear density verification for all three, including moisture content no higher than optimum. Gradation and physical properties testing for aggregate base. Soils engineers verify subgrade stability and frost susceptibility for needed correction.
MN	No QC on subgrade or aggregate base. QA (nongranular subgrade): LWD or specified density and quality compaction and test rolling. QA (granular subgrade): LWD, DCP, or specified density and quality compaction and test rolling. QA (aggregate base): LWD, DCP, or specified density and quality compaction and test rolling.
ND	Embankment and subgrade: require mostly 90% of AASHTO T 180. In some parts of the state require 95% of AASHTO T 99. Aggregate bases: not tested. Aggregate base compaction spec: "Compact aggregate, utilizing pneumatic-tired rollers, until no rutting or displacement occurs under the roller operation."
PA	Subbase: Compact to a condition of nonmovement as specified in Section 206.3(b). Subgrade: Compact and proof-roll the entire subgrade surface.
WI	Embankments: sometimes (special compaction, NDG); subgrade: same as embankments; aggregate base: sometimes (NDG), only asphalt surfaces.
<b><i>What test frequency is required for embankments, subgrades, and aggregate bases?</i></b>	
CA	For lime stabilization, every 500 yd <sup>3</sup> , the relative compaction and moisture content is checked. For bases, it is 500 yd <sup>3</sup> or 1 day production.
IA	New embankment or subgrade soil: 1 test per 1,500 ft (maximum volume of 1,300 yd <sup>3</sup> ).
MI	Subgrade, subbase, and aggregate base course: 1 test per 500 feet per width of 24 feet or less. Embankment: 1 test per 1,000 yd <sup>3</sup> of material with a minimum of 1 test per layer.
MN	Embankment: 1 test per 10,000 yd <sup>3</sup> and 100% test rolled. Aggregate Base: 1 test per 1,500 yd <sup>3</sup> or 1 test per 3,000 tons and 100% test rolled.
ND	Yes. Specific locations are selected by the engineer by random number table or a random number generator. Frequency is 1 test per 1,500 ft of compacted roadway.
PA	Embankment or fill: 1 QC test per lift for each 1,000 yd <sup>2</sup> placed; minimum 3 tests per lift per day. 1 acceptance test per lift for each 4,000 yd <sup>2</sup> placed; minimum 1 test per lift per day. Subgrade: 1 QC test per lift for each 800 yd <sup>2</sup> placed; minimum 4 tests per lift per day. 1 acceptance test per lift for each 3,000 yd <sup>2</sup> placed; minimum 1 test per lift per day.
WI	Embankments: Sometimes (special compaction, NDG); subgrade: same as embankments; aggregate base: Sometimes (NDG), only asphalt surfaces.

State	Response
<b><i>Is QC/QA testing selection based on random sampling (i.e., random number generator to determine locations), systematic sampling (e.g. every 500 ft or at location of poor quality), or some other approach?</i></b>	
CA	The QC/QA testing selection is based on systematic sampling.
IA	Random for moisture and/or density. Representative for Proctors.
MI	Density testing based on systematic approach with a preference to verify visually questionable areas. Aggregate testing is systematic. Subgrade verification is systematic with a preference to verify questionable areas.
MN	Since 100% is test rolled, spot tests are performed where most likely to fail.
ND	1 test per 1,500 ft of compacted roadway. Specific locations are selected by the engineer.
PA	At locations directed by the representative.
WI	Quality management program (QMP): Embankment/Subgrade one NDG test for 3,000 yd <sup>3</sup> random sampling (minimum 95% of AASHTO T 99); Aggregate base one NDG test for 1,500-foot lane-mile, random sampling (only asphalt surfaces).
<b><i>Are there any requirements for “uniformity” of support in the pavement foundation layers? Y/N. If yes, how is uniformity measured?</i></b>	
CA	No, there is no special requirement for uniformity of support.
IA	Require natural subgrade to be “uniformly firm.” Proof-roll required.
MI	Not through measurement.
MN	Yes, no defined measurement of uniformity. But all is test rolled.
ND	No.
PA	No.
WI	No, meeting the minimum density requirement for special compaction or minimum deflection requirement with standard compaction.

State	Response
<p><i>Are any of the following stabilization methods incorporated into pavement foundation design?</i></p> <p><i>(a) Subgrade stabilization using lime or fly ash? Y/N</i></p> <p><i>(b) Subgrade stabilization using cement? Y/N</i></p> <p><i>(c) Aggregate base stabilization using cement? Y/N</i></p> <p><i>(d) Aggregate base layer stabilization using geogrid? Y/N</i></p> <p><i>(e) Use of geosynthetics for separation or drainage? Y/N</i></p> <p><i>(f) Other stabilization practices in use?</i></p>	
CA	(a) Yes. (b) Yes. (c) Yes. (d) Yes. (e) Yes. (f) NA.
IA	(a) Generally, no, not in design; however, “Yes” as a construction expedient. (b) Generally, no. (c) No. (d) Yes, on Interstate projects. Occasionally on urban projects or when desired by District. (e) Typically, not in design; however, “Yes” in rare circumstances as a construction expedient. (f) None.
MI	(a) No. Used on some projects but not incorporated into design method. (b) No. Used on some projects but not incorporated into design method. (c) Yes. (d) No. Used on some projects but not incorporated into design method. (e) No. Used on most projects but not incorporated into design method. (f) No.
MN	(a) No. (b) Yes. (c) No. (d) Yes. (e) Yes. (f) Full-depth reclamation (FDR), cold in-place recycling (CIR), cold central-plant recycling.
ND	(a) No. (b) No. (c) Yes. (d) Yes, on rare occasions we use geogrid in the design. (e) No. (f) No.
PA	(a) Yes. (b) Yes. (c) Yes. (d) Yes. (e) Yes. (f) Asphalt-treated permeable base course.
WI	(a) Yes, rare (fly ash). (b) Allowed, very rare. (c) No. (d) Yes, sometimes. (e) Yes, sometimes. (f) Large aggregate bases/Select crushed material.

Note: The summary presented in this table is based on responses received from the states by October 2019.

At the time of the survey, one of the seven surveyed states (North Dakota) was using AASHTOWare Pavement ME Design, one state (Minnesota) was using earlier or modified versions of that software, one state (California) was using a design catalog-based method that was reportedly developed using an earlier version of AASHTOWare Pavement ME Design, two states (Pennsylvania and Michigan) were using the AASHTO (1993) design guide, one state (Iowa) was using the PCA (1984) design guide, and one state (Wisconsin) was using the AASHTO (1972) design guide.

The method for establishing foundation layer design inputs was different for each state. QC/QA testing is typically based on dry unit weight and moisture content. One state uses LWD and DCP testing. Testing frequency ranges are estimated to be between 0.01% and 0.004% of the work area using systematic or random sampling. No state has any specific requirements for uniformity,

and it is not clear if the actual pavement foundation design parameters are measured in situ. Various stabilization solutions are employed to improve the support conditions.

### **Framework for Performance-Based Mechanistic Pavement Foundation Testing**

This section presents a new framework that focuses on linking the design inputs assumed by the pavement designer to what is achieved during construction through performance-based mechanistic verification testing. The framework is outlined as a workflow for new construction and reconstruction (rehabilitation with full-depth repair) projects. Figure 51 and Figure 52 illustrate the key components of the workflow process and requirements.

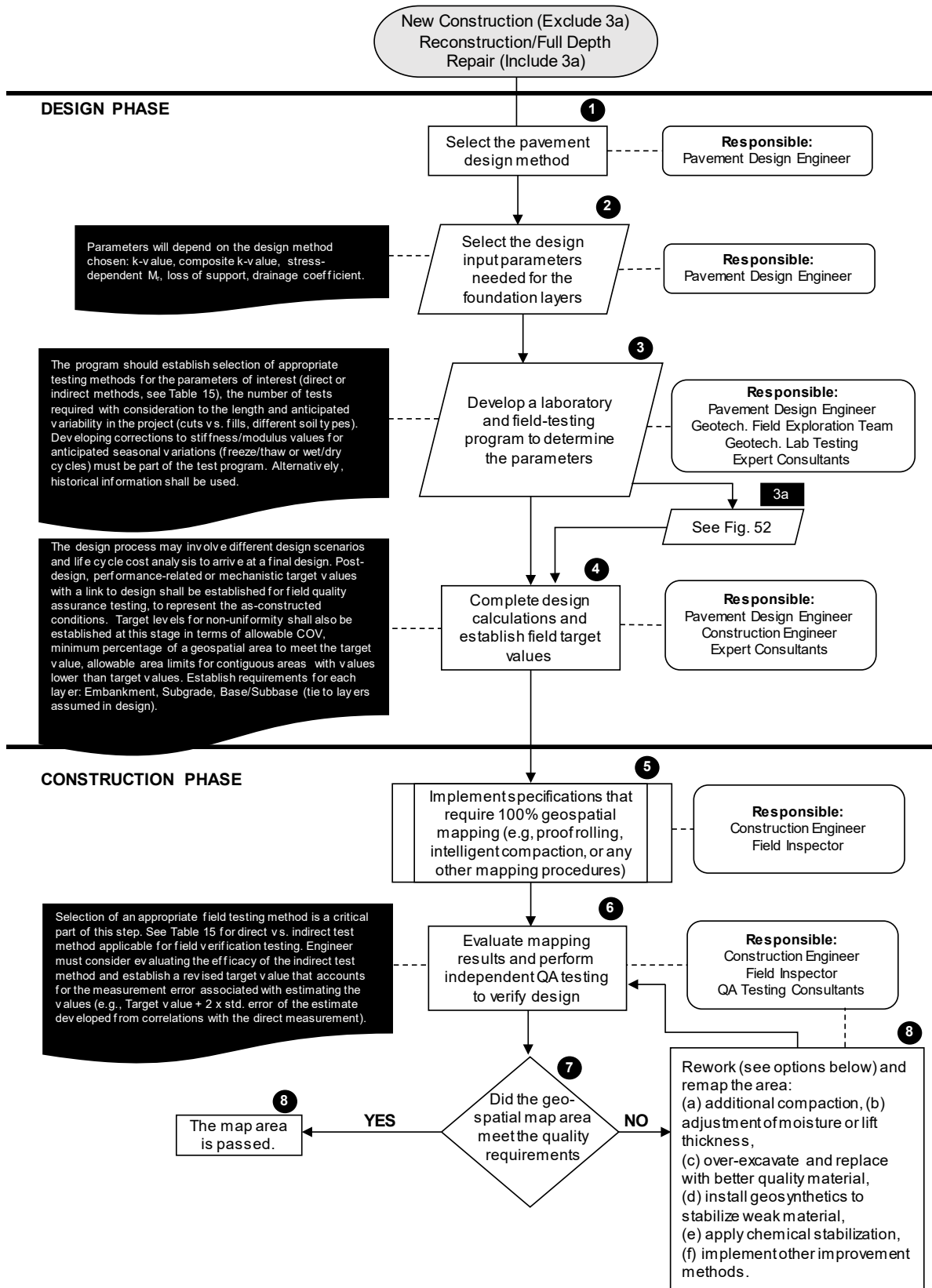
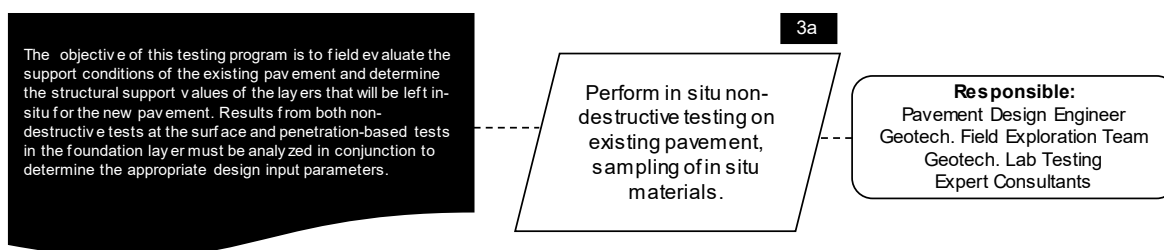


Figure 51. Workflow for field verification of pavement foundation design input parameters



## EVALUATION OF SUPPORT CONDITIONS UNDER EXISTING PAVEMENTS



**Figure 52. Step 3a of workflow for field verification of pavement foundation design input parameters – for evaluation of support conditions under existing pavements prior to rehabilitation**

The workflow involves eight steps, beginning with the selection of a design method and ending with field verification of whether the tested area met the design requirements, and identifies the responsible parties for each step. This is the structure of a performance-based specification, where performance entails delivery and verification of the required pavement foundation support conditions at the completion of construction.

Steps 1 through 4 are proposed requirements in the initial design phase, while Steps 5 through 8 are requirements in the construction phase. We are linking the pavement system design elements to the selection of target quality values to field construction process control and to quality inspection. A brief discussion of each of the steps is provided below.

### *Step 1: Selection of Pavement Design Method*

In this step, the pavement designer selects the pavement design methodology (e.g., AASHTOWare Pavement ME Design). This is a critical step because it establishes the type of foundation input parameters that must be evaluated in the following steps.

### *Step 2: Selection of Foundation Layer Design Input Parameters*

In this step, the pavement designer selects the key foundation layer design input parameters, which depend on the design methodology chosen. These parameters include the following:

- Modulus of subgrade reaction,  $k$  value (AASHTO 1972, AASHTO 1986, AASHTO 1993, PCA 1984)
- Composite modulus of subgrade reaction, composite  $k$  value (accounts for a subbase layer above the subgrade) (AASHTO 1986, AASHTO 1993, PCA 1984)
- Stress-dependent resilient modulus value,  $M_r$  (AASHTO 1986, AASHTO 1993, AASHTOWare Pavement ME Design)
- Elastic modulus value of subbase and stabilized layers,  $E$  (AASHTO 1986, AASHTO 1993, AASHTOWare Pavement ME Design)
- Universal model parameters for  $M_r$  (AASHTOWare Pavement ME Design)

- Drainage coefficient,  $C_d$  (AASHTO 1986, AASHTO 1993)
- Minimum coefficient of permeability,  $K_{sat}$  (PCA 1984, AASHTOWare Pavement ME Design)

*Step 3: Development of a Program/Method for Selection of These Input Parameters*

This step involves development of a program to select appropriate in situ testing methods for the parameters of interest. Table 15 provides a list of the direct and indirect laboratory and field test methods to be considered for determining  $M_r$ ,  $E$ , and  $k$  values.

**Table 15. Summary of testing methods to determine mechanistic properties of geomaterials**

Mechanical Property	Lab/ Field	Direct / Indirect	Test Method/ Reference	Measurement Device	Comments
Modulus of subgrade reaction ( $k$ )	Field	Direct	AASHTO T 222 USACE (1995) ASTM D1196	APLT	Can be determined using 30 in., 18 in., 12 in., and 8 in. diameter plates.
	Field	Indirect	ASTM D4694	FWD	Backcalculation analysis assumes static loading, but FWD applies dynamic loading. Empirical corrections are made. Very limited data directly comparing dynamic and static values.
	Lab	Indirect	ASTM D1883	CBR test device	Well-established test method, but source of correlations and the uncertainties associated with the relationships to $k$ value are not well understood. Sample is compacted in lab. Differences in field versus lab compaction and boundary conditions can influence results.
	Field	Indirect	ASTM D6951	DCP	Used to empirically estimate CBR or elastic modulus and convert to $k$ value. Can determine individual layer CBR in situ, but variations in penetration resistance with depth complicates interpretation.

Mechanical Property	Lab/Field	Direct / Indirect	Test Method/Reference	Measurement Device	Comments
Resilient Modulus ( $M_r$ ) or Elastic Modulus (E)	Lab	Indirect	AASHTO T 307 Witczak (2003)	Repetitive triaxial test device	Sample is compacted in lab. Differences in field versus lab compaction and boundary conditions can influence results.
	Field	Direct	ASTM E1196 AASHTO T 307	APLT	Can directly measure confining stress-dependent $M_r$ values to determine $k_1$ , $k_2$ , and $k_3$ values. Test measures composite moduli values, but layered moduli can be determined based on layered analysis.
		Indirect	ASTM D4694	FWD	Layered analysis can be performed to estimate individual layer moduli values.
		Indirect	ASTM E2583 ASTM E2835	LWD	Results can be empirically correlated to $M_r$ (Nazarian et al. 2014).
		Indirect	Nazarian et al. (1995)	Seismic pavement analyzer (SPA)	
	Lab	Indirect	ASTM D1883	CBR test device	Well-established test method, but source of correlations and the uncertainties associated with the relationships to $M_r$ or E values are not well understood in practice. Sample is compacted in lab. Differences in field versus lab compaction and boundary conditions can influence results.
	Field	Indirect	ASTM D6951	DCP	Used to empirically estimate CBR or elastic modulus. Can determine individual layer CBR in situ, but variations in penetration resistance with depth complicates interpretation.

Field testing plays a critical role in understanding the in situ foundation support conditions, and, as discussed earlier, the methods that can be selected have various limitations. Direct tests of the important mechanistic parameter value used in design are best, and technology that provides spatial uniformity assessment is important. Field testing can involve both nondestructive testing at the surface and some destructive testing where tests are performed directly on the foundation layer to ensure that the backcalculated values match the actual measured parameters. DCP penetration resistance testing can provide valuable information on the variability of stiffness/shear strength properties with depth. GPR profiles can also provide valuable information related to pavement and foundation layer thicknesses, trapped water, ice lenses within the foundation and pavement layers, and the ground water table. Additional guidance on the different testing methodologies is provided in AASHTO (2015).

The program should establish the number of tests required in consideration of the length of the project, the anticipated variability within it (e.g., cuts versus fills, different soil types), and (for indirect testing methods) the reliability of the testing method used. The testing program should also address the corrections required to the modulus values due to anticipated seasonal variations (freeze-thaw or wet-dry cycles). A critical outcome of these corrections is the determination of values pre- and post-saturation and in freeze-thaw conditions. The pre-saturation values are critical for establishing the field target values at the time of construction.

#### *Step 4: Complete Design Calculations and Establish Field Target Values*

In this step, the pavement designer completes the design calculations to establish the thickness of the PCC layer, joint spacing, reinforcement details, the mix design of the pavement layer, the thicknesses of the foundation layers, and any stabilization needed. The design process may involve analyzing and evaluating different design scenarios and conducting a life-cycle cost analysis, including material selection and stabilization options for the foundation layers. After design, the pavement designer establishes the mechanistic (performance) target values, linked to the design inputs, for field verification testing. The target values established for construction verification should represent the values for the as-constructed conditions (pre-saturation). To establish field target values, the following aspects must be evaluated:

- What stress conditions are anticipated on top of the tested foundation layer? This can be established by performing pavement analysis for the worst loading case and evaluating the range of stresses expected on the layer at critical loading locations (e.g., corner of the slab).
- What in situ testing method will be used for field evaluation? This is important to clarify. If the field testing method is an indirect testing method, then the reliability of the indirect testing method must be taken into account in establishing the target value. The reliability is evaluated by examining the regression relationship between the true measurement values and the values produced by the indirect testing method, and the standard error of the estimate. An example approach is to increase the target value for the indirect test method by adding two times the standard error of the estimate to account for the measurement error associated with the testing device/method. There is conclusive evidence from the field testing performed in the present study that dry unit weight measurements are not a direct indicator of the stiffness/modulus and do not capture the variability associated with support conditions. Emphasis should be placed on direct mechanistic measurement.
- What percentage of the project should meet the minimum target value? Based on the authors' field experience, it is impractical to expect that 100% of the project area will meet the target value, especially when the results of 100% mapping are used to evaluate a project during construction. The engineer should set expectations regarding the acceptable minimum percentage of the area that meet the target value (e.g., for practical purposes, 80% to 90%).
- What level of nonuniformity is acceptable? Using information gathered from 100% mapping coverage provides an opportunity to evaluate nonuniformity in the field. The results from the

present study have conclusively shown that nonuniformity affects pavement performance. However, quantifying the level of nonuniformity that is acceptable for a given project is a complex problem that needs additional research. If advanced pavement analysis tools are used, site- and material-specific target values can be established. As a rule of thumb, a COV of 20% is generally considered to indicate uniform support conditions, provided the variability is not geospatially concentrated with localized areas of weak support conditions. A requirement for a maximum allowable COV and an associated requirement that no contiguous areas of weak stiffness/modulus values (below the target value) be present that are greater than or equal to a minimum critical area (e.g., 200 ft<sup>2</sup>) should be established.

#### *Step 5: Implement Specifications with 100% Geospatial Mapping*

In this step, the construction engineer requires the contractor to produce mechanistic mapping results that provide 100% coverage of the foundation layers. Mapping can include proof-rolling, intelligent compaction, or any other suitable mapping procedures. The construction engineer shall have the responsibility of establishing the correct mapping and reporting procedures and the level of validation needed for the procedure, based on the project and site conditions.

#### *Steps 6, 7, and 8: Evaluate the Results and Perform Independent QA Testing*

In this step, the mapping results are evaluated to perform independent QA testing at selected test locations. The test method chosen for the verification testing will depend on the guidelines that the designer outlined in Step 4 for establishing the target values.

Following independent QA testing and evaluation of the mapping results, if the area meets the quality requirements established, the area is considered acceptable. If the area does not meet the quality requirements, the specifications should allow options for rework, such as the following:

- Additional compaction
- Adjustment of moisture content or lift thickness
- Overexcavation and replacement with better quality material
- Stabilization using geosynthetic products
- Stabilization using additives (e.g., cement, fibers)
- Potentially other innovative improvement methods

Following rework, the area is re-evaluated to verify that it meets the quality requirements.

The framework outlined in this section connects the selection of mechanistic field target values during design to construction and quality inspection verification and the selection of improvement options. The goal is to control the pavement foundation in the field to deliver the product intended by the design engineer.

## CHAPTER 5: CONCLUSIONS AND RECOMMENDATIONS

Pavement foundation systems for concrete pavements are critically important for providing economical and long-life pavement systems. This research program provided opportunities to collect a wealth of data at several sites in California, Iowa, Michigan, Pennsylvania, and Wisconsin. The volume of data and density of tests points and the emphasis on understanding the many mechanisms and index measurements relevant to the foundation layers allowed the research team to explore new approaches to characterizing pavement foundations. The following key challenges were documented from the field studies and analyses:

- The geomaterials used in pavement foundation construction are variable and complex.
- No field verification of the engineering parameters used in the mechanistic design of pavement foundations is being used for quality acceptance during construction.
- While parametric studies of pavement design have shown that pavement performance has a low sensitivity to the support conditions provided by the foundation materials, poor support conditions are well documented as affecting the long-term field performance of pavements.
- Substantial spatial variability (nonuniformity) exists in newly constructed pavement foundations for the range of materials tested.
- If the subgrade layer is nonuniform, the overlying aggregate base layer will be nonuniform.
- Uniformity of support is an important characteristic of pavement foundation systems. New finite element analyses quantify the effects of this characteristic on pavement performance.
- Loss of support due to irreversible plastic deformation in the foundation layer can significantly decrease the fatigue life of the pavement.
- Permanent (irreversible) deformation of the pavement foundation layers is not considered in modern pavement design or measured as part of the construction verification process.
- Limited geotechnical testing (covering less than 1% of a given work area) is used to accept the engineering support values of pavement foundations, resulting in low reliability.
- Pavement foundation layers are often constructed with locally available geomaterials of poor quality, which contributes to localized pavement performance issues.
- Limited technology is available to help earthwork and paving contractors improve the field control of pavement foundation layers during construction.

- Modern laboratory testing to determine the stress-dependent resilient modulus of foundation materials does not represent field boundary conditions.
- More frost heave and thaw testing is needed to characterize complex pavement foundation geomaterials, especially stabilized materials.
- The current practice for selecting design input parameters (e.g., modulus) is still largely empirical.
- Most methods for quality inspection testing do not qualify as direct mechanistic measurements.

Although numerous challenges regarding pavement foundations were discovered, it was determined that an ideal foundation layer for long-life concrete pavements (1) provides uniform support, (2) is neither too soft nor too stiff, (3) provides adequate drainage, (4) does not suffer from irreversible plastic deformation, and (5) makes use of sustainable methods and materials.

The full data record for all aspects of this project is documented in 15 previously published project reports and 11 peer-reviewed publications. The authors would also like to recognize that this project resulted in at least two PhD dissertations and four MS theses. The References section includes nearly all of these documents, given they are also cited in this report. Links to the completed final report PDFs are posted at <https://intrans.iastate.edu/research/completed/improving-the-foundation-layers-for-concrete-pavements/> and are also included in the References list.

Building on the field test results, new analyses, and a study of the origins of current practices for selecting pavement foundation parameters, a performance-based workflow for mechanistic pavement foundation testing was proposed. The next major steps toward improving pavement foundation longevity will be to improve the uniformity of the foundation layers, ensure the as-constructed condition meets the minimum mechanistic design requirements, and provide geospatial documentation of the foundation layers. These improvements will offer a new understanding of the relationships between the support conditions provided by the foundation layers and the ride quality and structural performance of the pavement.

The most important next steps are to measure modulus in situ, limit the reliance on empiricism, and document foundation layer conditions using reliable tests. The following is recommended:

- Encourage stakeholders to build on the proposed workflow within their organizations and to study how pavement design assumptions can be translated into field target values for use during construction.
- Establish field test protocols to directly measure the important mechanistic parameters.

- Enable inspectors and contractors to use real-time measurement technologies to implement improved moisture control, compaction, and stabilization practices for pavement foundation materials.
- Build robust databases of results that can be used to improve the selection of materials and processes that deliver the needed results in the field.
- Develop performance-based requirements and specifications that minimize methods-based process controls and emphasize the delivery of uniform, stable, and long-lasting pavement foundation support conditions. Moving the industry in this direction will require vastly different practices than those that currently exist.
- Share the knowledge gained through these processes on each new project to improve subsequent projects.



## REFERENCES

### **AASHTO Standards, American Association of State Highway and Transportation Officials, Washington, DC**

- AASHTO T 99: Standard Method of Test for Moisture–Density Relations of Soils Using a 2.5-kg (5.5-lb) Rammer and a 305-mm (12-in.) Drop.*
- AASHTO T 180: Standard Method of Test for Moisture–Density Relations of Soils Using a 4.54-kg (10-lb) Rammer and a 457-mm (18-in.) Drop.*
- AASHTO T 274-82: Resilient Modulus of Subgrade Soils, Standard Specifications for Transportation Materials and Methods of Sampling and Testing.*
- AASHTO T 307-99: Standard Method of Test for Determining the Resilient Modulus of Soils and Aggregate Materials, Standard Specifications for Transportation Materials and Methods of Sampling and Testing.*
- AASHTO T 221-81: Standard Method of Test for Repetitive Static Plate Load Tests of Soils and Flexible Pavement Components for Use in Evaluation and Design of Airport and Highway Pavements, Standard Specifications for Transportation Materials and Methods of Sampling and Testing.*
- AASHTO T 222-81: Standard Method of Test for Nonrepetitive Static Plate Load Test of Soils and Flexible Pavement Components for Use in Evaluation and Design of Airport and Highway Pavements, Standard Specifications for Transportation Materials and Methods of Sampling and Testing.*

### **ASTM Standards, ASTM International, West Conshohocken, PA**

- ASTM D1195 / D1196M-09: Standard Test Method for Repetitive Static Plate Load Tests of Soils and Flexible Pavement Components, for Use in Evaluation and Design of Airport and Highway Pavements.*
- ASTM D1196 / D1196M-12: Standard Test Method for Nonrepetitive Static Plate Load Tests of Soils and Flexible Pavement Components, for Use in Evaluation and Design of Airport and Highway Pavements.*
- ASTM D1883: Standard Test Method for California Bearing Ratio (CBR) of Laboratory-Compacted Soils.*
- ASTM D4123-82: Standard Test Method for Indirect Tension Test for Resilient Modulus of Bituminous Mixtures (Withdrawn 2003).*
- ASTM D4694: Standard Test Method for Deflections with a Falling-Weight-Type Impulse Load Device.*
- ASTM D5918-06: Standard Test Methods for Frost Heave and Thaw Weakening Susceptibility of Soils.*
- ASTM D5928: Standard Practice for Screening of Waste for Radioactivity.*
- ASTM D6951: Standard Test Method for Use of the Dynamic Cone Penetrometer in Shallow Pavement Applications.*
- ASTM E1196: Test Method for Determining the Anaerobic Biodegradation Potential of Organic Chemicals (Withdrawn 1998).*

*ASTM E2583: Standard Test Method for Measuring Deflections with a Light Weight Deflectometer (LWD).*  
*ASTM E2835: Standard Test Method for Measuring Deflections Using a Portable Impulse Plate Load Test Device.*

### Author-Date References

- AASHTO. 1972. *AASHTO Interim Guide for Design of Pavement Structures*. American Association of State Highway and Transportation Officials, Washington, DC.
- AASHTO. 1986. *AASHTO Guide for Design of Pavement Structures*. American Association of State Highway and Transportation Officials, Washington, DC.
- AASHTO. 1993. *AASHTO Guide for Design of Pavement Structures*. American Association of State Highway and Transportation Officials, Washington, DC.
- AASHTO. 2008. *Mechanistic-Empirical Pavement Design Guide: A Manual of Practice*. Interim edition, American Association of State Highway and Transportation Officials, Washington, DC.
- AASHTO. 2010. *Guide for the Local Calibration of the Mechanistic-Empirical Pavement Design Guide*. American Association of State Highway and Transportation Officials, Washington, DC.
- AASHTO. 2015. *Mechanistic-Empirical Pavement Design Guide: A Manual of Practice*. Second edition. American Association of State Highway and Transportation Officials, Washington, DC.
- ACPA. 1995. *Subgrades and Subbases for Concrete Pavements*. TB011P. American Concrete Pavement Association, Skokie, IL.
- ACPA. 2007. *Subgrades and Subbases for Concrete Pavements*. EB240P. American Concrete Pavement Association, Skokie, IL.
- ACPA. 2008. *Uniform Support in Concrete Pavement Structures*. Concrete Pavement Technology Series. TS201.1P. American Concrete Pavement Association, Skokie, IL.
- ACPA. 2012. Static K-Value Calculator. American Concrete Paving Association, Skokie, IL. <http://apps.acpa.org/applibrary/KValue/> accessed on July 15, 2012.
- Andrei, D. 2003. Development of a Predictive Model for the Resilient Modulus of Unbound Materials. PhD dissertation. Arizona State University, Tempe, AZ.
- ARA, Inc. ERES Division. 2000. *Guide for Mechanistic-Empirical Design of New and Rehabilitated Pavement Structures, Appendix DD-1: Resilient Modulus as Function of Soil Moisture – Summary of Predictive Models*. National Cooperative Highway Research Program, Washington, DC.
- Azam, A. M., D. A. Cameron, and M. M. Rahman. 2013. Model for Prediction of Resilient Modulus Incorporating Matric Suction for Recycled Unbound Granular Materials. *Canadian Geotechnical Journal*, Vol. 50, No. 11, pp. 1143–1158.
- Barker, W. R. and D. R. Alexander. 2012. *Determining the Effective Modulus of Subgrade Reaction for Design of Rigid Airfield Pavements Having Base Layers*. U.S. Army Corps of Engineers, Washington, DC.
- Beckemeyer, C. A., L. Khazanovich, and H. T. Yu. 2002. Determining Amount of Built-In Curling in Jointed Plain Concrete Pavement. *Transportation Research Record: Journal of the Transportation Research Board*, No. 1089, pp. 85–92.

- Bilodeau, J-P. and G. Dore. 2011. Water Sensitivity of Resilient Modulus of Compacted Unbound Granular Materials used as Pavement Base. *International Journal of Pavement Engineering*, Vol. 13, No. 5, pp. 459–471.
- Birkhoff, J. W. and B. F. McCullogh. 1979. *Detection of Voids Underneath Continuously Reinforced Concrete Pavements*. Texas State Department of Highways and Public Transportation, Austin, TX.
- Brand, A. S. and J. R. Roesler. 2014 *Improving the Foundation Layers for Pavements: Mechanistic-Empirical Pavement Design Guide (MEPDG) Sensitivity Analysis*. National Concrete Pavement Technology Center and Center for Earthworks Engineering Research, Iowa State University, Ames, IA.  
[https://intrans.iastate.edu/app/uploads/2018/07/improving\\_foundation\\_layers\\_UofI\\_mechanistic\\_soil\\_analysis\\_w\\_cvr-1.pdf](https://intrans.iastate.edu/app/uploads/2018/07/improving_foundation_layers_UofI_mechanistic_soil_analysis_w_cvr-1.pdf).
- Brand, A. S., J. R. Roesler, H. L. Chavan, and F. Evangelista, Jr. 2014. *Improving the Foundation Layers for Pavements: Effects of a Non-Uniform Subgrade Support on the Responses of Concrete Pavement*. National Concrete Pavement Technology Center and Center for Earthworks Engineering, Iowa State University, Ames, IA.  
[https://intrans.iastate.edu/app/uploads/2018/07/improving\\_foundation\\_layers\\_UofI\\_uniformity\\_w\\_cvr-1.pdf](https://intrans.iastate.edu/app/uploads/2018/07/improving_foundation_layers_UofI_uniformity_w_cvr-1.pdf).
- CalTrans. 2018. *Highway Design Manual*. Seventh edition. State of California Department of Transportation, Sacramento, CA.
- Cary, C. 2008. Resilient Modulus Testing for Unsaturated Unbound Materials. MS thesis. Arizona State University, Tempe, AZ.
- Cary, C. 2011. Pore Water Pressure Response of a Soil Subjected to Traffic Loading under Saturated and Unsaturated Conditions. PhD dissertation. Arizona State University, Tempe, AZ.
- Cary, C. and C. Zapata. 2010. Enhanced Model for Resilient Response of Soils Resulting from Seasonal Changes as Implemented in Mechanistic-Empirical Pavement Design Guide. *Transportation Research Record: Journal of Transportation Research Board*, No. 2170, pp. 36–44.
- Ceylan, H., S. Kim, K. Gopalakrishnan, and D. Ma. 2013. *Iowa Calibration of MEPDG Performance Prediction Models*. Institute for Transportation, Iowa State University, Ames, IA.  
[https://intrans.iastate.edu/app/uploads/2018/03/MEPDG\\_Iowa\\_calibration\\_w\\_cvrl.pdf](https://intrans.iastate.edu/app/uploads/2018/03/MEPDG_Iowa_calibration_w_cvrl.pdf).
- Christopher, B., C. Schwartz, and R. Boudreau. 2006. *Geotechnical Aspects of Pavements*. FHWA NHI-05-037. National Highway Institute and Federal Highway Administration, Washington, DC.
- Crovetti, J. A. 1994. Design and Evaluation of Jointed Concrete Pavement Systems Incorporating Open-Graded Bases. PhD dissertation. University of Illinois at Urbana-Champaign, IL.
- Darter, M. I., K. T. Hall, and C.-M. Kuo. 1995. *NCHRP Report 372: Support Under Portland Cement Concrete Pavements*. National Cooperative Highway Research Program, Washington, DC.
- Darter, M. I., L. Titus-Glover, H. Von Quntius, B. B. Bhattacharya, and J. Mallela. 2014. *Calibration and Implementation of the AASHTO Mechanistic-Empirical Pavement Design Guide in Arizona*. Arizona Department of Transportation, Phoenix, AZ.

- Devine, O. 2003. The Impact of Ignoring Measurement Error When Estimating Sample Size for Epidemiologic Studies. *Evaluation & Health Professions*, Vol. 26, No. 3, pp. 315–339.
- Drumm, E. C., J. S. Reeves, M. R. Madgett, and W. D. Trolinger. 1997. Subgrade Resilient Modulus Correction for Saturation Effects. *Journal of Geotechnical and Geoenvironmental Engineering*, Vol. 123, No. 7, pp. 663–670.
- Dupont, W. D. and W. D. Plummer, Jr. 1998. Power and Sample Size Calculations for Studies Involving Linear Regression. *Controlled Clinical Trials*, Vol. 19, No. 6, pp. 589–601.
- Edil, T. B. and S. E. Motan. 1979. Soil-Water Potential and Resilient Behavior of Subgrade Soils. *Transportation Research Record: Journal of the Transportation Research Board*, No 705, pp. 54–63.
- FAA. 2013. *Surface Drainage Design*. AC150/5320-5D. Federal Aviation Administration, Washington, DC.
- . 2016. *Airport Pavement Design and Evaluation*. AC150/5320-6F. Federal Aviation Administration, Washington, DC.
- Foxworthy, P. T. 1985. Concepts for the Development of a Nondestructive Testing and Evaluation System for Rigid Airfield Pavements. PhD thesis. University of Illinois at Urbana-Champaign, IL.
- Fredlund, D. G. and A. Xing. 1994. Equations for the Soil-Water Characteristic Curve. *Canadian Geotechnical Journal*, Vol. 31, No. 4, pp. 521–532.
- Fredlund, D. G., A. T. Began, and P. K. Wong. 1977. Relation between Resilient Modulus and Stress Conditions for Cohesive Subgrade Soils. *Transportation Research Record: Journal of the Transportation Research Board*, No 642, pp. 73–81.
- Gehling, D. G., J. A. Ceratti, W. P. Nunez, and M. R. Rodrigues. 1998. A Study on the Influence of Suction on the Resilient Behavior of Soils from Southern Brazil. *Proceedings of the Second International Conference on Unsaturated Soils*, Vol. 2. August 27–30, Beijing, China.
- Goldbeck, A. T. 1919. Thickness of Concrete Slabs. *Public Roads*, Vol. 1, No. 12, pp. 34–38, pp. 34–38.
- Griffiths, D. V., G. A. Fenton, and N. Manoharan. 2006. Undrained Bearing Capacity of Two-Strip Footings on Spatially Random Soil. *International Journal of Geomechanics*, Vol. 6, No. 6, pp. 421–427.
- Groeger, J. L., G. R. Rada, and A. Lopez. 2003. *AASHTO T 307 – Background and Discussion, Resilient Modulus Testing for Pavement Components*. STP 1437. ASTM International, West Conshohocken, PA.
- Gupta, S., A. Ranaivoson, T. Edil, C. Benson, and A. Sawangsuriya. 2007. *Pavement Design Using Unsaturated Soil Technology*. Minnesota Department of Transportation, St. Paul, MN.
- Haider, S. W., N. Buch, and K. Chatti. 2009. Simplified Approach for Quantifying Effect of Significant Input Variables and Designing Rigid Pavements Using M-EPDG. 88th Annual Meeting of the Transportation Research Board, January 11–15, Washington, DC.
- Hall, K. T., M. I. Darter, T. E. Hoerner, and L. Khazanovich. 1997. *LTPP Data Analysis – Phase I: Validation of Guidelines for k-Value Selection and Concrete Pavement Performance Prediction*. FHWA-RD-96-198. Federal Highway Administration, Turner-Fairbank Highway Research Center, McLean, VA.
- Highway Research Board. 1962. *The AASHTO Road Test Report 5 – Pavement Research*. Special Report 61E. Highway Research Board, Washington, DC.

- Hoerner, T. E., K. A. Zimmerman, K. D. Smith, and L. Cooley. 2007. *Mechanistic-Empirical Pavement Design Guide Implementation Plan*. South Dakota Department of Transportation, Pierre, SD.
- Hoffman, M. S. and M. R. Thompson. 1981. *Mechanistic Interpretation of Nondestructive Pavement Testing Deflections*. University of Illinois at Urbana-Champaign, IL.
- Huang, Y. H. 1974. Finite Element Analysis of Slabs on Elastic Solids. *Transportation Engineering Journal*, Vol. 100, No. TE2, pp. 403–416.
- Huang, Y. H. 2004. *Pavement Analysis and Design*. Second edition. Pearson Education, Inc., Upper Saddle River, NJ.
- Huang, Y. H. and S. T. Wang. 1974. Finite Element Analysis of Rigid Pavements with Partial Subgrade Contact. *Transportation Research Record: Journal of the Transportation Research Board*, No. 485, pp. 39–54.
- Hudson, W. R. and H. Matlock. 1966. Analysis of Discontinuous Orthotropic Pavement Slabs Subjected to Combined Loads, *Highway Research Record*, No. 131, pp. 1–48.
- Isaaks, E. H. and R. M. Srivastava. 1989. *An Introduction to Applied Geostatistics*. Oxford University Press, New York, NY.
- Jeong, J. H. and D. G. Zollinger. 2001. Characterization of Stiffness Parameters in Design of Continuously Reinforced and Jointed Pavements *Transportation Research Record: Journal of the Transportation Research Board*, No. 1778, pp. 54–63.
- Johnson, A. E. 2012. Freeze-Thaw Performance of Pavement Foundation Materials. MS thesis. Civil, Construction, and Environmental Engineering, Iowa State University, Ames, IA.
- Jung, Y.-s., D. G. Zollinger, and A. J. Wimsatt. 2010. Test Method and Model Development of Subbase Erosion for Concrete Pavement Design. *Transportation Research Record: Journal of the Transportation Research Board*, No. 2154, pp. 22–31.
- Kannekanti, V. and J. Harvey. 2005. *Sensitivity Analysis of 2002 Design Guide Rigid Pavement Distress Prediction Models*. Draft Report. Pavement Research Center, University of California-Davis and University of California-Berkeley, CA.
- Khanum, T. 2005. Kansas Rigid Pavement Analysis Following New Mechanistic-Empirical Design Guide. MS thesis. Kansas State University, Manhattan, KS.
- Kher, R. K., W. R. Hudson, and B. F. McCullough. 1971. *A System Analysis of Rigid Pavement Design*. Center for Highway Research, University of Texas, Austin, TX.
- Khoury, N. N. and M. Zaman. 2004. Correlation Among Resilient Modulus, Moisture Variation and Soil Suction for Subgrade Soils. *Transportation Research Record: Journal of the Transportation Research Board*, No 1874, pp. 99–107.
- Khoury, N. N., R. Brooks, M. M. Zaman, and C. H. Khoury. 2009. Variations of Resilient Modulus of Sub-Grade Soils with Post-Compaction Moisture Contents. *Transportation Research Record: Journal of the Transportation Research Board*, No 2101, pp. 72–81.
- Kim, R. Y., F. M. Jadoun, T. Hou, and N. Muthadi. 2011. *Local Calibration of the MEPDG for Flexible Pavement Design*. North Carolina Department of Transportation, Raleigh, NC.
- Larralde, J. 1984. Structural Analysis of Ridge Pavements with Pumping. PhD dissertation. Purdue University, West Lafayette, IN.
- Leonards, G. A. and M. E. Harr. 1959. Analysis of Concrete Slabs on Ground, *Journal of the Soil Mechanics and Foundation Divisions*, Vol. 85 (SM3), pp. 35–58.
- Levey, J. R. and E. J. Barenberg. 1970. A Procedure for Evaluating Pavements with Nonuniform Paving Materials. Paper sponsored by Committee on Theory of Pavement Design and presented at the 49th Annual Meeting. *Highway Research Record*, No 337, pp. 55–69.

- Li, J., D. J. White, and P. Vennapusa. 2018. *Improving the Foundation Layers for Pavements: Field Assessment of Variability in Pavement Foundation Properties*. National Concrete Pavement Technology Center and Center for Earthworks Engineering Research, Iowa State University, Ames, IA.  
[https://intrans.iastate.edu/app/uploads/2018/07/improving\\_foundation\\_layers\\_field\\_assessment\\_of\\_variability\\_w\\_cvr-1.pdf](https://intrans.iastate.edu/app/uploads/2018/07/improving_foundation_layers_field_assessment_of_variability_w_cvr-1.pdf).
- Liang, R. Y., S. Rabab'ah, and M. Khasawneh. 2008. Predicting Moisture-Dependent Resilient Modulus of Cohesive Soils Using Soil Suction Concept. *Journal of Transportation Engineering*, Vol. 134, No. 1, pp. 34–40.
- Lytton, R. L., X. Luo, S. Saha, Y. Chen, Y. Deng, F. Gu, and M. Ling. 2019. *NCHRP Web-Only Document 264: Proposed Enhancements to Pavement ME Design: Improved Consideration of the Influence of Subgrade and Unbound Layers on Pavement Performance*. National Cooperative Highway Research Board, Washington, DC.
- Mallela, J., L. Titus-Glover, S. Sadasivam, B. Bhattacharya, M. Darter, and H. Von Quintus. 2013. *Implementation of the AASHTO Mechanistic-Empirical Pavement Design Guide for Colorado*. Colorado Department of Transportation – Research, Denver, CO.
- Markow, M. J. and B. D. Brademeyer. 1984. *EAROMAR*, v. 2. FHWA/RD-82/086. Federal Highway Administration, Turner-Fairbank Highway Research Center, McLean, VA.
- McPeak, T. J., L. Khazanovich, M. I. Darter, and C. Beckemeyer. 1998. Determination of In-Service Asphalt Pavement Subgrade Support for Concrete Pavement Design. *Proceedings of Fifth International Conference on the Bearing Capacity of Roads and Airfields*. Norwegian University of Science and Technology, Trondheim, Norway.
- Mohammad, L. N., A. J. Puppala and P. Alavilli. 1995. Resilient Properties of Laboratory Compacted subgrade Soils. *Transportation Research Record: Journal of the Transportation Research Board*, No 1504, pp. 87–102.
- Mooney, A. M., V. R. Rinehart, W. N. Facas, M. O. Musimbi, J. D. White, and K. R. P. Vennapusa. 2010. *NCHRP Report 676: Intelligent Soil Compaction Systems*. National Cooperative Highway Research Program, Washington, DC.
- Mostyn, G. R. and K. S. Li. 1993. Probabilistic Slope Analysis: State-of-Play. In *Probabilistic Methods in Geotechnical Engineering*. K. S. Li and S-C. R. Lo, eds., Balkema, Rotterdam, The Netherlands, pp. 89–109.
- Nazarian, S., M. Baker, and K. Crain. 1995. Use of Seismic Pavement Analyzer in Pavement Evaluation. *Transportation Research Record: Journal of the Transportation Research Board*, No 1505, pp. 1–8.
- Nazarian S., M. Mazari, I. Abdallah, A. J. Puppala, L. N. Mohammad, and M. Y. Abu-Farsakh. 2014. *Modulus-Based Construction Specification for Compaction of Earthwork and Unbound Aggregate*. Draft final report for NCHRP Project 10-84. National Cooperative Highway Research Program, Washington, DC.
- Nokkaew, K., J. M. Tinjum, W. J. Likos, and T. B. Edil. 2014. Effect of Matric Suction on Resilient Modulus for Compacted Recycled Base Course in Postcompaction State. *Transportation Research Record: Journal of the Transportation Research Board*, No 2433, pp. 68–78.
- Older, C. 1924. Highway Research in Illinois. *Transactions*, Vol 87, Paper No. 1546, pp. 1180–1222.

- Ooi, P. S, A. R. Archilla, and K. G. Sandefur. 2004. Resilient Modulus Models for Compacted Cohesive Soils. *Transportation Research Record: Journal of the Transportation Research Board*, No 1874, pp. 115–124.
- Packard, R. C. 1973. *Design of Concrete Airport Pavement*. Engineering Bulletin, Portland Cement Association, Skokie, IL.
- Parreira, A. B. and R. F. Goncalves. 2000. The Influence of Moisture Content and Soil Suction on the Resilient Modulus of a Lateritic Subgrade Soil. GeoEng - An International Conference on Geotechnical & Geological Engineering, International Society for Rock Mechanics and Rock Engineering (ISRM) International Symposium, November 19–24, Melbourne, Australia.
- PCA. 1984. *Thickness Design for Concrete Highway and Street Pavements*. Portland Cement Association, Skokie, IL.
- Pennsylvania DOT. 2009. *Section ITEM 9000-0001–Slab Stabilization*. Supplemental Specifications. Pennsylvania Department of Transportation, Harrisburg, PA.
- Phoon, K.-K., F. H. Kulhawy, and M. D. Grigoriu. 2000. Reliability Based Design for Transmission Line Structure Foundations. *Computers and Geotechnics*, Vol. 26, Nos. 3–4, pp. 169–346.
- Pickett, G. M., M. E. Raville, W. C. Janes, and F. J. McCormick. 1951. *Deflections, Moments, and Reactive Pressures for Concrete Pavements*. Bulletin No. 65. Engineering Experiment Station, Kansas State College, Manhattan, KS.
- Rada, G. 1981. Evaluation of Design Parameters for MSHA Unbound Granular Materials. MS thesis. University of Maryland, College Park, MD.
- Rada, G. and M. W. Witczak. 1981. Comprehensive Evaluation of Laboratory Resilient Moduli Results for Granular Material. *Transportation Research Record: Journal of the Transportation Research Board*, No. 810, pp. 23–33.
- Rauhut, J. B., R. L. Lytton, and M. I. Darter. 1982. *Pavement Damage Functions for Cost Allocation Volume 1: Damage Functions and Load Equivalency Factors*. FHWA/RD-82/126. Federal Highway Administration, Turner-Fairbank Highway Research Center, McLean, VA.
- Richart, F. E., Jr. and P. Zia. 1962. Effect of Local Loss of Support on Foundation Design. *Journal of the Soil Mechanics and Foundation Divisions*, Vol. 88 (SM1), pp. 1–27.
- Saeed, A. 2008. *NCHRP Report 598: Performance-Related Tests of Recycled Aggregates for Use in Unbound Pavement Layers*. National Highway Cooperative Highway Research Program, Washington, DC.
- Santha B. L. 1994. Resilient Modulus of Subgrade Soils: Comparison of Two Constitutive Equations. *Transportation Research Record: Journal of the Transportation Research Board*, No 1462, pp. 79–90.
- Smith, K. D., M. J. Wade, J. E. Bruinsma, K. Chatti, J. M. Vandenbossche, H. T. Yu, T. E. Hoerner, and S. D. Tayabji. 2007. *Using Falling Weight Deflectometer Data with Mechanistic-Empirical Design and Analysis*. Draft Interim Report. Federal Highway Administration, Washington, DC.
- Substad, R. N., Y. J. Jiang, and E. O. Lukanen. 2006. *Guidelines for Review and Evaluation of Backcalculation Results*. FHWA-RD-05-152. Federal Highway Administration, Turner-Fairbank Highway Research Center, McLean, VA.
- Teller, L. W. and E. C. Sutherland. 1935a. The Structural Design of Concrete Pavements, Part 1, A Description of the Investigation. *Public Roads*, Vol. 16, No. 8.



- Teller, L. W. and E. C. Sutherland. 1935b. The Structural Design of Concrete Pavements, Part 2, Observed Effects of Variations in Temperature and Moisture on the Size, Shape and Stress Resistance of Concrete Pavement Slabs. *Public Roads*, Vol. 16, No. 9.
- Teller, L. W. and E. C. Sutherland. 1935c. The Structural Design of Concrete Pavements, Part 3, A Study of Concrete Pavement Cross Sections. *Public Roads*, Vol. 16, No. 10.
- Teller, L. W. and E. C. Sutherland. 1936. The Structural Design of Concrete Pavements, Part 4, A Study of the Structural Action of Several Types of Transverse and Longitudinal Joint Designs. *Public Roads*, Vol. 17, Nos. 7 and 8.
- Teller, L. W. and E. C. Sutherland. 1943. The Structural Design of Concrete Pavements, Part 5, An Experimental Study of the Westergaard Analysis of Stress Conditions in Concrete Pavements of Uniform Thickness. *Public Roads*, Vol. 23, No. 8.
- Terzaghi, K. 1955. Evaluation of Coefficients of Subgrade Reaction. *Geotechnique*, Vol. 5, No. 1, pp. 297–326.
- Terzaghi, K. and R. B. Peck. 1967. *Soil Mechanics in Engineering Practice*. Second edition. John Wiley and Sons, New York, NY.
- Thadkamalla, G. B. and K. P. George. 1995. Characterization of Subgrade Soils at Simulated Field Moisture. *Transportation Research Record: Journal of the Transportation Research Board*, No 1481, pp. 21–27.
- Tutumluer, E. 2013. *NCHRP Synthesis 445: Practices for Unbound Aggregate Pavement Layers*. National Cooperative Highway Research Board, Washington, DC.
- Tutumluer, E., M. Moaveni, and I. Qamiha. 2018. *NCHRP Synthesis 524: Aggregate Quality Requirements for Pavements*. National Cooperative Highway Research Board, Washington, DC.
- Ullidtz, P. 1987. *Pavement Analysis*. Elsevier, Amsterdam, Netherlands.
- USACE. 1943. *Report of Special Field Bearing Tests on Natural Subgrade and Prepared Subbase Using Different Size Bearing Plates*. Ohio River Division, Office of the Division Engineer, Cincinnati Testing Laboratory Soils Division, U.S. Army Corps of Engineers, Mariemont, OH.
- USACE. 1953. *Determination of the High Values of the Subgrade Modulus, k, from the Plate Bearing Test*. Ohio River Division, Office of the Division Engineer, Cincinnati Testing Laboratory Soils Division, U.S. Army Corps of Engineers, Mariemont, OH.
- USACE. 1966. *Airfield Rigid Pavement Evaluation – Air Force Emergency Construction*. TM 5-888-9. U.S. Army Corps of Engineers, Washington, DC.
- USACE. 1995. *Handbook for Concrete and Cement Standard Test Method for Determining the Modulus of Soil Reaction*. COE CRD-C 655-95. U.S. Army Corps of Engineers, Washington, DC.
- U.S. Departments of the Army and the Air Force. 1958. *Rigid Airfield Pavements*. TM 5-825-3/AFM 88-6. Departments of the Army and the Air Force, Washington, DC.
- . 1979. *Rigid Airfield Pavements*. TM 5-824-3/AFM 88-6. Departments of the Army and the Air Force, Washington, DC.
- U.S. Department of Defense. 2018. *UFC 3-270-01 O&M Manual: Asphalt and Concrete Pavement Maintenance and Repair*. U.S. Department of Defense, Washington, DC.
- Velasquez, R., K. Hoegh, I. Yut, N. Funk, G. Cochran, M. Marasteanu, and L. Khazanovich, 2009. *Implementation of the MEPDG for New and Rehabilitated Pavement Structures for Design of Concrete and Asphalt Pavements in Minnesota*. Minnesota Department of Transportation, St. Paul, MN.



- Vennapusa, P. 2004. Determination of the Optimum Base Characteristics for Pavements. MS thesis. Civil, Construction, and Environmental Engineering, Iowa State University, Ames, IA.
- Vennapusa, P. and D. J. White. 2009. Comparison of Light Weight Deflectometer Measurements for Pavement Foundation Materials. *Geotechnical Testing Journal*, Vol. 32, No. 3, pp. 239–251.
- Vennapusa, P., P. Taylor, and D. J. White. 2015. *Improving the Foundation Layers for Pavements: Field Evaluation of Premature Pavement Joint Deterioration – Iowa Urbandale Drive Field Study*. National Concrete Pavement Technology Center and Center for Earthworks Engineering Research, Iowa State University, Ames, IA. [https://intrans.iastate.edu/app/uploads/2018/07/improving\\_foundation\\_layers\\_Urbandale\\_Drive\\_w\\_cvr-1.pdf](https://intrans.iastate.edu/app/uploads/2018/07/improving_foundation_layers_Urbandale_Drive_w_cvr-1.pdf).
- Vennapusa, P., D. J. White, and M. Morris. 2010. Geostatistical Analysis for Spatially Referenced Roller-Integrated Compaction Measurements. *Journal of Geotechnical and Geoenvironmental Engineering*, Vol. 136, No. 6, pp. 813–822.
- Vessely, M., W. Robert, W., S. Richrath, V. R. Schaefer, O. Smadi, E. Loehr, and A. Boeckmann. 2019. *NCHRP Research Report 903: Geotechnical Asset Management for Transportation Agencies: Volume 2 – Implementation Manual*. National Cooperative Highway Research Program, Washington, DC.
- Vinson, T. S. 1989. *Fundamentals of Resilient Modulus Testing*. Workshop on Resilient Modulus Testing, Oregon State University, Corvallis, OR.
- Yang, R. R., W. H. Huang, and Y. T. Tai. 2005. Variation of Resilient Modulus with Soil Suction for Compacted Subgrade Soils. *Transportation Research Record: Journal of the Transportation Research Board*, No 1913, pp. 99–106.
- Westergaard, H. M. 1926a. Analysis of Stresses in Concrete Pavements due to Variations of Temperature. *Highway Research Board*, Vol. 6, pp. 201–215.
- Westergaard, H. M. 1926b. Stresses in Concrete Pavements Computed by Theoretical Analysis. *Public Roads*, Vol. 7, pp. 25-35.
- Westergaard, H. M. 1927. Theory of Concrete Pavement Design. *Highway Research Board*, Vol. 7, pp. 175–181.
- Westergaard, H. M. 1948. New Formulas for Stresses in Concrete Pavements of Airfields. *Transactions*, Vol. 113, pp. 425–444.
- White, D. J. and P. Vennapusa. 2014. *Optimizing Pavement Base, Subbase, and Subgrade Layers for Cost and Performance of Local Roads*. Center for Earthworks Engineering Research, Iowa State University, Ames, IA.
- White, D. J., H. Ceylan, C. Jahren, T. H. Phan, S. H. Kim, K. Gopalakrishnan, and M. Suleiman. 2008. *Performance Evaluation of Concrete Pavement Granular Subbase and Pavement Surface Condition Evaluation*. Center for Transportation Research and Education, Iowa State University, Ames, IA.
- White, D. J., T. Rupnow, and H. Ceylan. 2005. Influence of Subgrade/Subbase Nonuniformity on Pavement Performance. Geotechnical Special Publication No. 126. Geo-Trans 2004 – Geotechnical Engineering for Transportation Projects, Los Angeles, CA, pp. 1058–1065.
- White, D. J., P. Vennapusa, and C. T. Jahren. 2004. *Determination of Optimum Base Characteristics for Pavements*. Center for Transportation Research and Education, Iowa State University, Ames, IA.

- White, D. J., P. Vennapusa, C. T. Suleiman, and C. T. Jahren. 2007. An In Situ Device for Rapid Determination of Permeability of Granular Bases. *Geotechnical Testing Journal*, Vol. 30, No. 4, pp. 282–291.
- White, D. J., P. K. R. Vennapusa, and H. H. Gieselman, H. 2011. Field Assessment and Specification Review for Roller-Integrated Compaction Monitoring Technologies. *Advances in Civil Engineering Advances in Instrumentation and Monitoring in Geotechnical Engineering*, Vol. 2011.
- White, D. J., P. Vennapusa, and L. Zhao. 2013. Verification and Repeatability Analysis for the In Situ Air Permeability Test. *Geotechnical Testing Journal*, Vol. 37, No. 2.
- White, D. J., P. Vennapusa, and A. Wolfe. 2015. *Improving the Foundation Layers for Pavements: Jointed Concrete Pavement Rehabilitation with Injected High Density Polyurethane Foam and Dowel Bar Retrofitting – Pennsylvania US 422 Field Study*, National Concrete Pavement Technology Center and Center for Earthworks Engineering Research, Iowa State University, Ames, IA.  
[https://intrans.iastate.edu/app/uploads/2018/07/improving\\_foundation\\_layers\\_PA\\_US\\_422\\_w\\_cvr-1.pdf](https://intrans.iastate.edu/app/uploads/2018/07/improving_foundation_layers_PA_US_422_w_cvr-1.pdf).
- White, D. J., P. Vennapusa, H. Gieselman, A. J. Wolfe, S. Douglas, and J. Li. 2016a. *Improving the Foundation Layers for Pavements: Pavement Foundation Layer Reconstruction Michigan I-94 Field Study*. National Concrete Pavement Technology Center and Center for Earthworks Engineering Research, Iowa State University, Ames, IA.  
[https://intrans.iastate.edu/app/uploads/2018/07/improving\\_foundation\\_layers\\_MI\\_I-94\\_w\\_cvr-1.pdf](https://intrans.iastate.edu/app/uploads/2018/07/improving_foundation_layers_MI_I-94_w_cvr-1.pdf).
- White, D. J., P. Vennapusa, Y. Zhang, H. Gieselman, and M. Prokudin. 2016b. *Improving the Foundation Layers for Pavements: Pavement Foundation Layer Reconstruction IA US 30 Field Study*. National Concrete Pavement Technology Center and Center for Earthworks Engineering Research, Iowa State University, Ames, IA.  
[https://intrans.iastate.edu/app/uploads/2018/07/improving\\_foundation\\_layers\\_IA\\_US\\_30\\_w\\_cvr-1.pdf](https://intrans.iastate.edu/app/uploads/2018/07/improving_foundation_layers_IA_US_30_w_cvr-1.pdf).
- White, D. J., P. Vennapusa, and Y. Zhang. 2016c. *Improving the Foundation Layers for Pavements: Field Assessment of Jointed Portland Cement Concrete Pavement with Premature Distresses — Iowa US 34 Field Study*. National Concrete Pavement Technology Center and Center for Earthworks Engineering Research, Iowa State University, Ames, IA.  
[https://intrans.iastate.edu/app/uploads/2018/07/improving\\_foundation\\_layers\\_IA\\_US\\_34\\_w\\_cvr-1.pdf](https://intrans.iastate.edu/app/uploads/2018/07/improving_foundation_layers_IA_US_34_w_cvr-1.pdf).
- White, D. J., P. Vennapusa, and Y. Zhang. 2016d. *Improving the Foundation Layers for Pavements: Jointed Concrete Pavement Rehabilitation with Precast Concrete Pavement – California I-15 Field Study*. Field Project Report. National Concrete Pavement Technology Center and Center for Earthworks Engineering Research, Iowa State University, Ames, IA.  
[https://intrans.iastate.edu/app/uploads/2018/07/improving\\_foundation\\_layers\\_CA\\_I-15\\_w\\_cvr-1.pdf](https://intrans.iastate.edu/app/uploads/2018/07/improving_foundation_layers_CA_I-15_w_cvr-1.pdf).

- White, D. J., P. Vennapusa, P. Becker, J. Rodriguez, Y. Zhang, and C. White. 2018. *Central Iowa Expo Pavement Test Sections: Pavement and Foundation Construction Testing and Performance Monitoring*. Center for Earthworks Engineering Research, Iowa State University, Ames, IA.  
[https://intrans.iastate.edu/app/uploads/2018/03/Central\\_Iowa\\_Expo\\_pvmt\\_section\\_perf\\_w\\_cvr.pdf](https://intrans.iastate.edu/app/uploads/2018/03/Central_Iowa_Expo_pvmt_section_perf_w_cvr.pdf).
- White, D. J., P. Vennapusa, J. R. Roesler, and W. Vavrik. 2019. Plate Load Testing on Layered Pavement Foundation System to Characterize Mechanistic Parameters. GeoCongress 2019 – 8th International Conference on Case Histories in Geotechnical Engineering, March 24–27, Philadelphia, PA.
- White, D. J., P. Vennapusa, and T. Cackler. 2019. *In Situ Modulus Measurement Using Automated Plate Load Testing for Statewide Mechanistic-Empirical Design Calibration*. Ingios Geotechnics, Inc., Ames, IA.  
[http://publications.iowa.gov/30753/1/ST003\\_Final%20Report\\_In-Situ%20Modulus%20Testing%20Using%20APLT%20for%20MEPDG.pdf](http://publications.iowa.gov/30753/1/ST003_Final%20Report_In-Situ%20Modulus%20Testing%20Using%20APLT%20for%20MEPDG.pdf).
- Wijk, A. J. V. 1985. *Rigid Pavement Pumping – (1) Subbase Erosion and (2) Economic Modeling*. Joint Highway Research Project, School of Civil Engineering, Purdue University, West Lafayette, IN.
- Witczak, M. W. 2003. *NCHRP 1-28A: Harmonized Test Methods for Laboratory Determination of Resilient Modulus for Flexible Pavement Design, Volume I: Unbound Granular Material*. National Cooperative Highway Research Program, Washington, DC.
- Witczak, M. W., D. Andrei, and W. N. Houston. 2000. *NCHRP 1-37A: Resilient Modulus as Function of Soil Moisture – Summary of Predictive Models. Development of the 2002 Guide for the Development of New and Rehabilitated Pavement Structures*. Inter Team Technical Report (Seasonal 1). Arizona State University, Tempe, AZ.
- Yang, R. R., W. H. Huang, and Y. T. Tai. 2005. Variation of Resilient Modulus with Soil Suction for Compacted Subgrade Soils. *Transportation Research Record*, No 1913, pp. 99–106.
- Zapata, C. E. and W. N. Houston. 2008. *NCHRP Report 602: Calibration and Validation of the Enhanced Integrated Climatic Model for Pavement Design*. National Cooperative Highway Research Program, Washington, DC.
- Zhang, Y. 2013. Frost-Heave and Thaw-Weakening of Pavement Foundation Materials. MS thesis. Civil, Construction, and Environmental Engineering, Iowa State University, Ames, IA.
- Zhang, Y. 2016. Assessing Seasonal Performance, Stiffness, and Support Conditions of Pavement Foundations. PhD dissertation. Civil, Construction, and Environmental Engineering, Iowa State University, Ames, IA.
- Zhang, Y., A. E. Johnson, and D. J. White. 2016. Laboratory Freeze-Thaw Assessment of Cement, Fly Ash, and Fiber Stabilized Pavement Foundation Layers. *Cold Regions Science and Technology*, Vol. 122, pp. 50–57.
- Zhang, Y., D. J. White, P. Vennapusa, and A. E. Johnson. 2018. Investigating Frost Heave Deterioration at Pavement Joint Locations. *Journal of Performance of Constructed Facilities*, Vol. 32, No. 2.





**National Concrete Pavement  
Technology Center**

